Phosphorus Characterization and Transport in Traditionally Fertilized No-Till vs. Conventionally Managed Systems and Greenhouse Growth Trials Using Dairy Manure-Amended Soils

A Thesis

Presented in Partial Fulfillment of the Requirements for the

Degree of Master of Science

with a

Major in Soil and Land Resources

in the

College of Graduate Studies

University of Idaho

by

Maggi Marie Laan

Approved by:

Major Professor: Daniel Strawn, Ph.D.; Zachary Kayler, Ph.D.

Committee Members: Gregory Möller, Ph.D.; Jeff Langman, Ph.D.

Department Administrator: Jodi Johnson-Maynard, Ph.D.

August 2022

Abstract

Phosphorus (P) is a limiting nutrient in freshwater systems that can cause harmful algal blooms even at low concentrations. Excessive application of both conventional fertilizers and manure for crop production has caused a build-up of legacy phosphorus stores in surface soils, which continue to export phosphorus from agricultural fields for decades after fertilizer application has ceased. In this thesis, soil P availability and cycling were evaluated in two unique systems: 1) P in soil amendments derived from dairy, and 2) P leached from a dryland agricultural field and tile drain in the Northwestern Wheat Growing Region. Isotopic tracing of phosphorus (P-$\delta^{18}O$) was used in the field study to understand temporal P leaching patterns through the soils. In the field study, P-$\delta^{18}O$ signatures were used to identify key source areas of phosphorus transport in small watersheds and showed that seasonal climate drivers, not land management, controlled the turnover and transport of legacy phosphorus through the soil and into tile drains. To understand P cycling from dairy-derived nutrients, isotopic tracing, nuclear magnetic resonance (^{31}P-NMR), x-ray absorbance near-edge structure spectroscopy (XANES), and chemical sequential extraction methods were used in a greenhouse study. Results show that P cycling and transformations, determined by isotopic and spectroscopic analysis, differed between dairy-derived and synthetic fertilizers, which could not be determined from chemical extractions alone. XANES analysis showed that soils were comprised mostly of Ca-P species (53.6 - 86.7%), but Ca-P species in soils amended with dairy-derived fertilizers were present in more soluble forms. Plant available P was similar between dairy-derived and synthetic fertilizer treatments within high and low levels, suggesting that the amendments generated from dairy wastes are a possible way to help recycle nutrients from dairy waste streams, helping to close the dairy bioeconomy in Idaho.

Phosphorus Characterization and Transport in Traditionally Fertilized No-Till vs. Conventionally Managed Systems and Greenhouse Growth Trials Using Dairy Manure-Amended Soils

Acknowledgments

I'd like to thank the USDA National Institute of Food and Agriculture for funding my Master's program in Soil and Land Resources. My advisors, Dr. Dan Strawn and Dr. Zack Kayler, have been crucial for my success at the University of Idaho. I would not be here today without their support and guidance through this process. I'd also like to thank my committee members, Dr. Jeff Langman and Dr. Greg Möller, for their input in completing this thesis. Dr. Barbara Cade-Menun and Dr. Alexander Blumenfeld were especially helpful for completing NMR analysis. Alex Crump and Martin Baker were helpful in the completion of lab and field work, which I could not have done on my own.

Dedication

I would like to dedicate this thesis to people who supported me throughout this process. Thank you to my family and friends for keeping me grounded over the last two years. From long phone calls to dinner parties to cribbage nights, thank you for reminding me to take some time for fun.

Table of Contents

Abstract ii
Acknowledgments iii
Dedication iv
Table of Contents v
List of Tables vii
List of Figures x
Chapter 1: Isotopic Tracing of Phosphorus (P-^{18}O) in Till and No-Till Systems 1
1.1 ABSTRACT 1
1.2 INTRODUCTION 1
1.2.1 Land Management Effects on Phosphorus Fluxes 1
1.2.2 Isotope Tracing 5
1.2.3 Research Gaps 9
1.2.4 Research Goals 11
1.3 MATERIALS & METHODS 11
1.3.1 Site Background 11
1.3.2 Soil and Water Sampling 12
1.3.3 P-δ^{18}O Extraction of Soil and Water 13
1.3.4 Statistical Analysis 14
1.4 RESULTS 14
1.4.1 Phosphorus concentrations in soil and tile drains at CAF 14
1.4.2 P-δ^{18}O dynamics at CAF 17
1.5 DISCUSSION 22
1.5.1 Land Management Effects 22
1.5.2 Climate Drivers of P Transport 22
1.5.3 Legacy P at CAF 25
1.5.4 Future Directions 26
1.6 CONCLUSION 27
1.7 REFERENCES 28
Chapter 2: Phosphorus Speciation and Availability in Soils with Dairy-Derived Amendments. 37
2.1 ABSTRACT 37
2.2 INTRODUCTION 37
2.2.1 Phosphorus in Agriculture 37

2.2.2 Dairy Waste Management 38
2.2.3 Methods Background 40
2.2.4 Research Goals 42
2.3 MATERIALS & METHODS 42
2.3.1 Dairy-Derived Amendments 42
2.3.2 Greenhouse Setup 50
2.3.3 Soil Characterization 51
2.3.4 Barley Characterization and Harvest 52
2.3.5 Soil Total P 52
2.3.6 Hedley Sequential Extraction 52
2.3.7 Extractable Soil P Isotopic Analysis 54
2.3.8 Soil P Speciation by P-NMR Analysis 55
2.3.9 Phosphorus K-Edge XANES Analysis 56
2.3.10 Statistical Analysis 57
2.4 RESULTS 57
2.4.1 Soil Characterization 57
2.4.2 Plant Characterization 60
2.4.3 Soil Total P 62
2.4.4 Hedley P Characterization 64
2.4.5 NMR Speciation 69
2.4.7 XANES Fitting 76
2.4.8 Hedley Isotope Extraction 82
2.5 DISCUSSION 86
2.5.1 Plant Availability of Dairy-Derived Fertilizers 86
2.5.2 P Speciation 86
2.5.3 Dairy-derived fertilizer impacts on plant biomass 89
2.5.4 P Cycling as Determined by P-δ^{18}O Signatures 91
2.6 CONCLUSION 95
2.7 REFERENCES 98
Appendix A. Supplemental Tables and Figures for Chapter 1. 107
Appendix A.1. P-δ^{18}O Extraction Protocol. 107
Appendix B. Supplemental Introduction, Discussion, Tables and Figures for Chapter 2. 116
Appendix B.1. Supplementary Material for Chapter 2 Introduction 116
Appendix B.2. Supplementary Material for Chapter 2 Discussion. 119

List of Tables

Table 1.1. P-$\delta^{18}O$ of various sources and pools from Tamburini et al. (2014). 7
Table 1.2. Water-extractable phosphorus values for monthly soil samples. 15
Table 1.3. H_2O-P_{MR} concentrations (mg/L) for tile drain samples. 17
Table 2.1. Al, Ca, Fe, K, Mg, Mn, Na, P, and S content in digested 0.5% Fe-modified biochars after mixing with dairy lagoon water at 1:20, 1:100, and 1:400 solid:solution ratios for two hours. 0.5% Fe-modified biochar was also mixed with DI water at 1:100 solid:solution ratio to serve as a control. 44
Table 2.2. Concentration of Al, Ca, Fe, K, Mg, Mn, Na, P, and S in lagoon water before and after mixing with 0.5% Fe-modified at 1:20, 1:100, and 1:400 solid:solution ratios for two hours. 0.5% Fe-modified biochar was also mixed with DI water at 1:100 solid:solution ratio to serve as a control. 45
Table 2.3. Summary of dairy lagoon characteristics before and after 1% Fe biochar mixing. Values are averaged from two replicate samples (±standard error). 47
Table 2.4. Summary of biochar and fermented biosolids properties. Values are averaged over replicates where applicable (± standard error). 49
Table 2.5. Amendment application rate and total P addition at high and low rates for each treatment. 51
Table 2.6. Comparison of $NaHCO_3$-P_i analyzed by ICP and colorimetrically. 54
Table 2.7. Summary of pH and EC (± standard error) of samples before and after use in the greenhouse. Time final values are averaged from five treatment replicates (n = 5). 58
Table 2.8. Summary of soil characteristics of amended soil samples before use in the greenhouse. Standard errors denoted in parentheses for control (n = 3). 59
Table 2.9. Estimated marginal means for main effects of treatment and level on root mass, dried plant biomass, yield, and number of barley heads per plant. Values in parentheses are standard errors. Main effects indicated by superscript letters are statistically not different at a 95% confidence level. 61
Table 2.10. Estimated marginal means for average biomass, root biomass, yield mass, and number of grain heads for GemCraft barley harvested from greenhouse pot trial. Values in parentheses are standard errors. Pairwise comparisons of treatments within each level and comparisons to control indicated by superscript letters are not statistically different at a 95% confidence level within the level of application. Significant differences at a 95% confidence level for the same treatment at high and low level of application are indicated by an asterisk. 62

Table 2.11. Estimated marginal means for total P by incineration (TP), organic P (P_o), and % P_o for all treatments and levels. Values in parentheses represent standard errors. 64
Table 2.12. Estimated marginal means for main effects of treatment and level on Hedley H_2O, $NaHCO_3$, NaOH, and HNO_3 P pools. Values in parentheses are standard errors. Main effects indicated by superscript letters are statistically not different at a 95% confidence level. 66
Table 2.13 Estimated marginal means for Hedley H_2O, $NaHCO_3$, NaOH, and HNO_3 P pools. Values in parentheses are standard errors. Pairwise comparisons of treatments within each level and comparisons to control indicated by superscript letters are not statistically different at a 95% confidence level within the Hedley pool and level of application. Significant differences at a 95% confidence level for the same treatment at high and low level of application are indicated by an asterisk. 67
Table 2.14. Mean H_2O-P concentrations determined by ICP and colorimetrically. Standard error in parentheses. 69
Table 2.15. ^{31}P-NMR results from NaOH-EDTA extraction of selected soil samples. 73
Table 2.16. Summed ^{31}P-NMR results from NaOH-EDTA extraction of soil samples. 74
Table 2.17. ^{31}P-NMR results from NaOH-EDTA extraction of amendments. 75
Table 2.18. Summed ^{31}P-NMR results from NaOH-EDTA extraction of amendments. 76
Table 2.19. Percent composition of phosphorus species of soil samples and amendments from greenhouse pot trials determined by linear combination fitting of K-edge XANES spectra. 80
Table 2.20. Isotopic values of CF and FS amendments and Hedley pools of soils before and after use in greenhouse pot trial. 85
Table 2.21. % P_o species determined by ^{31}P-NMR, XANES LCF, and ignition. 89
Table 2.22. Optimized τ values for individual samples, averaged within treatment for each extractable soil pool and treatment, and total average for the extractable soil pool. Coefficients of variation were calculated to determine the spread of values in each pool. 95
Table A.1. Estimated marginal means for main effects of catchment and month for soil H_2O-P_{TF}, H_2O-P_{MR}, and P-$\delta^{18}O$ values. Values in parentheses are standard errors. 112
Table A.2. Estimated marginal means and p-values for differences in H_2O-P_{TF} by catchment for each month. 113
Table A.3. Estimated marginal means and p-values for differences in H_2O-P_{MR} by catchment for each month. 114
Table A.4. Estimated marginal means and p-values for differences in P-$\delta^{18}O$ values by catchment for each month. 115
Table B.1. %RSD values for analytical replicates in each run. 121

Table B.2. Plant height measurements (cm) taken weekly and averaged across treatment (± standard error)..... 122
Table B.3. Average concentrations for Al, Ca, Fe, Mg, Mn (± standard error) for the H_2O-P Hedley extraction..... 123
Table B.4. Average concentrations for Al and Ca (± standard error) for the NaOH-P Hedley extraction..... 124
Table B.5. Average concentrations for Al, Ca, Fe, Mg, and Mn (± standard error) for the HNO_3-P Hedley extraction. 125
Table B.6. Elemental concentrations in freeze-dried NMR extracts. 127
Table B.7. Chemical shifts of peaks detected in ^{31}P-NMR spectra. 128
Table B.8. R-Factors for LCF processing of XANES soil samples. 129
Table B.9. Average $\delta^{18}O_w$ values from collected greenhouse water (± standard error) and average high and low equilibrium values calculated using high and low average greenhouse temperatures. .. 130

List of Figures

Figure 1.1. Phosphorus fluxes in artificially drained agricultural systems.....4
Figure 1.2. Seasonal variation in resin-extractable P-δ18O pools from Angert et al. (2011). 8
Figure 1.3. Map of CAF with sampling points.....13
Figure 1.4. Soil H2O-P concentrations (mg/kg) for CT and NT sites for November 2020 - May 2021. 16
Figure 1.5. Tile drain H_2O-P_{MR} concentrations (mg/L) at CAF for storm and baseline samples from February 2021 - June 2021.....17
Figure 1.6. Average soil P-δ18O values by month for CT and NT side of CAF. Error bars represent standard error from averaged P-δ18O values for each side. 19
Figure 1.7. Monthly P–$\delta^{18}O$ equilibrium values normalized to zero, shown by gray bars, calculated using two-inch soil temperature and standard deviation of $\delta^{18}O_W$ measurements. Normalized deviation of samples was calculated by subtracting the sample P-$\delta^{18}O$ value.....22
Figure 1.8. Correlation between soil H_2O-P_{MR} (mg P/kg) and tile drain H_2O-P_{MR} (mg P/L) concentrations and P-$\delta^{18}O$ value. 25
Figure 2.1. Total organic and inorganic P in soils used in greenhouse pot trials determined by difference of H_2SO_4 extraction of incinerated and non-incinerated soils. Numbers within bars are percent organic P. Error bars denote standard error (n = 5). 63
Figure 2.2. Total phosphorus extracted from soils used in greenhouse pot trial. Error bars denote standard error (n = 5).....68
Figure 2.3. NMR spectra from NaOH-EDTA extracts of soil from all treatments at high application rate. Magnification shows monoester and diester phosphate peaks from PBC-H sample. 70
Figure 2.4. Percentage of P species in NaOH-EDTA extraction and measured using ^{31}P-NMR analysis. Monoester and diester values were corrected for degradation and denoted with "c" prefix. Inorganic P is the sum of the inorganic orthophosphate and polyphosphate compounds. Organic P is the sum of diesters, monoesters, and phosphonates. 72
Figure 2.5. P K-edge XANES spectra for nine standards used in linear combination fitting for soil samples.....77
Figure 2.6. P K-edge XANES spectra for eight samples used in greenhouse pot trials. 79
Figure 2.7. Phosphorus species composition of soil samples used in greenhouse pot trial determined by linear combination fitting of K-edge XANES spectra. Soil phosphorus was fit with phosphorus adsorbed on goethite, apatite, DCDP, DCDP 50:50 Ca:Mg, and phytic acid. 81
Figure 2.8. P-K edge XANES spectra for three biochar amendments used in greenhouse pot trials...82

Figure 2.9. Average isotopic values (± standard deviation) for the Hedley pools for CFH, FSH, control, and untreated soils. Equilibrium range is denoted by gray bar across graph. The total isotopic value for CFH is not reported because of experimental error in extraction. 84

Figure 2.10. Modelled turnover times of P-$\delta^{18}O$ signatures present in the a) H_2O, b) $NaHCO_3$, c) HNO_3, and d) Total extractable soil pools. Points are measured values of P-$\delta^{18}O$ signatures and lines are predictions from the numerical model with average τ calculated for each amendment and for the entire average soil pool. 94

Figure A.1. Precipitation and no till tile drain discharge from the 2018 water year. Dashed line at 0.64 cm is the threshold determined for when to sample storms. 111

Figure B.1. Pearson correlation coefficients for soil properties, plant characteristics, Hedley pool concentrations, total P, and total organic P. 126

Chapter 1: Isotopic Tracing of Phosphorus (P-^{18}O) in Till and No-Till Systems

1.1 ABSTRACT

The buildup of legacy P from fertilization practices continues to impact water quality. Conservation till management reduces soil erosion and particulate bound P losses. However, dissolved P losses increase in the presence of preferential flow pathways, which are kept intact in the absence of tilling. At Cook Agronomy Farm (CAF), surface soils of the toe slope region were determined to be the largest transporters of dissolved P species to the tile drain under no-till management. The objective of this research was to confirm the source and transport of dissolved P species from toe-slope surface soils to the tile drain under no-till and conventional till management using P-δ^{18}O tracing. Isotopic values of tile drain effluent under both management types were similar to toe-slope surface soils under high flow conditions identifying these areas as the main contributors to P in tile drains. Under low flow conditions, isotopic values of tile drain effluent were not similar to isotopic values of toe-slope surface soils under either management type, suggesting that the source and turnover of P changes over the course of the year. These results show that seasonal changes in temperature and precipitation control the source and transport of legacy P from soils to the tile drain.

1.2 INTRODUCTION

1.2.1 Land Management Effects on Phosphorus Fluxes

Phosphorus (P) is an essential element for plant growth as well as a chemical backbone for many fundamental biomolecules. P is often a limiting nutrient in crop yields and is commonly applied as a mineral fertilizer. However 80% of P is sorbed by soil, immobilizing P from plant uptake (Prasad & Chakraborty, 2019). With annual P fertilizer applications nearing five million tons (Mosheim, 2019), the agricultural sector is a primary contributor to nonpoint source pollution of P in surface waters (Jarvie, Sharpley, Withers, et al., 2013; Kleinman et al., 2011; Sharpley et al., 2006). Eutrophication of aquatic systems downstream from agricultural soils with excessive P loading remains a pervasive water quality issue in the US (Sharpley et al., 2006). Additionally, the build-up of legacy P, or the P left sorbed in soils when application is greater than crop uptake, continues to impact water quality after fertilization stops. Although P loss is also influenced by fertilizer application method, rate, source, and timing, as well as hydrological properties and soil type, land management plays a large role in the type of P being lost from a system (Carter, 2005; King et al., 2015; Kleinman et al., 2011). Previous attempts to elucidate P transport response to land management has focused on correlations between concentrations in soil and water. To confirm these results, another method of P tracing is necessary.

Differing management practices in agricultural systems affect soil properties. Tillage, the act of breaking soil for crop growth, helps to prepare seedbeds for planting, suppresses weed growth, and incorporates soil amendments (Carter, 2005). However, tillage decreases soil and surface water quality by increasing erosion and surface runoff, transporting important crop nutrients from soil into nearby waterways (Franklin & Bergtold, 2020). Conventionally tilled systems retain less than 30% crop residue on the soil surface, while conservation till practices retain at least 30% of crop residue on the soil surface, and minimize soil and water losses in comparison to conventionally tilled systems (Carter, 2005). Conservation till mitigates erosion and water losses through increased residue cover and surface organic matter, protecting the soil surface and increasing infiltration from hydrological events (Rust & Williams, n.d.). Reduced till systems may leave up to 30% of harvest biomass as residue on the soil surface (Carter, 2005). No-till management, included in conservation till management, leaves all crop residue on the soil surface after crop harvest, resulting in soil disturbances only to plant, harvest, and apply nutrients to the field. Overall, conservation tillage, or a reduction in tillage disturbances, increases surface soil organic matter (SOM), reduces soil erosion, and increases water infiltration, subsequently reducing surface runoff and the transport of sediment bound nutrients, compared to conventionally tilled counterparts.

In agricultural systems, P generally enters waterways through either surface or subsurface flow. In the first attempts to reduce P loading from agricultural fields, particulate-bound P transported by surface runoff was targeted. By the 1990s, the importance of dissolved phosphorus species began to take hold, as water quality measures had not improved with particulate P reductions (Kleinman et al., 2011). Dissolved species are considered to be highly bioavailable, and are associated with decreasing water quality (Baker et al., 2019; Sharpley & Smith, 1993). Conservation tillage, when implemented in an effort to minimize P loading from nonpoint sources, decreased surface and sediment bound P losses by reducing erosion but increased P losses through subsurface flow (Carter, 2005; King et al., 2015; Kleinman et al., 2011). Under conservation till regimes, P concentrations in surface soils are heightened as fertilizer is broadcast onto the soil surface without incorporation into the soil profile (Sharpley et al., 1994). Additionally, subsurface dissolved P transport is greater under reduced tillage than conventional tillage systems due to an increase in preferential flow pathways (Moore, 2016). In the absence of tillage, macropores (>0.08 mm diameter), formed from earth worm burrows, root channels, and fissures, facilitate the movement of air and water through soil and are left intact (*Soil Quality Indicators*, 2008). Macropores act as preferential flow pathways whereby nutrients rapidly move past the sorption capacity of the soil matrix (King et al., 2015). An increase in labile P in the surface soils, in conjunction with preferential flow pathways that allow P to bypass the sorption capacity of the soil matrix, increases the connectivity between surface soil P and P in

subsurface drainage water (Hooda et al., 2001; Kleinman et al., 2011; Smith et al., 2015; S. Xu et al., 2020). Although conventional till methods reduce macropore connectivity and soil infiltration capacity, leading to a significant decrease in subsurface dissolved P runoff compared to no-till systems, P leached below the root zone in conventionally tilled soil has also been reported to be high (Moore, 2016; Williams et al., 2016).

The accumulation of legacy P reverses the buffering capacity of soils turning them into potential P sources instead of sinks (Kleinman et al., 2011; Sharpley et al., 2009). Though fertilizer predominantly enters the soil in a soluble, plant available, inorganic form, it is not completely taken up by plants due to sorption to soil mineral surfaces and incorporation into soil organic matter (SOM) (Frossard et al., 2000; Shen et al., 2011). Once sorbed, these inputs, which escape initial plant uptake, become legacy P stores, residing in labile and sorbed forms that help to preserve P in the soil solution, as well as in stable forms that are unavailable for plant uptake (Johnston et al., 2014; Negassa & Leinweber, 2009; Rowe et al., 2015). Greater legacy P buildup at the soil surface has been associated with the switch from conventional to conservation tillage due to crop residue breakdown and surface application of fertilizer without incorporation by tillage (Jarvie et al., 2017). Increased legacy P stores, in turn, negate water quality improvements from the implementation of source controls, such as managing soil P inputs (Jarvie, Sharpley, Withers, et al., 2013; Sharpley et al., 2006). Legacy P stores release P as soil P sorption capacities become saturated, redox conditions change, or under changing land management regimes (Jarvie, Sharpley, Spears, et al., 2013). P sorption capacity describes the amount of dissolved P forms soils are able to adsorb (Hooda et al., 2000; Kleinman, 2017). For hydrologically connective soils, the desorption of P from P saturated soils is primarily associated with legacy P losses (Kleinman, 2017; Pionke et al., 2000). Desorption of P from legacy stores makes soil a chronic source of P to waterways, impacting aquatic systems for decades after fertilizer applications are reduced (Figure 1.1) (Hamilton, 2012; Jarvie, Sharpley, Withers, et al., 2013; Kleinman et al., 2011; Meals et al., 2010; Vadas et al., 2018). Legacy P reserves are decreased through crop uptake and biomass removal, and as such reducing legacy P stores is a decades long process (Fiorellino et al., 2017; Vadas et al., 2018). Additionally, this removal process depends on management changes that reduce legacy P stores as well as prevent erosion and runoff losses (Vadas et al., 2018). During this time, legacy P stores can still release P to waterways, stimulating eutrophication (R. McDowell et al., 2020). McDowell et al. (2020) found that, in some areas, legacy P stores could be reduced to agronomic targets in less than one year, while a decrease in the H_2O-P pool associated with runoff could take 25 – 50 years. Thus, managing legacy P stores over many years is necessary for preserving waterway health.

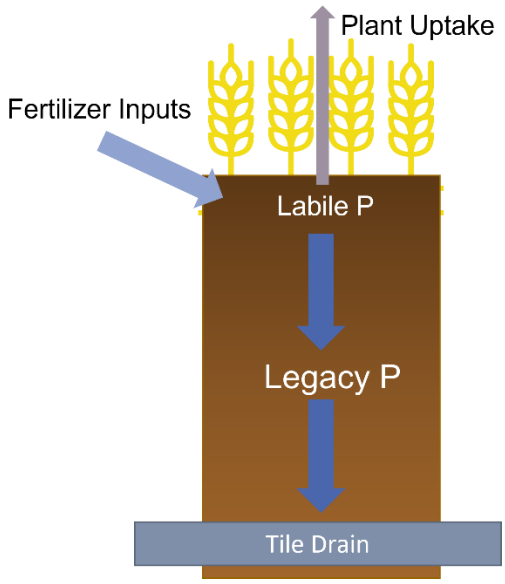

Figure 1.1. Phosphorus fluxes in artificially drained agricultural systems.

Artificial drains are necessary in agricultural systems where excess water hinders crop production. In the Midwest, the environmental impacts of tile drains have been studied extensively (Kleinman, Smith, et al., 2015; Williams et al., 2016). On the Palouse region of Northern Idaho and Eastern Washington, tile drains are commonly found in low-lying regions where they remove excess water and reduce surface ponding. However, tile drains also provide direct transport to waterways, allowing nutrients to circumvent the sorption capacity of the soil matrix (Kleinman, Smith, et al., 2015). Often, these nutrients are exported in a dissolved form, exacerbating eutrophication issues (Baker et al., 2019). Tile drain discharge varies between baseflow and event flow, as well as seasonally. Hydrological response of the artificial drains depends on the amount and intensity of rainfall, initial moisture conditions, and hydrogeology (Macrae et al., 2010; Moore, 2016; Outram et al., 2016; Vidon et al., 2012). During storm events, tile drain discharge tends to increase (King et al., 2015; Vidon et al., 2012). P loading from tile drains can show strong correlations with tile drain discharge, whereby P concentrations increase with an increase in tile drain discharge (Kleinman & Sharpley, 2003; Ortega-Pieck et al., 2020). Similar observations have been made during storm events, although P concentrations do not consistently respond to storm events (Macrae et al., 2010; Williams et al., 2016). In general, the correlation of storm hydrographs and chemographs support the claim that the majority of P loss occurs during peak flows, potentially due to mixing of matrix and macropore flows (King et al., 2015; Moore, 2016; Vidon et al., 2012). Multiple studies have demonstrated that macropore connectivity enhances P loss during storm events (King et al., 2015; Kleinman, Smith, et al., 2015; Williams et al., 2016). Williams et al. (2016) found that dissolved phosphorus

concentrations in tile drain water were elevated during storm events following fertilizer application, although tillage decreased P loading from the tile drain by a factor of nearly four. Artificial drains also vary seasonally in flow rate and dissolved phosphorus output, with the majority of P loss associated with high tile drain flow in cooler, wetter months, often during the non-growing season (King et al., 2015; Macrae et al., 2010; Ortega-Pieck et al., 2020). In much of the United States, this corresponds with the months between October and May, when large volumes of water flows through tile drains due to greater moisture in the soil profile.

1.2.2 Isotope Tracing

To understand the impact of P fertilization levels and legacy pools a means of tracing P through the system is needed. The oxygen stable isotope of orthophosphate has been proposed for this purpose. Carbon (C) and nitrogen (N) isotope tracing has been used to track transfers of elements between pools and to understand the processes that mediate the transfers (Amundson et al., 2003; Brüggemann et al., 2011). To identify sources of P to ecosystems, the use of oxygen isotope ratios ($\delta^{18}O$) from orthophosphate (PO_4), the most prevalent form of P in soil, is used. While phosphorus only has one stable isotope, ^{31}P, oxygen has three (^{16}O, ^{17}O, and ^{18}O), allowing isotopic ratios to be calculated between the two most abundant isotopes, ^{16}O and ^{18}O, that are bound to P in soil (Equation 1.1). The international standard value used for oxygen is the Vienna Standard Mean Ocean Water (VSMOW). In isotopic notation, a positive value indicates the sample is enriched with the heavier isotope compared to the standard, while a negative isotopic value indicates a lighter isotopic composition compared to standard values.

$$\delta^{18}O = \left(\frac{(\frac{^{18}O}{^{16}O})_{\text{sample}}}{(\frac{^{18}O}{^{16}O})_{\text{standard}}} - 1 \right) * 1000 \qquad \text{Equation 1.1}$$

The P-O bonds in orthophosphate are stable against hydrolysis at low pH and have little isotopic exchange with oxygen (O) in water at ambient temperatures (Blake et al., 2005; Tonderski et al., 2017). In principle, P-$\delta^{18}O$ isotopic signals, which vary by source, remain constant, except in the presence of microbial enzymes and fluctuating soil water signals. Microbial enzymatic processes can shift the isotopic signal toward an equilibrium with the oxygen of soil water through intracellular and extracellular enzymatic reactions, overwriting the phosphorus source signature (Blake et al., 2005). When mineralized, P_i is kinetically fractionated resulting in values lower than the original source signature and equilibrium (Liang & Blake, 2009). Microbial enzymatic reactions are a form of kinetic isotope fractionation, whereby the lighter isotopic form of orthophosphate (P-$\delta^{16}O$) is preferentially

bound to the microbial enzyme resulting in a remaining soil P pool that is isotopically heavier. Intracellular cycling is mediated by the pyrophosphatase enzyme which catalyzes the hydrolysis of the phosphoester bond in phosphate, leading to a temperature-dependent equilibrium with the oxygen isotope of ambient water (Blake et al., 2005). This equilibrium exchange was first predicted using the empirical equation (Equation 1.2) from Longinelli and Nuti (1973) as a paleoclimate indicator for biogenic phosphate minerals, where T is the average temperature in °C during the duration of the sample collection and $\delta^{18}O_W$ is the oxygen isotope signature of water (‰).

$$P\text{-}\delta^{18}O = \frac{111.4 - T}{4.3} + \delta^{18}O_W \qquad \text{Equation 1.2}$$

Chang and Blake (2015) defined a new experimentally-determined equilibrium equation (Equation 1.3) for temperatures from 3-37°C, which offsets the Longinelli and Nuti (1973) equation by +0.5 to 0.7‰. This new equilibrium equation is based on dissolved inorganic phosphate equilibration with water, making it more applicable to water quality studies.

$$\delta^{18}O = e^{\left(\frac{14.43}{T} - \frac{26.54}{1000}\right)} * (\delta^{18}O_W + 1000) - 1000 \qquad \text{Equation 1.3}$$

In Equation 1.3, T is temperature in Kelvin.

Only a handful of studies have used P-δ^{18}O to trace P through different matrices and systems. These studies tend to have low sample size, little spatial or temporal variation, and apply various sample extraction methods, highlighting the complexities of using P-δ^{18}O as a tracing method. Recent studies attempted to use P-δ^{18}O values to differentiate between effluent from wastewater treatment plants and P fertilizers (Gruau et al., 2005; Young et al., 2009), as well as signatures of various parent materials and soil phosphorus pools (Table 1.1) (Angert et al., 2012; Elsbury et al., 2009; McLaughlin et al., 2004; Tamburini et al., 2014; Zohar et al., 2010). Although overlap in P-δ^{18}O values between P sources is evident, statistical differences in the isotopic ratios of multiple sources in several fresh water systems where P-δ^{18}O values were not in equilibrium with water have been reported, allowing P-δ^{18}O values to be used as tracers in some systems (Elsbury et al., 2009; Young et al., 2009). Additionally, Tonderski et al. (2017) found significant differences between stream water P-δ^{18}O values and equilibrium values in an agricultural catchment, suggesting that isotope ratios may be preserved in streams with short residence times.

Hydrological dynamics have a notable impact on seasonal and spatial variability of P-δ^{18}O values, as preferential flow pathways help preserve isotopic signatures in drain effluent by allowing

water to bypass plant uptake (Ford et al., 2018; King et al., 2015; Tonderski et al., 2017). Angert et al. (2011, 2012) reported that fractionation and equilibration in plant leaves may create litter that is up to 25‰ heavier than those in soils, influencing P-$\delta^{18}O$ values in soil pools when organic P (P_o) from the litter is converted into an inorganic form. Still, the efficacy of using phosphate as a source tracer is often debated. Gruau et al. (2005) discouraged the use of isotopic ratios as source tracers when attempting to distinguish two sources with similar P-$\delta^{18}O$ values or if source P-$\delta^{18}O$ values overlap with equilibrium values.

Table 1.1. P-$\delta^{18}O$ of various sources and pools from Tamburini et al. (2014).

Type	Material	Min. ^{18}O-P	Max. ^{18}O-P	Reference
		‰†		
Lithogenic material	carbonatite	0.2	10	Mizota et al., 1992
	hydrothermal	2.4	12.2	Mizota et al., 1992
	volcanic ash	5.3	6.2	Mizota et al., 1992
	silt	8.6	16.9	Markel et al., 1994
	sand	9.1	12.8	Markel et al., 1994
	clay	12.7	22.5	Markel et al., 1994
	aerosol (Israel)	14.2	24.9	Young et al., 2009
	phosphate rock	16.7	19.1	Ayliffe et al., 1992
	phosphorite (Florida)	17.2	23.2	Gruau et al., 2005
	phosphorite (Morocco)	18.5	20.5	Gruau et al., 2005
	dust (Israel)	19.5	22.6	Gross et al., 2013
	calcarenite	20.1	22.8	Ayliffe et al., 1992
	Santa Barbara sediment	21		McLaughlin et al., 2006c
Soil pools	HCl-P	5.6	17.8	Zohar et al., 2010b
	HCl-P	6	15.1	Tamburini et al., 2012b
	NaOH-P	7.8	22.5	Zohar et al., 2010b
	HCl-P	8.2	21.3	Angert et al., 2012
	Acetic acid-P	10.1	20.6	Mizota et al., 1992
	Bray-P	10.6	24.3	McLaughlin et al., 2006a
	H_2O-extractable P	10.7	24.5	Zohar et al., 2010b
	Microbial P	11.2	17.8	Tamburini et al., 2012b
	HNO_3–P	11.7		McLaughlin et al., 2006c
	Resin-P	12.7	19.8	Tamburini et al., 2012b
	NH_4F-P	12.7	24.8	Mizota et al., 1992
	Resin-P	14.5	19.1	Angert et al., 2011
	Resin-P	14.5	20	Angert et al., 2012
	HCl-P	16.1	16.9	Angert et al., 2011
	Resin-P	17.4	22.8	Gross et al., 2013
	HNO_3–P	19	27	McLaughlin et al., 2006a
	$NaHCO_3$–P	19	23.7	Zohar et al., 2010b
Phosphate in organic material	vegetation (TCA‡ extract)	12.4	31.4	Tamburini et al., 2012b
	vegetation (H_2O extract)	14.2	23.1	Young et al., 2009
	animal feces	15.7	18.3	Young et al., 2009
	soybean leaves (TCA extract)	16.9	27.5	Pfahler et al., 2013
	ivory and skulls	18.6	24	Mizota et al., 1992
	guano	19.8	23.1	Ayliffe et al., 1992
	humus	21.8		Ayliffe et al., 1992
	plankton	22.9	23.4	McLaughlin et al., 2006c
	algae	27.6	28.6	McLaughlin et al., 2006c
	soybean leaves (HNO_3 extract)	42.6	57.1	Pfahler et al., 2013
Industrial products	detergent	13.3	18.6	Young et al., 2009
	fertilizers	14.8	27	McLaughlin et al., 2006a
	fertilizers	15.5	22.3	Young et al., 2009
	toothpaste	17.7		Young et al., 2009
	fertilizers	19.6	23.1	Gruau et al., 2005
Waters	marine waters (San Francisco Bay)	7.8	20.1	McLaughlin et al., 2004, 2006b
	wastewater treatment plant	8.4	14.2	Young et al., 2009
	river and groundwater	9.2	16.4	Young et al., 2009
	Lake Erie waters (surface)	9.7	17.1	Elsbury et al., 2009
	river water (California)	14.1	20.3	McLaughlin et al., 2006a
	discharge water (France)	16.6	18.4	Gruau et al., 2005
	open ocean (Pacific)	18.6	22	McLaughlin et al., 2004

† With respect to Vienna Standard Mean Ocean Water.
‡ TCA, trichloroacetic acid.

Isotopic values also vary temporally (Figure 1.2). Equilibrium values for rapidly cycled soil pools can vary seasonally due to changes in soil temperature, while stable pools may trend toward the isotopic signature of parent material (Angert et al., 2012), or towards equilibrium values (Angert et

al., 2011; Tamburini et al., 2010; Zohar et al., 2010). The trend towards equilibrium for stable P pools may be from the redistribution of biologically cycled P from more available pools to the stable pool (Joshi et al., 2016). Stable pools nearing equilibrium is not indicative of bioavailability or of microbial cycling within the pool, but from precipitation of P from the preceding pools, whose isotopic values have been mediated by microbial cycling (Joshi et al., 2016). Often, periods that correspond with high flow events from snow runoff and rainfall events may also correspond with low biological activity, such as autumn and spring, preserving isotopic signatures (Tonderski et al., 2017). However, Tonderski et al. (2017) also found that water samples collected during a peak flow event from snowmelt had an isotopic value in equilibrium, potentially due to a buildup from microbial P turnover. Angert et al. (2011) suggests that the rate of change to equilibrium is dependent on biological activity, which slows during the drier conditions that can occur during summer months in Mediterranean climates.

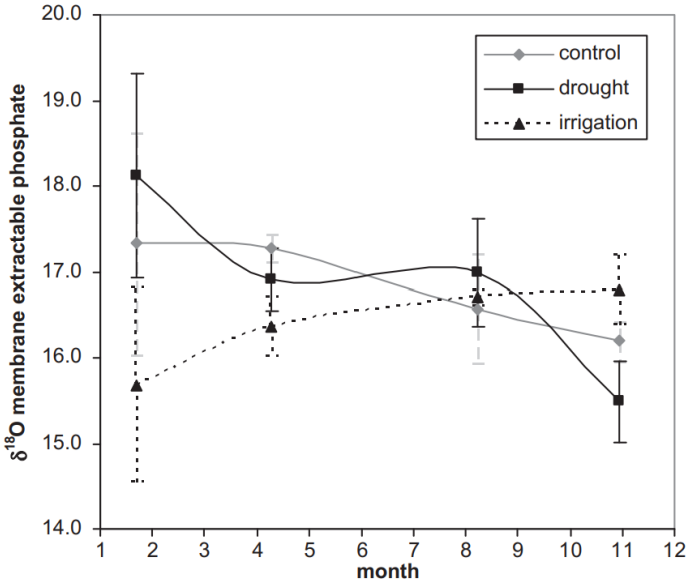

Figure 1.2. Seasonal variation in resin-extractable P-δ18O pools from Angert et al. (2011).

In addition to seasonal variation, isotopic signatures in runoff may vary over the duration of events. Ford et al. (2018) found that in an agricultural field with large available P stores, tile drain P-$\delta^{18}O$ dynamics varied over the course of a storm event. Despite not being fertilized in the previous decade, P-$\delta^{18}O$ values of water extractable P (H_2O-P) in the surface soil from the study differed from the predicted equilibrium value, implying that this P pool had not been completely cycled by microorganisms and may be transporting legacy P. At the beginning of a storm event, tile drain effluent P-$\delta^{18}O$ values were at the soil-water equilibrium value. However, during peak flow and soon after the conclusion of the event, P-$\delta^{18}O$ values from the tile drain rose from equilibrium to values

near the P-$\delta^{18}O$ of H_2O-P_i soil values (Ford et al., 2018). Gooddy et al. (2016) also found variable P-$\delta^{18}O$ values dependent on flow conditions, which could be due to changes in stream equilibrium values at low and high flow. Previous studies found that the H_2O extractable P-$\delta^{18}O$ approached isotopic equilibrium within 30 – 150 days (Joshi et al., 2016; Zohar et al., 2010). On the other hand, when the system is not P-limited, source signature in the H_2O-P pool may be preserved (Ford et al., 2018; Gross et al., 2015). Ford et al. (2018) suggests that enriched P-$\delta^{18}O$ signatures in long-term fertilized soils were evidence of legacy P stores. Additionally, the authors proposed that legacy P transport occurred during and after a storm event based on the correlation of P-$\delta^{18}O$ signatures in the H_2O-P soil pool and tile drain effluent (Ford et al., 2018). Gross et al. (2015) found that bioavailable P in plots receiving recurrent P applications only slightly diverged from the isotopic value of added P, while plots without a history of P application converged to equilibrium, suggesting that microbial turnover rates are slower when microbial growth is not P limited. So, in areas with high P content, P-$\delta^{18}O$ signatures may be preserved and traceable.

Currently, multiple methods are available for determining P-$\delta^{18}O$ values for different matrices, e.g., water, soil, and seawater, making it difficult to determine the best way to prepare and analyze samples. Originally, P crystals were precipitated as bismuth phosphate ($BiPO_4$), a hygroscopic material that required large amounts of precipitates to analyze, that then underwent fluorination or bromination to release oxygen for analysis (Tamburini et al., 2014). Halogenation of $BiPO_4$ required hazardous materials and resulted in low O_2 yields from large sample sizes (Davies et al., 2014). Silver phosphate (Ag_3PO_4) precipitation is now the most widely used method for phosphate analysis due to a large number of improved extraction protocols for a variety of sample types (McLaughlin et al., 2004; Nisbeth et al., 2019; Tamburini et al., 2010; T. Weiner et al., 2011; Z. Xu et al., 2018; Zohar et al., 2010). A wide range of extraction steps are needed for Ag_3PO_4 precipitation due to the heterogeneity of sample matrices. Furthermore, manipulation of published procedures to fit samples is often required, resulting in numerous extraction methods for all sample types (Tamburini et al., 2014).

1.2.3 Research Gaps

The R.J. Cook Agronomy Farm (CAF) in the Palouse region of eastern Washington is a Long Term Agroecological Research (LTAR) site owned by Washington State University and managed in conjunction with the United States Department of Agriculture Agricultural Research Service (USDA-ARS). Since 1998, the farm has operated on a three-year crop rotation with a goal of producing continual cereal crops without using conventional till methods. Intensive tillage practices on the rolling hills of the Palouse have led to high erosion rates and movement of topsoil. Erosion rates drove many farmers in the region to adopt conservation till practices, reducing the amount of topsoil

lost but increasing preferential flow pathways (Brooks et al., 2012; Montgomery et al., 1999; *Palouse Co-Operative River Basin Study*, 1978). Although no total maximum daily load (TMDL) for P exists for the region in Washington that contains CAF, a TMDL of 0.10 mg/L total phosphorus (TP) is established across the border in Idaho for the South Fork of the Palouse River (Idaho Department of Environmental Quality, 2016). Dissolved phosphorus in tile drain effluent at CAF continues to exceed the Idaho TMDL during high water flow months, even with the cessation of fertilizer application (I. Leslie, personal communication, November 20, 2020; Ortega-Pieck et al., 2020). The majority of dissolved phosphorus in tile drain effluent is assumed to originate from the H_2O-P pools from the 0-10 cm depth of the toe slope area on the no till side of the system, implying that "P hotspots" exist at the toe slope (Ortega-Pieck et al., 2020). Toe slope areas accumulate P throughout the growing season and through long-term deposition processes (Burke et al., 1995; Schlatter et al., 2019). These pools are flushed during snowmelt and rainfall events, releasing large amounts of dissolved P to the tile drain, potentially due to connectivity of surface soils with high P concentrations and the tile drain resulting from preferential flow. Under high flow, large amounts of nitrate and dissolved organic matter are also transported through artificial drain lines at CAF (Bellmore et al., 2015; Keller et al., 2008; Kelley et al., 2017). Although the increase in P loading in tile drain flow under high flow is most likely due to surface P sources being transported to tile drains through preferential flow pathways, the mechanisms of transport are not well understood. By analyzing P-$\delta^{18}O$ values from soil H_2O-P, baseline tile drain flow, and storm event tile drain flow, we hope to understand the seasonal dynamics of subsurface transport of P from soil to waterways. This helps to bridge gaps in the current understanding about leaching potential from land management regimes and the effects of long-term fertilizer use on phosphorus in subsurface runoff.

Though much progress has been made on PO_4^{3-} precipitation methods, cycling extent, and potential sources, using oxygen isotopes as phosphate tracers in agroecosystems is still a recent field of study with only limited temporal and spatial applications. For example, Joshi et al (2016) and Zohar et al (2010) applied phosphate treatments directly to plots and measured isotopic signatures only within one growing season. Tian et al (2016) determined P-$\delta^{18}O$ values for multiple soil P pools in an agricultural field, but did not characterize surface or subsurface flow dynamics (Tian et al., 2016). Many studies have characterized P-$\delta^{18}O$ values that have a low potential for leaching, thus not capturing the transport of the most available P from land to waterways (Granger et al., 2017; Gross & Angert, 2015). Finally, multiple studies are based in large watersheds with many P inputs, making it difficult to determine specific source areas (Ishida et al., 2019; Tonderski et al., 2017). To our knowledge, the Ford et al. (2018) study is the first and only to attempt to capture $\delta^{18}O$ values in an agricultural catchment during precipitation events.

1.2.4 Research Goals

The goal of this research was to understand differences in subsurface phosphorus transport from soils to tile drains under different land management practices during baseline flow and during precipitation events using isotopic analysis. To achieve this goal, our objective was to determine seasonal P soil sources to the watershed in conventional and no till agricultural systems at Cook Agronomy Farm using P-$\delta^{18}O$ as a tracer for phosphate transport from the soil to subsurface flow. To accomplish this objective, we analyzed the isotopic values of soil and water samples at CAF from November 2020 to June 2021. We hypothesized that land management effects would be the largest driver of P-$\delta^{18}O$ transport at CAF due to the increased presence of preferential flow pathways under conservation tillage.

1.3 MATERIALS & METHODS

1.3.1 Site Background

CAF is a paired watershed site, with fields under conventional and conservation till management. 370 georeferenced locations across the site are used for research on soil type, nutrients, and water distribution (*Research at Cook Agronomy Farm*, n.d.). Annual average precipitation on the Palouse from 1981-2010 was 520 mm, with most occurring in the fall and winter months (*Cooperative Climatological Data Summaries. PULLMAN 2 NW, WASHINGTON (456789)*, 2021). Artificial drain lines, located about one meter below the surface on both sides of the farm, divert up to 24% of annual precipitation (Kelley et al., 2017). Additionally, Keller et al (2008) suggested that 150 mm of precipitation, typically occurring in January and February, is needed to overcome the discharge threshold of the tile drain and increase flow through the drains. Water flow from artificial drain lines is measured using 1-inch Parshall flumes at drain tile outlets and automated ISCO water samplers. Although no total maximum daily load (TMDL) for P exists for the region in Washington that contains CAF, a TMDL of 0.10 mg/L total phosphorus (TP) is established across the border in Idaho for the South Fork of the Palouse River (Idaho Department of Environmental Quality, 2016). The artificial tile drain outlet at CAF discharges into Missouri Flat Creek, which eventually drains into the South Fork of the Palouse River in Pullman, WA. Dissolved phosphorus in tile drain effluent at CAF continues to exceed the Idaho TMDL during high water flow months, even with the cessation of fertilizer application (I. Leslie, personal communication, November 20, 2020; Ortega-Pieck et al., 2020). Available P from the 0-10 centimeter depth is proposed to be the main sources of dissolved P to the tile drain outlet in the no-till catchment (Norby, 2018; Ortega-Pieck et al., 2020).

1.3.2 Soil and Water Sampling

Three points along the toe slope on the conventional till (CT1, CT2, CT3) and no till (NT1, NT2, NT3) side of CAF were chosen from existing georeferenced locations that have been identified as contributors of P to tile drain outlets and to represent variability along the toe slope region (Figure 1.3). Six soil subsamples were taken from 0 to 10 cm depth within a 1.5 m diameter area around each of the georeferenced points and composited to form a representative sample of the area. These points were sampled three times to represent seasonal variation (November/December, March, and May). Soil H_2O-P was determined by shaking soil samples at 100 rotations per minute in a 1:10 solid:solution ratio using deionized water for one hour following the Self-Davis method (Self-Davis et al., 2000). Debris was removed by hand before shaking. Samples were filtered through a 0.45 μm polyether sulfone (PES) membrane filter before determining molybdate reactive phosphorus (H_2O-P_{MR}) colorimetrically at 880 nm and total filterable phosphorus (H_2O-P_{TF}) concentrations by inductively coupled plasma – optical emission spectrometry (ICP-OES) were also analyzed. H_2O-P_{TF} is total dissolved phosphorus in the sample and includes H_2O-P_{MR} and molybdate unreactive phosphorus (H_2O-P_{MU}). H_2O-P_{MR} is an estimation of inorganic P in solution, however due to hydrolysis of P_o and incomplete reactions with some inorganic compounds, it may not be entirely P_i species (Haygarth & Sharpley, 2000). H_2O-P_{MU} is considered to be organic, colloidal, and non-hydrolysable forms of P (Haygarth & Sharpley, 2000). Two samples were extracted in triplicate for H_2O-P_{MR} (RSD ranged from 1.12 – 3.97%) and H_2O-P_{TF} (RSD ranged from 1.73 – 2.65%). Quality control standards were also included in the analysis for H_2O-P_{MR} (RSD = 0.57%) and H_2O-P_{TF} (RSD = 0.59%).

Baseline water samples were taken about once per month from February to June. Only storm events generating at least 0.64 cm of precipitation were sampled. This threshold value is based on hydrographs from previous years. After receiving over 0.64 cm of precipitation, discharge from the no till tile drain increased in less than 24 hours (Appendix Figure A.1). Using Pearson correlation coefficients of storm precipitation and tile drain flow, we determined that tile drain flow increased within the same 24-hour period as precipitation fell. Water was collected from tile drains using peristaltic pumps with acid-washed nylon tubing and collected in acid-washed 5-gallon buckets. 15 gallons of water were collected at each sampling event. Water samples were analyzed for P concentration as both H_2O-P_{MR} using spectrophotometry at 880 nm and H_2O-P_{TF} using ICP-OES. Samples were used for isotopic extraction within 48 hours of collection. If sample extraction did not begin within 2 hours of collection, samples were stored at 4°C for up to 48 hours.

Precipitation samples were collected about once every two weeks from January through June to use for $\delta^{18}O_w$ values for equilibrium calculations. These samples were analyzed using a cavity ring

down spectrometer (CRDS) (Picarro, Santa Clara, CA). USGS 45 and USGS 46 were used as internal standards. Internal standard deviation of the samples was 0.5‰.

Figure 1.3. Map of CAF with sampling points.

1.3.3 P-$\delta^{18}O$ Extraction of Soil and Water

A modified Nisbeth et al. (2019) protocol was used to extract silver phosphate (Ag_3PO_4) crystals from the soil and water samples. This method was developed for use in freshwater systems and results in the precipitation of Ag_3PO_4. Due to the nature of our matrix, an organic matter removal step (DAX-8) was added to the protocol, as per Tamburini et al. (2010). The complete method can be found in Appendix A. In short, magnesium-induced co-precipitation of brucite (MagIC) adsorbs P from the sample solution, reducing sample size. Dissolved organic matter is removed using DAX-8 resin, followed by removal of contaminants soluble at low pH through ammonium phospho-molybdate (APM) precipitation and removal of contaminants soluble at high pH by magnesium ammonium phosphate (MAP) precipitation. Finally, cations are removed through a cation resin wash and residual chloride ions are removed with silver nitrate ($AgNO_3$). Silver ammine solution is added to facilitate the precipitation of Ag_3PO_4. Precipitated crystals are rinsed with deionized water and dried before analyzing using a high temperature conversion elemental analyzer coupled to a Delta V Advantage continuous flow isotope ratio monitoring mass spectrometer (TCEA-IRMS) (Thermo Fisher Scientific, Waltham, Massachusetts). Ag_3PO_4 and benzoic acid standards (ThermoFisher Scientific, Waltham, Massachusetts and HEKAtech GmbH, Wegberg, Germany) were used to calibrate samples. Internal standard deviation of standards was 0.4‰, leading us to assume that differences of greater than 0.4‰ were not due to instrument variation. The measured P-$\delta^{18}O$ values are reported relative to Vienna Standard Mean Oceanic Water (VSMOW) in per mil (‰) notation.

1.3.4 Statistical Analysis

Data analysis was performed using R version 4.1.2 (R Studio Team, 2020). Statistical analysis on soil H_2O-P_{TF}, H_2O-P_{MR}, and P-$\delta^{18}O$ values were analyzed in a linear mixed effect model with site (NT or CT) and month of sampling as fixed effects and sample position in the field as a random effect. Model fit was assessed by examining log-likelihoods and examining residual plots. Package "nlme" (Pinheiro et al., 2022) was used for model building and ANOVA. Means comparisons were performed using R package "emmeans" (Lenth et al., 2022). Significance was determined at a $p < 0.05$ using a Tukey test.

1.4 RESULTS

1.4.1 Phosphorus concentrations in soil and tile drains at CAF

Soil H_2O-P_{TF} values at CAF varied by site ($p = 0.0567$) and by date ($p = 0.0056$) (Table 1.2, Table A.1, Table A.2, and Figure 1.4). In November/December, H_2O-P_{TF} was greater in NT soils than CT soils ($p = 0.0432$). Similarly, in February, H_2O-P_{TF} in NT soils was again greater than CT soils ($p = 0.0697$). In May, as the growing season began, there was no significant difference between H_2O-P_{TF} concentrations in NT and CT soils ($p = 0.2459$). H_2O-P_{MR} concentrations also varied by site ($p = 0.070$) (Table 1.2, Table A.1, Table A.3, and Figure 1.4). In November/December, the NT side had greater H_2O-P_{MR} than CT ($p = 0.0375$). In February and May, H_2O-P_{MR} concentrations were not significantly different by site. The amount of H_2O-P_{MR} in the total filterable pool ranged from 45% to 100%. Average percentage of H_2O-P_{TF} that is H_2O-P_{MR} was 70% for NT and 71% for CT.

Table 1.2. Water-extractable phosphorus values for monthly soil samples.

Month	Sample	H_2O-P_{TF} (mg/kg)	H_2O-P_{MR} (mg/kg)	H_2O-P_{MU} (mg/kg)
November/December	NT1	8.06	4.71	3.35
	NT2	10.24	7.00	3.24
	NT3	11.55	9.57	1.98
	CT1	6.01	2.72	3.29
	CT2	7.64	4.54	3.1
	CT3	3.29	2.65	0.64
February	NT1	7.78	4.03	3.75
	NT2	10.06	5.31	4.75
	NT3	10.73	6.28	4.45
	CT1	6.59	3.09	3.5
	CT2	7.95	5.33	2.62
	CT3	3.09	1.77	1.32
May	NT1	5.46	4.53	0.93
	NT2	5.95	5.35	0.6
	NT3	5.99	5.11	0.88
	CT1	4.12	4.47	0
	CT2	5.56	4.41	1.15
	CT3	1.75	2.00	0

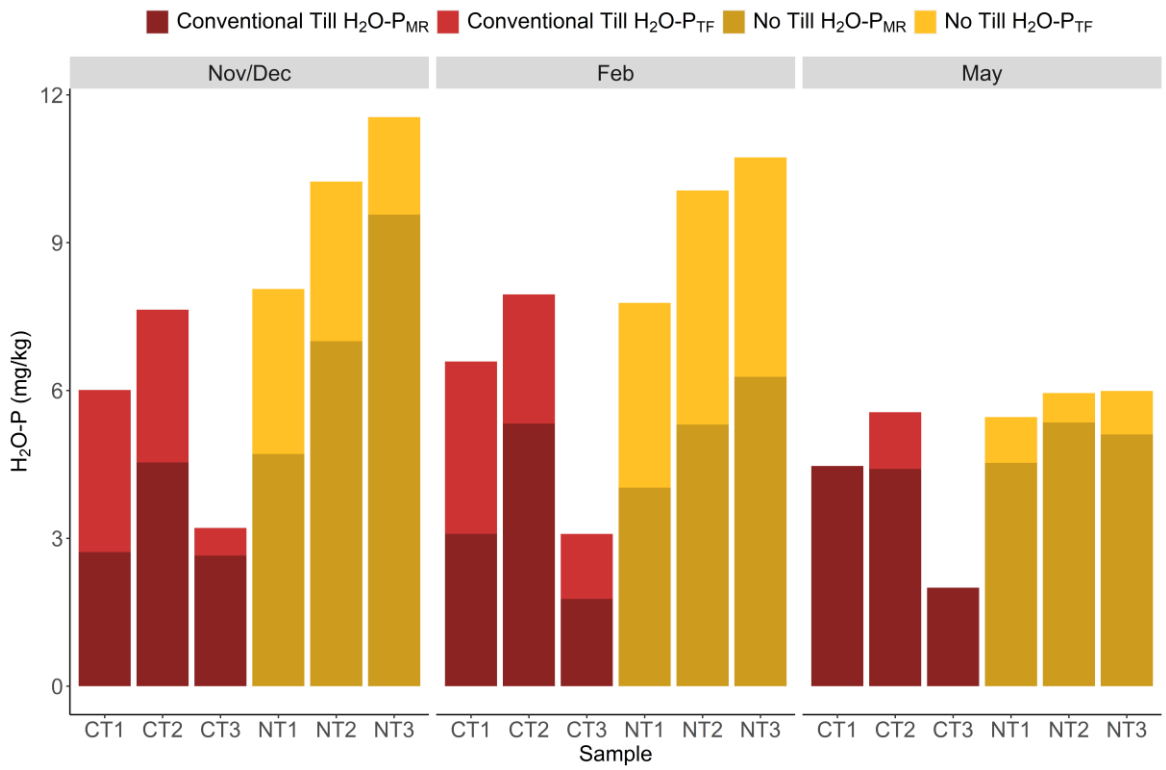

Figure 1.4. Soil H2O-P concentrations (mg/kg) for CT and NT sites for November 2020 - May 2021.

Tile drains at CAF began flowing in January 2021. The first tile drain sample was collected in February 2021. Over the course of the sampling season, tile drain $H_2O\text{-}P_{MR}$ concentrations ranged from 0.047 mg P/L to 0.093 mg P/L. Samples did not exceed the 0.1 mg P/L Idaho TMDL for the Palouse region, although most samples had an $H_2O\text{-}P_{TF}$ P concentration of greater than 0.05 mg P/L (Table 1.3 and Figure 1.5).

Table 1.3. H_2O-P_{MR} concentrations (mg/L) for tile drain samples.

Month	Site	Sample Type	H_2O-P_{MR} (mg/L)
February	CT	Baseline	0.064
	CT	Storm	0.47
	NT	Storm	0.073
March	CT	Baseline	0.063
	NT	Baseline	0.067
April	CT	Baseline	0.074
	NT	Baseline	0.063
May	CT	Baseline	0.093
	NT	Baseline	0.056
June	NT	Baseline	0.076

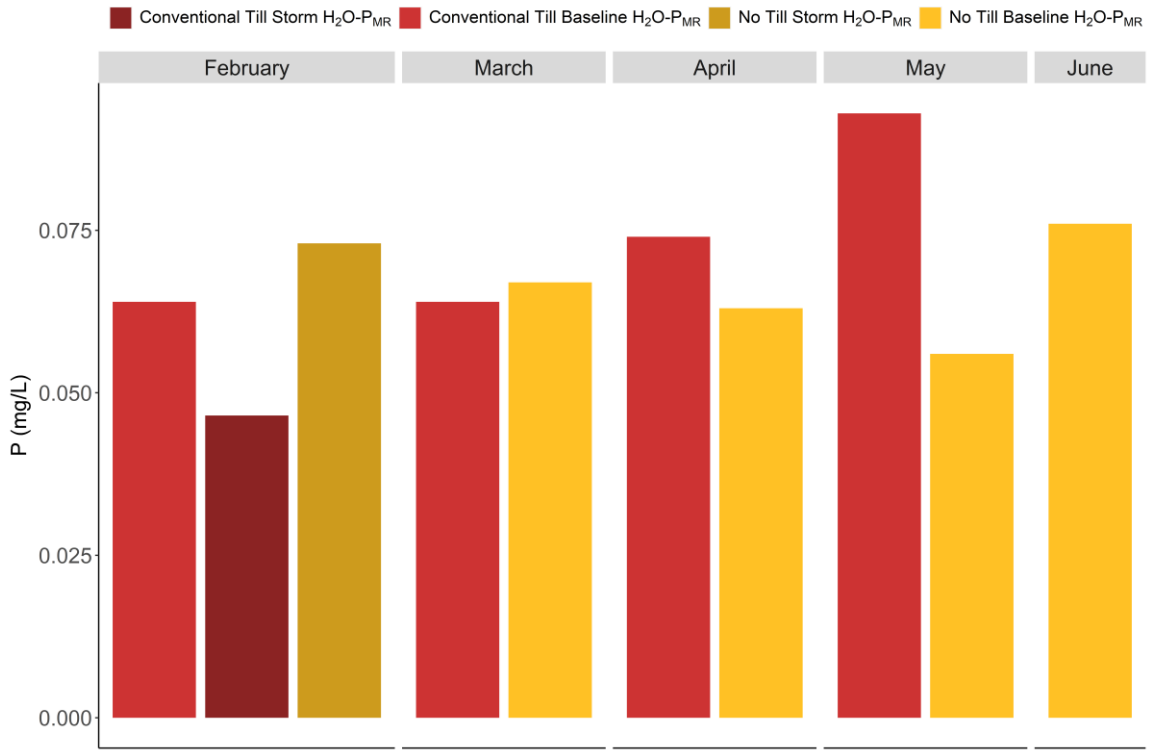

Figure 1.5. Tile drain H_2O-P_{MR} concentrations (mg/L) at CAF for storm and baseline samples from February 2021 - June 2021.

1.4.2 P-$\delta^{18}O$ dynamics at CAF

The calculation of a microbially-mediated equilibrium range over the sampling season helped to determine seasonal cycling and deviation of P-$\delta^{18}O$ signatures of soil and water P. The equilibrium range was calculated using collected precipitation from the site for $\delta^{18}O_w$ and high and low average temperatures from 2 inches below the soil surface. Calculated average equilibrium values for

November to June ranged from 10.2 – 16.4‰ (Table 1.4). Equilibrium values increased with increasing temperature and more enriched $\delta^{18}O_w$ samples, such as those coming from rain instead of snow (*Isotopes-Oxygen 18*, n.d.). The month of December had the highest equilibrium value, 1.5‰ above the other months, due to enriched $\delta^{18}O_w$ values.

Water extractable soil P-δ^{18}O signatures for the six georeferenced points at CAF remained enriched compared to equilibrium values across the sampling season. Soil P-δ^{18}O signatures varied slightly by catchment ($p = 0.0816$), with more enriched P-δ^{18}O signatures on the NT side of the farm, mostly in the month of May ($p = 0.0254$) (Table A.1 and Table A.4). Differences in soil P-δ^{18}O values between the CT and NT sides of the farm during November/December and May were not significantly different. NT soil samples ranged from 15 – 18.6‰ over the sampling season, with values 2.4 – 7.3‰ above the corresponding monthly equilibrium values (Table 1.4, Figure 1.6, and Figure 1.7). Similar values were present on the CT side, with a range from 14.1 – 16.7‰, with an enrichment from 0 – 6.3‰ compared to equilibrium (Table 1.4, Figure 1.6, and Figure 1.7). Because the December equilibrium value was much greater compared to other months, the December CT soil samples fell into the equilibrium range, although actual P-δ^{18}O values were similar to other soil samples.

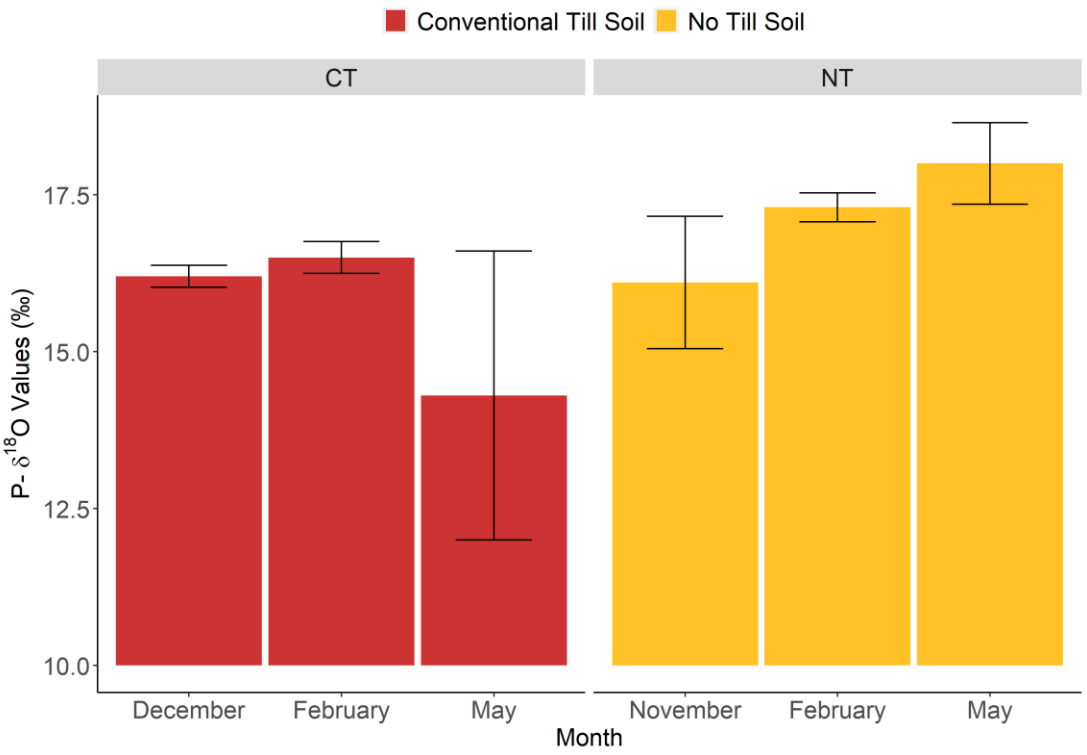

Figure 1.6. Average soil P-δ18O values by month for CT and NT side of CAF. Error bars represent standard error from averaged P-δ18O values for each side.

Baseline tile drain water samples on the conventional till side of the farm ranged from 13.1‰ to 15.4‰, with a deviation from equilibrium of 1.3‰ to 4.1‰ (Table 1.4 and Figure 1.7). In February, March, and May, CT tile drain baseline (CT TD BL) samples were above the equilibrium value. In April, the CT tile drain baseline sample was below equilibrium, although the sample value only varied from the March and May samples by 0.1 -0.4‰. NT baseline tile drain (NT TD BL) water samples were collected in March and June, with values of 13.4‰ and 10.8‰, with deviation from equilibrium ranging from 1.1‰ to -1.7‰, respectively (Table 1.4 and Figure 1.7). Storm samples were collected in February (16.7‰) and March (12.7‰) with a deviation from equilibrium of 6.3‰ and 0.2‰, respectively. In March, a drought began on the Palouse; precipitation from March to May decreased by up to 85% of average precipitation values. Thus, sampling storm events was not possible.

In February, tile drain samples on both sides of the farm had the greatest deviation from equilibrium at baseline flow and during storm events. The CT baseline tile drain sample in February was 4.1‰ enriched compared to equilibrium, while the storm (CT TD S) sample was 6.3‰ enriched compared to equilibrium. Additionally, the storm and baseline samples deviated from CT soil samples collected in February by 0.2‰ and 1.0‰, respectively. The NT tile drain storm (NT TD S) sample for February deviated from equilibrium by 5.3‰ and from NT surface soil values by 1.6‰. In March,

baseline and storm tile drain P-$\delta^{18}O$ values for both NT and CT trended towards equilibrium values. NT baseline and storm samples deviated from equilibrium by 1.1‰ and 0.2‰, respectively while the CT baseline sample deviated from equilibrium by 1.3‰. Tile drain samples collected from March until June did not trend towards surface soil values, and only deviated from equilibrium by 0.7‰ to 1.7‰. Because the internal standard deviation of our instrument was 0.4‰, we assume that this difference is due to real variation at CAF.

Table 1.4. Soil and tile drain P-$\delta^{18}O$ signatures. Equilibrium range for each month located underneath month. Baseline tile drain samples are denoted by TD BL. Storm tile drain samples are denoted by TD S.

Month (Equilibrium Range)	Type	Point	Value (‰)	Dev. from equilibrium (‰)
November (12.4‰ ± 0.2)	Soil	NT1	15	2.4
		NT2	16.2	3.6
		NT3	17.1	4.5
December (16.1‰ ± 0.3)	Soil	CT1	16.3	0
		CT2	16.3	0
		CT3	16	0
February (10.3‰ ± 0.1)	Soil	NT1	17.2	6.8
		NT2	17.2	6.8
		NT3	17.6	7.2
		CT1	16.4	6.0
		CT2	16.7	6.3
		CT3	16.2	5.8
	Water	CT TD BL	14.5	4.1
		CT TD S	16.7	6.3
		NT TD S	15.7	5.3
March (12.0‰ ± 0.3)	Water	NT TD BL	13.4	1.1
		NT TD S	12.5	0.2
		CT TD BL	13.6	1.3
April (14.6‰ ± 0.3)	Water	CT TD BL	13.2	-1.1
May (12.3‰ ± 0.1)	Soil	NT1	18.6	6.2
		NT2	17.3	4.9
		NT3	18	5.6
		CT1	11.2	-1.0
		CT2	16.6	4.2
		CT3	15.3	2.9
	Water	CT TD BL	13.6	1.3
June (12.8‰ ± 0.3)	Water	NT TD BL	10.8	-1.7

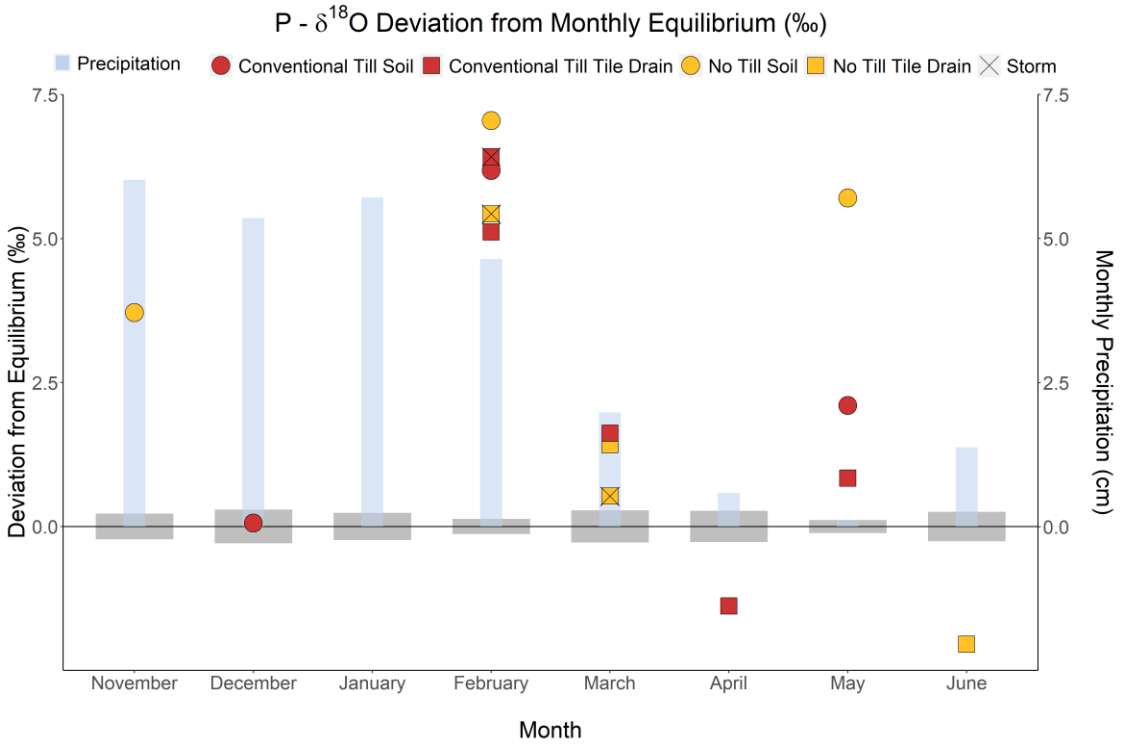

Figure 1.7. Monthly P–$\delta^{18}O$ equilibrium values normalized to zero, shown by gray bars, calculated using two-inch soil temperature and standard deviation of $\delta^{18}O_W$ measurements. Normalized deviation of samples was calculated by subtracting the sample P-$\delta^{18}O$ value

1.5 DISCUSSION

1.5.1 Land Management Effects

The use of paired watersheds at CAF is conducive for understanding differences in nutrient transport under conventional and conservation till management. We hypothesized that land management type would play a larger role in P-$\delta^{18}O$ transport from surface soils to tile drains based on the presence of preferential flow pathways. Surface soil P-$\delta^{18}O$ signatures remained enriched relative to equilibrium values on both sides of the farm throughout the sampling season. Actual soil and tile drain P-$\delta^{18}O$ values varied slightly with land management, indicating that land management may play a secondary role in P transport in this system, compared to other drivers.

Using surface soil P-$\delta^{18}O$ signatures as a source signature for phosphorus tracing from the soil to the tile drain allows for insight into the dynamics of P transport and cycling across the sampling season. Soil P-$\delta^{18}O$ values became slightly more enriched on the no till side of the farm as the season progressed compared to the conventional till values. Changes in soil P-$\delta^{18}O$ values do not describe the changes in tile drain values, which decreased as the season progressed.

1.5.2 Climate Drivers of P Transport

Seasonal variation of P-$\delta^{18}O$ signatures and the deviation of those values from monthly average equilibrium at CAF suggests that climate drivers influence the source and transport of P

through tile drains during the year. Past studies have shown very little deviation from equilibrium (<3‰) in large spatial areas with multiple P sources, suggesting that the temporal variation that we see in P-$\delta^{18}O$ values for tile drain samples potentially provides insight into P dynamics at CAF (Ford et al., 2018; Granger et al., 2017; Gruau et al., 2005). Under high flow conditions, tile drain P-$\delta^{18}O$ values were more similar to surface soil P-$\delta^{18}O$ values than throughout low flow conditions for the rest of the year. When the soil and tile drain are hydrologically connected, isotopic data corroborates that P is transported from toe-slope surface soils, even when tile drain P concentrations are low (Ortega-Pieck et al., 2020). Seasonal tile drain dynamics help to describe P-$\delta^{18}O$ and concentration transports similar to nitrate and dissolved organic matter transport through artificial drain lines at CAF (Bellmore et al., 2015; Keller et al., 2008; Kelley et al., 2017). I hypothesize that high flow conditions similarly facilitate the transport of P from surface soils to tile drains independent of land management.

After receiving ~150 mm of precipitation, tile drains begin to flow on both sides of the farm. Following this precipitation threshold, the soil profile remains saturated and drains continuously throughout the rainy season (Keller et al., 2008). Following precipitation or melt events, the tile drain becomes flashy, with discharge that can increase by an order of magnitude following precipitation or melt events (Keller et al., 2008). This same mechanism has been proposed to also transport P from surface soils to the tile drain during flushing events at CAF (Ortega-Pieck et al., 2020) and artificial drains throughout the country (Christianson et al., 2016; King et al., 2015; R. W. McDowell & Sharpley, 2001).

In February, the large, positive deviation from equilibrium in tile drain samples (4.1 – 6.3‰) on both sides of CAF resembles surface soils isotopic values and indicates a period of high connectivity during baseline flow and storm events due to saturated macropore flow. At this site, precipitation and melt events at this time rapidly saturate macropore flow, transporting nutrients from surface soils to the tile drain (Bellmore et al., 2015; Keller et al., 2008; Kelley et al., 2017; Ortega-Pieck et al., 2020). Under high flow conditions with fast transit time from surface to tile drain, source P-$\delta^{18}O$ signature may be preserved in the tile drain signal (Ford et al., 2018; Gooddy et al., 2016; Tonderski et al., 2017). Ford et al. (2018) found that P-$\delta^{18}O$ signatures were also dynamically tied to soil moisture conditions, and suggested that under saturated soil conditions, storm events mobilize phosphorus from surface soil H_2O-P pools, transporting P through the soil matrix to tile drains. Ortega-Pieck et al. (2020) found that tile drains at CAF flush large amounts of dissolved P early in the water year, potentially due to the accumulation and mineralization of P pools in the surface soils of toe slope areas at CAF. Because our first tile drain sample was collected in February after the tile drain began to flow, we likely missed this initial flush of P. Cold temperatures during the month of

February may help to preserve the source signatures of soil P-$\delta^{18}O$ due to a decrease in microbial activity (Tonderski et al., 2017). This suggests that soil water extractable P during this time period is slowly turned over by microbially processes and that microbial activity during winter months at this site is low, in contrast to other snow dominated sites where winter mineralization is common (Groffman et al., 2001).

Beginning in March, tile drain P-$\delta^{18}O$ values began to more closely reflect equilibrium values (0.2‰ to 1.3‰ deviation). Baseline tile drain flow conditions are reestablished as precipitation declines and the growing season begins. Little water is leached during this time and tile drain discharge begins to slow or cease. Low baseline flow at this time reflects diffuse matrix percolation, with residual H_2O-P leaching from the soil matrix (Bellmore et al., 2015; Keller et al., 2008; Kelley et al., 2017). Soil moisture conditions influence biological processes that drive P-$\delta^{18}O$ cycling, with faster P mineralization being promoted under warmer and wetter conditions (Angert et al., 2011; Chang & Blake, 2015; Tonderski et al., 2017). As connectivity from surface soils decreases, H_2O-P transported from surface soils to the tile drain may have a greater amount of time to be cycled by microorganisms, reflecting P-$\delta^{18}O$ values that are closer to equilibrium (Ford et al., 2018). Ford et al. (2018) also found that under baseline flow conditions, P-$\delta^{18}O$ signatures in tile drains reflected equilibrium values. The CT TD BL April sample has a P-$\delta^{18}O$ value below equilibrium; however, it does not vary much from the March and May tile drain samples ((13.1 – 13.6‰), indicating that the response to equilibrium change is slow or the source is in equilibrium with deep sources. Deep soil water and water traveling from hill slope positions may begin to impact P-$\delta^{18}O$ equilibrium values at this time (Bellmore et al., 2015). P in equilibrium with deep soil water may have a different value of equilibration due to differences in temperature and $\delta^{18}O_w$ at depth (Ford et al., 2018; Joshi et al., 2016). Ford et al. (2018) found that equilibrium ranges could vary by nearly 6‰ within the soil profile, with more enriched values deeper within the soil profile. Tile drain P-$\delta^{18}O$ values at this time may reflect P in various stages of microbial equilibration within the soil profile, making it difficult to determine the exact P source.

Under low flow conditions where connectivity from the soil surface is weak, subsurface soil P may become the dominant tile drain P source. Although available P decreases by over half in toe slope subsurface soils compared to surface soils, P contents are great enough that these areas are likely to contribute to P leaching (Ortega-Pieck et al., 2020). Subsurface soil P concentrations have been related to P concentrations in leachate, although with less certainty than transport from surface soils (Kleinman, Church, et al., 2015). Soil P-$\delta^{18}O$ values have been shown to vary with depth in some studies on agricultural fields, however in other systems soil P-$\delta^{18}O$ has remained similar throughout the soil profile (Amelung et al., 2015; Joshi et al., 2016, 2018). Amelung et al. (2015)

found a decreasing gradient of P-$\delta^{18}O$ values with depth in fields with historical fertilization due to changes in equilibrium values and surface inputs. However, phosphate pools considered unavailable to plants and microbes were measured, which equilibrate slower, and may not reflect P that is being lost to runoff (Amelung et al., 2015; Joshi et al., 2016). Without verifying P-$\delta^{18}O$ signatures for the entire soil profile, it is difficult to determine if differences in soil P-$\delta^{18}O$ values with depth at CAF are driving changes in tile drain P-$\delta^{18}O$ values under low flow conditions. Additionally, P transport from other areas of the field may contribute to changing P-$\delta^{18}O$ values at this time (Ortega-Pieck et al., 2020). More research is needed to corroborate this hypothesis.

Throughout the sampling campaign, we found no correlation between soil and tile drain P concentrations with P-$\delta^{18}O$ values (Figure 1.8). Climate drives change the connectivity between surface soils and tile drains at CAF, altering the source and concentration of P in tile drains. Tile drain P concentrations have been correlated to available P concentrations in toe slope surface soils at CAF (Ortega-Pieck et al., 2020). Under low flow conditions, high concentrations of H_2O-P_{MR} were measured, while under high flow conditions, low concentrations of H_2O-P_{MR} were measured ,with no correlation to isotopic values from the surface soils. Poor relationships between H_2O-P_{MR} concentration and P-$\delta^{18}O$ signatures have been reported in aquatic and terrestrial systems (Elsbury et al., 2009; Ford et al., 2018; Granger et al., 2017; Tonderski et al., 2017) but the opposite has also been reported (Gooddy et al., 2016), suggesting that the coupling of dissolved phosphorus and P-$\delta^{18}O$ signatures is system dependent.

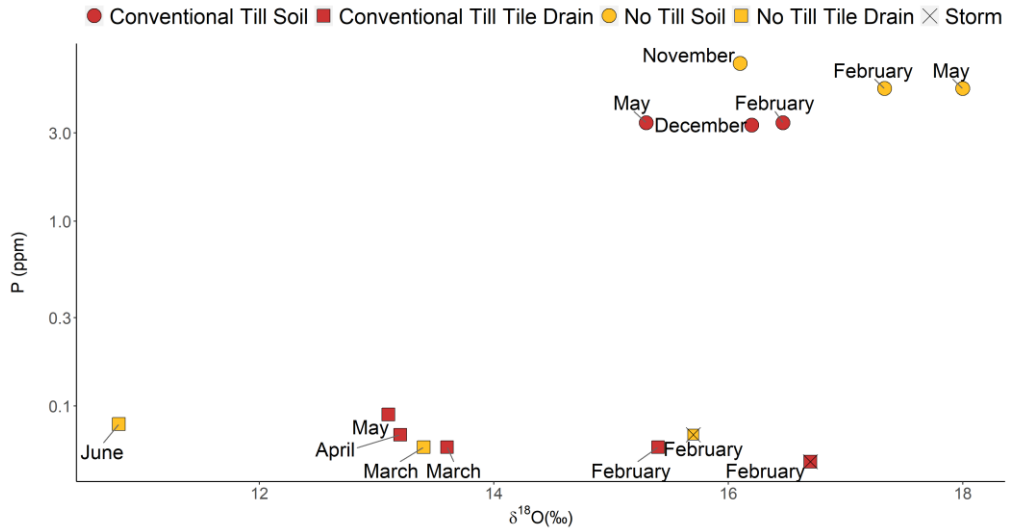

Figure 1.8. Correlation between soil H_2O-P_{MR} (mg P/kg) and tile drain H_2O-P_{MR} (mg P/L) concentrations and P-$\delta^{18}O$ value.

1.5.3 Legacy P at CAF

Phosphorus fertilizer at CAF has not been applied in the last five years, thus soil P at the site is from legacy sources. Both NT and CT surface soil H_2O-P P-$\delta^{18}O$ signatures remained enriched

compared to equilibrium over multiple months of sampling. Enrichment of both CT and NT soil P-$\delta^{18}O$ values with reference to equilibrium throughout the year suggests the presence of legacy P from historical fertilization practices on the Palouse. Past studies have found mixed results in the deviation of soil H_2O-P with equilibrium (Bi et al., 2018; Ford et al., 2018; Gross et al., 2015; Joshi et al., 2016; Tamburini et al., 2012; Zohar et al., 2010). Results from studies with enriched soil P-$\delta^{18}O$ values in labile P pools following long-term fertilization suggest that P-$\delta^{18}O$ signatures are preserved when microorganisms are not P-limited (Ford et al., 2018; Gross et al., 2015). In P-limited systems, however, labile P pools may be quickly cycled to equilibrium values (Gross et al., 2015). Ford et al. (2018) found that H_2O-P P-$\delta^{18}O$ signatures surface soils was enriched compared to equilibrium values ten years after P fertilizer had been applied. At CAF, accumulation of P in toe slope surface soils from erosion and historical fertilization may have resulted in microbial biomass that were not P-limited, allowing the source signature of legacy P fertilizer to be retained (Gross et al., 2015; Ortega-Pieck et al., 2020). We cannot discount, however, evaporative effects near the soil surface, which could result in the accumulation of heavier $\delta^{18}O_w$. Evaporative enrichment of surface soil water could lead to equilibrium values that are more enriched than we accounted for using only collected precipitation. Studies are split on the collection of water for $\delta^{18}O_w$, with some studies using $\delta^{18}O_w$ from precipitation to calculate equilibrium (Angert et al., 2011, 2012; Ford et al., 2018), and some using soil water $\delta^{18}O_w$ values (Amelung et al., 2015; Bi et al., 2018; Hsieh et al., 1998; Pfahler et al., 2020; Roberts et al., 2015). Despite this, differences in soil P-$\delta^{18}O$ values and tile drain P-$\delta^{18}O$ values throughout the year suggests that climate drivers may be influencing source and microbial turnover of P at CAF. P-$\delta^{18}O$ signatures indicated the direct transport of legacy P from surface soils to the tile drain under high flow conditions, regardless of land management.

1.5.4 Future Directions

For a better understanding of phosphorus dynamics and cycling at CAF, a closer look at soil and water P-$\delta^{18}O$ signatures is necessary. Using a finer resolution sampling scheme for storm and baseline tile drain flow dynamics would lead to a better understanding of the mixing of deep and shallow water sources over the course of events, as well as to differentiate variability in transport time of event water between the conventional and no till land management schemes. To understand the nuances of soil P-$\delta^{18}O$ variation, soil samples should be collected from multiple depths as well as from various hill slope positions on the no till and conventionally tilled sides of CAF. Additionally, water samples collected with lysimeters from multiple depths within the soil profile would provide insight to understand change in equilibrium range and change in soil water P-$\delta^{18}O$ signatures and surface connectivity with depth. Analyzing $\delta^{18}O_w$ and hydrogen isotopes ($\delta^{2}H_w$) from soil water with depth and through the tile drain would also shed light on the main sources of tile drain flow

throughout the year. Overall, stable isotopic tracing of P-$\delta^{18}O$ has the potential to be a powerful tool for studying phosphorus processing and transport at CAF.

1.6 CONCLUSION

Historical use of phosphorus fertilizer continues to impact water quality in the US. Long-term tillage and erosion led to large stores of legacy P in depositional areas at CAF in the Palouse region of eastern Washington. The majority of subsurface P transport at CAF was proposed to come from the surface soils of toe slope depositional areas on the no-till side of the farm based on correlations between soil and tile drain P concentrations (Ortega-Pieck et al., 2020). This study sought to test two tillage regimes impact on the transport of legacy P from toe slope surface soils to the tile drain using isotopic tracing of phosphorus and to determine the effects of land management. Using stable isotope tracing, we provide evidence that climate, not land management, was the largest driver for the source of P at CAF, rejecting our initial hypothesis. Under high flow conditions, similar isotopic values in surface soils and tile drain outlet show that phosphorus is primarily transported from toe slope surface soils on both the conventional till and no till side of the farm to the tile drain under saturated macropore flow. Under low flow conditions, isotopic tile drain values are not similar to surface soils, indicating that connectivity from surface soils to the tile drain is lost on both sides of the farm. This indicates that the primary phosphorus source and extent of microbial cycling may change over the course of the year depending on hydrologic conditions. We found no correlation between H_2O-P_{MR} concentrations and isotopic values of the soil or tile drain, indicating that concentration and isotopic values are not coupled in this system. Characterizing P-$\delta^{18}O$ values for more areas of CAF would help to determine major source areas under changing hydrologic conditions. Closely examining patterns and the extent of hydrologic connectivity under baseline and high flow conditions at CAF would provide better insight into the yearly phosphorus dynamics that control P loading to the surrounding waterways.

1.7 REFERENCES

Amelung, W., Antar, P., Kleeberg, I., Oelmann, Y., Lücke, A., Alt, F., Lewandowski, H., Pätzold, S., & Barej, J. (2015). The δ18O signatures of HCl-extractable soil phosphates: Methodological challenges and evidence of the cycling of biological P in arable soil. *European Journal of Soil Science*, *66*. https://doi.org/10.1111/ejss.12288

Amundson, R., Austin, A. T., Schuur, E. a. G., Yoo, K., Matzek, V., Kendall, C., Uebersax, A., Brenner, D., & Baisden, W. T. (2003). Global patterns of the isotopic composition of soil and plant nitrogen. *Global Biogeochemical Cycles*, *17*(1). https://doi.org/10.1029/2002GB001903

Angert, A., Weiner, T., Mazeh, S., & Sternberg, M. (2012). Soil Phosphate Stable Oxygen Isotopes across Rainfall and Bedrock Gradients. *Environmental Science & Technology*, *46*(4), 2156–2162.

Angert, A., Weiner, T., Mazeh, S., Tamburini, F., Frossard, E., Bernasconi, S. M., & Sternberg, M. (2011). Seasonal variability of soil phosphate stable oxygen isotopes in rainfall manipulation experiments. *Geochimica et Cosmochimica Acta*, *75*(15), 4216–4227. https://doi.org/10.1016/j.gca.2011.05.002

Baker, D. B., Johnson, L. T., Confesor, R. B., Crumrine, J. P., Guo, T., & Manning, N. F. (2019). Needed: Early-term adjustments for Lake Erie phosphorus target loads to address western basin cyanobacterial blooms. *Journal of Great Lakes Research*, *45*(2), 203–211. https://doi.org/10.1016/j.jglr.2019.01.011

Bellmore, R. A., Harrison, J. A., Needoba, J. A., Brooks, E. S., & Kent Keller, C. (2015). Hydrologic control of dissolved organic matter concentration and quality in a semiarid artificially drained agricultural catchment. *Water Resources Research*, *51*(10), 8146–8164. https://doi.org/10.1002/2015WR016884

Bi, Q.-F., Zheng, B.-X., Lin, X.-Y., Li, K.-J., Liu, X.-P., Hao, X.-L., Zhang, H., Zhang, J.-B., Jaisi, D. P., & Zhu, Y.-G. (2018). The microbial cycling of phosphorus on long-term fertilized soil: Insights from phosphate oxygen isotope ratios. *Chemical Geology*, *483*, 56–64. https://doi.org/10.1016/j.chemgeo.2018.02.013

Blake, R. E., O'Neil, J. R., & Surkov, A. V. (2005). Biogeochemical cycling of phosphorus: Insights from oxygen isotope effects of phosphoenzymes. *American Journal of Science*, *305*(6–8), 596–620. https://doi.org/10.2475/ajs.305.6-8.596

Brooks, E. S., Boll, J., & McDaniel, P. A. (2012). Hydropedology in Seasonally Dry Landscapes: The Palouse Region of the Pacific Northwest USA. In H. Lin (Ed.), *Hydropedology: Synergistic Integration of Soil Science and Hydrology* (1st ed., p. Chapter 10: 329-350). Elsevier.

Brüggemann, N., Gessler, A., Kayler, Z., Keel, S. G., Badeck, F., Barthel, M., Boeckx, P., Buchmann, N., Brugnoli, E., Esperschütz, J., Gavrichkova, O., Ghashghaie, J., Gomez-Casanovas, N., Keitel, C., Knohl, A., Kuptz, D., Palacio, S., Salmon, Y., Uchida, Y., & Bahn, M. (2011). Carbon allocation and carbon isotope fluxes in the plant-soil-atmosphere continuum: A review. *Biogeosciences*, *8*(11), 3457.

Burke, I. C., Elliott, E. T., & Cole, C. V. (1995). Influence of Macroclimate, Landscape Position, and Management on Soil Organic Matter in Agroecosystems. *Ecological Applications*, *5*(1), 124–131. https://doi.org/10.2307/1942057

Carter, M. R. (2005). CONSERVATION TILLAGE. In D. Hillel (Ed.), *Encyclopedia of Soils in the Environment* (pp. 306–311). Elsevier. https://doi.org/10.1016/B0-12-348530-4/00270-8

Chang, S. J., & Blake, R. E. (2015). Precise calibration of equilibrium oxygen isotope fractionations between dissolved phosphate and water from 3 to 37°C. *Geochimica et Cosmochimica Acta*, *150*, 314–329. https://doi.org/10.1016/j.gca.2014.10.030

Christianson, L. E., Harmel, R. D., Smith, D., Williams, M. R., & King, K. (2016). Assessment and Synthesis of 50 Years of Published Drainage Phosphorus Losses. *Journal of Environmental Quality*, *45*(5), 1467–1477. https://doi.org/10.2134/jeq2015.12.0593

Cooperative climatological data summaries. PULLMAN 2 NW, WASHINGTON (456789). (2021). Western Regional Climate Center (WRCC). https://wrcc.dri.edu/cgi-bin/cliMAIN.pl?wa6789

Davies, C. L., Surridge, B. W. J., & Gooddy, D. C. (2014). Phosphate oxygen isotopes within aquatic ecosystems: Global data synthesis and future research priorities. *Science of The Total Environment*, *496*, 563–575.

Elsbury, K. E., Paytan, A., Ostrom, N. E., Kendall, C., Young, M. B., McLaughlin, K., Rollog, M. E., & Watson, S. (2009). Using Oxygen Isotopes of Phosphate To Trace Phosphorus Sources and Cycling in Lake Erie. *Environmental Science & Technology*, *43*(9), 3108–3114. https://doi.org/10.1021/es8034126

Fiorellino, N., Kratochvil, R., & Coale, F. (2017). Long-Term Agronomic Drawdown of Soil Phosphorus in Mid-Atlantic Coastal Plain Soils. *Agronomy Journal*, *109*(2), 455–461. https://doi.org/10.2134/agronj2016.07.0409

Ford, W., Williams, M. R., Young, M. B., King, K. W., & Fischer, E. (2018). Assessing Intra-Event Phosphorus Dynamics in Drainage Water Using Phosphate Stable Oxygen Isotopes. *Transactions of the ASABE*, *61*(4), 1379–1392. https://doi.org/10.13031/trans.12804

Franklin, D. H., & Bergtold, J. (2020). Chapter 2: Conservation Tillage Systems: History, the Future and Benefits. In J. Bergtold & M. Sailus (Eds.), *Conservation Tillage Systems in the Southeast: Production, Profitability and Stewardship* (pp. 19–28). https://www.sare.org/publications/conservation-tillage-systems-in-the-southeast/chapter-2-conservation-tillage-systems-history-the-future-and-benefits/a-historical-perspective/

Frossard, E., Condron, L. M., Oberson, A., Sinaj, S., & Fardreau, J. C. (2000). Processes governing phosphorus availability in temperate soils. *Journal of Environmental Quality*, *29*(1). http://search.proquest.com/docview/197381913?accountid=14551&rfr_id=info%3Axri%2Fsid%3Aprimo

Gooddy, D. C., Lapworth, D. J., Bennett, S. A., Heaton, T. H. E., Williams, P. J., & Surridge, B. W. J. (2016). A multi-stable isotope framework to understand eutrophication in aquatic ecosystems. *Water Research*, *88*, 623–633. https://doi.org/10.1016/j.watres.2015.10.046

Granger, S. J., Heaton, T. H. E., Pfahler, V., Blackwell, M. S. A., Yuan, H., & Collins, A. L. (2017). The oxygen isotopic composition of phosphate in river water and its potential sources in the Upper River Taw catchment, UK. *Science of The Total Environment*, *574*, 680–690. https://doi.org/10.1016/j.scitotenv.2016.09.007

Groffman, P. M., Driscoll, C. T., Fahey, T. J., Hardy, J. P., Fitzhugh, R. D., & Tierney, G. L. (2001). Colder Soils in a Warmer World: A Snow Manipulation Study in a Northern Hardwood Forest Ecosystem. *Biogeochemistry*, *56*(2), 135–150.

Gross, A., & Angert, A. (2015). What processes control the oxygen isotopes of soil bio-available phosphate? *Geochimica et Cosmochimica Acta*, *159*, 100–111. https://doi.org/10.1016/j.gca.2015.03.023

Gross, A., Turner, B. L., Wright, S. J., Tanner, E. V. J., Reichstein, M., Weiner, T., & Angert, A. (2015). Oxygen isotope ratios of plant available phosphate in lowland tropical forest soils. *Soil Biology and Biochemistry*, *88*, 354–361. https://doi.org/10.1016/j.soilbio.2015.06.015

Gruau, G., Legeas, M., Riou, C., Gallacier, E., Martineau, F., & Hénin, O. (2005). The oxygen isotope composition of dissolved anthropogenic phosphates: A new tool for eutrophication research? *Water Research*, *39*(1), 232–238. https://doi.org/10.1016/j.watres.2004.08.035

Hamilton, S. K. (2012). Biogeochemical time lags may delay responses of streams to ecological restoration. *Freshwater Biology*, *57*(s1), 43–57. https://doi.org/10.1111/j.1365-2427.2011.02685.x

Haygarth, P. M., & Sharpley, A. N. (2000). Terminology for phosphorus transfer. *Journal of Environmental Quality*, *29*(1), 10.

Hooda, P. S., Rendell, A. R., Edwards, A. C., Withers, P. J. A., & al, et. (2000). Relating soil phosphorus indices to potential phosphorus release to water. *Journal of Environmental Quality*, *29*(4), 1166.

Hooda, P. S., Truesdale, V. W., Edwards, A. C., Withers, P. J. A., Aitken, M. N., Miller, A., & Rendell, A. R. (2001). Manuring and fertilization effects on phosphorus accumulation in soils and potential environmental implications. *Advances in Environmental Research*, *5*(1), 13–21. https://doi.org/10.1016/S1093-0191(00)00037-X

Hsieh, J. C. C., Chadwick, O. A., Kelly, E. F., & Savin, S. M. (1998). Oxygen isotopic composition of soil water: Quantifying evaporation and transpiration. *Geoderma*, *82*(1–3), 269–293. https://doi.org/10.1016/S0016-7061(97)00105-5

Idaho Department of Environmental Quality. (2016). *Palouse River Subbasin Five-Year Review*.

Ishida, T., Uehara, Y., Iwata, T., Cid-Andres, A. P., Asano, S., Ikeya, T., Osaka, K., Ide, J., Privaldos, O., De Jesus, I. B. B., Peralta, E. M., Trino, E. M. C., Ko, C.-Y., Paytan, A., Tayasu, I., & Okuda, N. (2019). Identification of Phosphorous Sources in a Watershed using a phosphate oxygen isoscape approach. *Environmental Science & Technology*, *53*(9), 4707–4716.

Isotopes-Oxygen 18. (n.d.). Retrieved May 26, 2022, from http://snobear.colorado.edu/Daniel/isotopes/oxygen18.html

Jarvie, H. P., Johnson, L. T., Sharpley, A. N., Smith, D. R., Baker, D. B., Bruulsema, T. W., & Confesor, R. (2017). Increased Soluble Phosphorus Loads to Lake Erie: Unintended Consequences of Conservation Practices? *Journal of Environmental Quality*, *46*(1). https://acsess-onlinelibrary-wiley-com.uidaho.idm.oclc.org/doi/full/10.2134/jeq2016.07.0248

Jarvie, H. P., Sharpley, A. N., Spears, B., Buda, A. R., May, L., & Kleinman, P. J. A. (2013). Water Quality Remediation Faces Unprecedented Challenges from "Legacy Phosphorus." *Environmental Science & Technology*, *47*(16), 8997–8998.

Jarvie, H. P., Sharpley, A., Withers, P., Scott, T., & Haggard, B. (2013). Phosphorus Mitigation to Control River Eutrophication: Murky Waters, Inconvenient Truths, and "Postnormal" Science. *Journal of Environmental Quality*, *42*(2), 295–304.

Johnston, A. E., Poulton, P. R., Fixen, P. E., & Curtin, D. (2014). Phosphorus. In *Advances in Agronomy* (Vol. 123, pp. 177–228). Elsevier. https://doi.org/10.1016/B978-0-12-420225-2.00005-4

Joshi, S. R., Li, W., Bowden, M., & Jaisi, D. P. (2018). Sources and Pathways of Formation of Recalcitrant and Residual Phosphorus in an Agricultural Soil. *Soil Systems*, *2*(3), 45. https://doi.org/10.3390/soilsystems2030045

Joshi, S. R., Li, X., & Jaisi, D. P. (2016). Transformation of Phosphorus Pools in an Agricultural Soil: An Application of Oxygen-18 Labeling in Phosphate. *Soil Science Society of America Journal*, *80*(1), 69–78. https://doi.org/10.2136/sssaj2015.06.0219

Keller, C. K., Butcher, C. N., Smith, J. L., & Allen-King, R. M. (2008). Nitrate in Tile Drainage of the Semiarid Palouse Basin. *Journal of Environmental Quality*, *37*(2), 353–361.

Kelley, C. J., Keller, C. K., Brooks, E. S., Smith, J. L., Orr, C. H., & Evans, R. D. (2017). Water and nitrogen movement through a semiarid dryland agricultural catchment: Seasonal and decadal trends. *Hydrological Processes*, *31*(10), 1889–1899. https://doi.org/10.1002/hyp.11152

King, K. W., Williams, M. R., Macrae, M. L., Fausey, N. R., Frankenberger, J., Smith, D. R., Kleinman, P. J. A., & Brown, L. C. (2015). Phosphorus Transport in Agricultural Subsurface Drainage: A Review. *Journal of Environmental Quality*, *44*(2), 467–485. https://doi.org/10.2134/jeq2014.04.0163

Kleinman, P. J. A. (2017). The Persistent Environmental Relevance of Soil Phosphorus Sorption Saturation. *Current Pollution Reports*, *3*(2), 141–150. https://doi.org/10.1007/s40726-017-0058-4

Kleinman, P. J. A., Church, C., Saporito, L. S., McGrath, J. M., Reiter, M. S., Allen, A. L., Tingle, S., Binford, G. D., Han, K., & Joern, B. C. (2015). Phosphorus Leaching from Agricultural Soils of the Delmarva Peninsula, USA. *Journal of Environmental Quality*, *44*(2), 524–534. https://doi.org/10.2134/jeq2014.07.0301

Kleinman, P. J. A., & Sharpley, A. N. (2003). Effect of broadcast manure on runoff phosphorus concentrations over successive rainfall events. *Journal of Environmental Quality*, *32*(3), 1072–1081.

Kleinman, P. J. A., Sharpley, A. N., Buda, A., McDowell, R., & Allen, A. (2011). Soil controls of phosphorus in runoff: Management barriers and opportunities. *Canadian Journal of Soil Science*, *91*(3), 329–338. https://doi.org/10.4141/cjss09106

Kleinman, P. J. A., Smith, D. R., Bolster, C. H., & Easton, Z. M. (2015). Phosphorus Fate, Management, and Modeling in Artificially Drained Systems. *Journal of Environmental Quality*, *44*(2), 460–466. https://doi.org/10.2134/jeq2015.02.0090

Lenth, R. V., Buerkner, P., Herve, M., Love, J., Miguez, F., Riebl, H., & Singmann, H. (2022). *emmeans: Estimated Marginal Means, aka Least-Squares Means* (1.7.3) [Computer software]. https://CRAN.R-project.org/package=emmeans

Leslie, I. (2020, November 20). [Personal communication].

Liang, Y., & Blake, R. E. (2009). Compound- and enzyme-specific phosphodiester hydrolysis mechanisms revealed by δ18O of dissolved inorganic phosphate: Implications for marine P cycling. *Geochimica et Cosmochimica Acta*, *73*(13), 3782–3794. https://doi.org/10.1016/j.gca.2009.01.038

Longinelli, A., & Nuti, S. (1973). Revised phosphate-water isotopic temperature scale. *Earth and Planetary Science Letters*, *19*(3), 373–376. https://doi.org/10.1016/0012-821X(73)90088-5

Macrae, M. L., English, M. C., Schiff, S. L., & Stone, M. (2010). Influence of antecedent hydrologic conditions on patterns of hydrochemical export from a first-order agricultural watershed in Southern Ontario, Canada. *Journal of Hydrology*, *389*(1–2), 101–110. https://doi.org/10.1016/j.jhydrol.2010.05.034

McDowell, R., Dodd, R., Pletnyakov, P., & Noble, A. (2020). The Ability to Reduce Soil Legacy Phosphorus at a Country Scale. *Frontiers in Environmental Science*, *8*. https://www.frontiersin.org/article/10.3389/fenvs.2020.00006

McDowell, R. W., & Sharpley, A. N. (2001). Approximating phosphorus release from soils to surface runoff and subsurface drainage. *Journal of Environmental Quality*, *30*(2), 508–520.

McLaughlin, K., Silva, S., Kendall, C., Stuart-Williams, H., & Paytan, A. (2004). A precise method for the analysis of δ18O of dissolved inorganic phosphate in seawater. *Limnology and Oceanography*, *2*(7). https://aslopubs-onlinelibrary-wiley-com.uidaho.idm.oclc.org/doi/abs/10.4319/lom.2004.2.202

Meals, D. W., Dressing, S. A., & Davenport, T. E. (2010). Lag Time in Water Quality Response to Best Management Practices: A Review. *Journal of Environmental Quality*, *39*(1), 85–96. https://doi.org/10.2134/jeq2009.0108

Montgomery, J. A., McCool, D. K., Busacca, A. J., & Frazier, B. E. (1999). Quantifying tillage translocation and deposition rates due to moldboard plowing in the Palouse region of the Pacific Northwest. *Soil and Tillage Research*, *51*(3), 175–187. https://doi.org/10.1016/S0167-1987(99)00036-7

Moore, J. (2016). *Literature Review: Tile Drainage and Phosphorus Losses from Agricultural Land* (Technical No. 83; p. 79). Lake Champlain Basin Program.

Mosheim, R. (2019, October 30). *USDA ERS - Summary of Findings* [United States Department of Agriculture-Economic Research Service]. https://www.ers.usda.gov/data-products/fertilizer-use-and-price/summary-of-findings/

Negassa, W., & Leinweber, P. (2009). How does the Hedley sequential phosphorus fractionation reflect impacts of land use and management on soil phosphorus: A review. *Journal of Plant Nutrition and Soil Science*, *172*(3), 305–325. https://doi.org/10.1002/jpln.200800223

Nisbeth, C. S., Tamburini, F., Kidmose, J., Jessen, S., & O'Connell, D. W. (2019). Analysis of oxygen isotopes of inorganic phosphate ($\delta^{18}O_p$) in freshwater: A detailed method description. *Hydrology and Earth System Sciences Discussions*, 1–18. https://doi.org/10.5194/hess-2019-469

Norby, J. (2018). *Subsurface Phosphorus Transport through a no-till Field in the Semiarid Palouse Region* [M.S., University of Idaho]. http://search.proquest.com/docview/2115829115/abstract

Ortega-Pieck, A., Norby, J., Brooks, E. S., Strawn, D., Crump, A. R., & Huggins, D. R. (2020). Sources and subsurface transport of dissolved reactive phosphorus in a semiarid, no-till catchment with complex topography. *Journal of Environmental Quality*, *49*(5), 1286–1297. https://doi.org/10.1002/jeq2.20114

Outram, F. N., Cooper, R. J., Sünnenberg, G., Hiscock, K. M., & Lovett, A. A. (2016). Antecedent conditions, hydrological connectivity and anthropogenic inputs: Factors affecting nitrate and phosphorus transfers to agricultural headwater streams. *Science of The Total Environment*, *545–546*, 184–199. https://doi.org/10.1016/j.scitotenv.2015.12.025

Palouse Co-Operative River Basin Study (p. 248). (1978). [U.S. Gov. Print.]. United States Department of Agriculture, Economics, Statistics and Cooperatives Service, Forest Service, Soil Conservation Service. http://pnwsteep.wsu.edu/resourcelinks/Palouse_Basin_Study.pdf

Pfahler, V., Macdonald, A., Mead, A., Smith, A. C., Tamburini, F., Blackwell, M. S. A., & Granger, S. J. (2020). Changes of oxygen isotope values of soil P pools associated with changes in soil pH. *Scientific Reports*, *10*(1), 2065. https://doi.org/10.1038/s41598-020-59103-2

Pinheiro, J., Bates, D., DebRoy, S., Sarkar, D., Heisterkamp, S., Willigen, B. V., Ranke, J., & R Core Team. (2022). *nlme: Linear and Nonlinear Mixed Effects Models* (3.1-158) [Computer software]. https://CRAN.R-project.org/package=nlme

Pionke, H. B., Gburek, W. J., & Sharpley, A. N. (2000). Critical source area controls on water quality in an agricultural watershed located in the Chesapeake Basin. *Ecological Engineering*, *14*(4), 325–335. https://doi.org/10.1016/S0925-8574(99)00059-2

Prasad, R., & Chakraborty, D. (2019). *Phosphorus Basics: Understanding Phosphorus Forms and Their Cycling in the Soil*. Alabama Cooperative Extension System.

R Studio Team. (2020). *RStudio: Inegrated Development for R* [RStudio]. PBC. http://www.rstudio.com/

Research at Cook Agronomy Farm. (n.d.). Retrieved January 20, 2021, from https://css.wsu.edu/facilities/cook/research/

Roberts, K., Defforey, D., Turner, B. L., Condron, L. M., Peek, S., Silva, S., Kendall, C., & Paytan, A. (2015). *Oxygen isotopes of phosphate and soil phosphorus cycling across a 6500 year chronosequence under lowland temperate rainforest*. https://doi.org/10.1016/j.geoderma.2015.04.010

Rowe, H., Withers, P. J. A., Baas, P., Chan, N. I., Doody, D., Holiman, J., Jacobs, B., Li, H., MacDonald, G. K., McDowell, R., Sharpley, A. N., Shen, J., Taheri, W., Wallenstein, M., & Weintraub, M. N. (2015). Integrating legacy soil phosphorus into sustainable nutrient management strategies for future food, bioenergy and water security. *Nutrient Cycling in Agroecosystems*, *104*, 393–412.

Rust, B., & Williams, J. D. (n.d.). *How Tillage Affects Soil Erosion and Runoff* (pp. 1–9) [Technical Note]. USDA/ARS Columbia Plateau Conservation Research Center.

Schlatter, D. C., Reardon, C. L., Johnson-Maynard, J., Brooks, E., Kahl, K., Norby, J., Huggins, D., & Paulitz, T. C. (2019). Mining the Drilosphere: Bacterial Communities and Denitrifier Abundance in a No-Till Wheat Cropping System. *Frontiers in Microbiology*, *10*. https://doi.org/10.3389/fmicb.2019.01339

Self-Davis, M. L., Moore, P. A., & Joern, B. C. (2000). Determination of Water- and/or Dilute Salt-Extractable Phosphorus. In J. L. Kovar & G. M. Pierzynski (Eds.), *Methods of Phosphorus Analysis for Soils, Sediments, Residuals, and Waters* (pp. 24–26). Southern Extension/Research Activity-Information Exchange Group 17-A USDA-CSREES Regional Commiittee. http://www.sera17.ext.vt.edu/Documents/P_Methods2ndEdition2009.pdf

Sharpley, A. N., Chapra, S. C., Wedepohl, R., Sims, J. T., Daniel, T. C., & Reddy, K. R. (1994). Managing Agricultural Phosphorus for Protection of Surface Waters: Issues and Options. *Journal of Environmental Quality*, *23*(3), 437–451. https://doi.org/10.2134/jeq1994.00472425002300030006x

Sharpley, A. N., Daniel, T., Gibson, G., Bundy, L., Cabrera, M., Sims, T., Stevens, R., Lemunyon, J., Kleinman, P., & Parry, R. (2006). *Best Management Practices to Minimize Agricultural Phosphorus Impacts on Water Quality* (No. 163). United States Department of Agriculture-Agricultural Research Service. https://www.ars.usda.gov/is/np/bestmgmtpractices/best%20management%20practices.pdf

Sharpley, A. N., Kleinman, P. J. A., Jordan, P., Bergstrom, L., & Allen, A. L. (2009). Evaluating the Success of Phosphorus Management from Field to Watershed. *Journal of Environmental Quality*, *38*(5), 1981–1988.

Sharpley, A. N., & Smith, S. J. (1993). Prediction of Bioavailable Phosphorus Loss in Agricultural Runoff—Sharpley—1993—Journal of Environmental Quality—Wiley Online Library. *Journal of Environmental Quality*, *22*(1), 32–37.

Shen, J., Yuan, L., Zhang, J., Li, H., Bai, Z., Chen, X., Zhang, W., & Zhang, F. (2011). Phosphorus Dynamics: From Soil to Plant. *Plant Physiology*, *156*(3), 997–1005. https://doi.org/10.1104/pp.111.175232

Smith, D. R., King, K. W., Johnson, L., Francesconi, W., Richards, P., Baker, D., & Sharpley, A. N. (2015). Surface Runoff and Tile Drainage Transport of Phosphorus in the Midwestern United States. *Journal of Environmental Quality*, *44*(2), 495–502. https://doi.org/10.2134/jeq2014.04.0176

Soil Quality Indicators. (2008). United States Department of Agriculture Natural Resources Conservation Service. https://www.nrcs.usda.gov/Internet/FSE_DOCUMENTS/nrcs142p2_053261.pdf

Tamburini, F., Bernasconi, S. M., Angert, A., Weiner, T., & Frossard, E. (2010). A method for the analysis of the δ18O of inorganic phosphate extracted from soils with HCl. *European Journal of Soil Science*, *61*(6), 1025–1032. https://doi.org/10.1111/j.1365-2389.2010.01290.x

Tamburini, F., Pfahler, V., Bünemann, E. K., Guelland, K., Bernasconi, S. M., & Frossard, E. (2012). Oxygen Isotopes Unravel the Role of Microorganisms in Phosphate Cycling in Soils. *Environmental Science & Technology*, *46*(11), 5956–5962. https://doi.org/10.1021/es300311h

Tamburini, F., Pfahler, V., Sperber, C. von, Frossard, E., & Bernasconi, S. M. (2014). Oxygen Isotopes for Unraveling Phosphorus Transformations in the Soil–Plant System: A Review. *Soil Science Society of America Journal*, *78*(1), 38–46. https://doi.org/10.2136/sssaj2013.05.0186dgs

Tian, L., Guo, Q., Zhu, Y., He, H., Lang, Y., Hu, J., Zhang, H., Wei, R., Han, X., Peters, M., & Yang, J. (2016). Research and application of method of oxygen isotope of inorganic phosphate in Beijing agricultural soils. *Environmental Science and Pollution Research*, *23*(23), 23406–23414. https://doi.org/10.1007/s11356-016-7482-7

Tonderski, K., Anderson, L., Lindstrom, G., St Cyr, R., Schonberg, R., & Taubald, H. (2017). Assessing the use of δ18O in phosphate as a tracer for catchment phosphorus sources. *Science of the Total Environment*, *607–608*, 1–10.

Vadas, P. A., Fiorellino, N. M., Coale, F. J., Kratochvil, R., Mulkey, A. S., & McGrath, J. M. (2018). Estimating Legacy Soil Phosphorus Impacts on Phosphorus Loss in the Chesapeake Bay Watershed. *Journal of Environmental Quality*, *47*(3), 480–486. https://doi.org/10.2134/jeq2017.12.0481

Vidon, P., Hubbard, H., Cuadra, P., & Hennessy, M. (2012). Storm phosphorus concentrations and fluxes in artificially drained landscapes of the US Midwest. *Agricultural Sciences*, *03*(04), 474–485. https://doi.org/10.4236/as.2012.34056

Weiner, T., Mazeh, S., Tamburini, F., Frossard, E., Bernasconi, S. M., Chiti, T., & Angert, A. (2011). A method for analyzing the δ18O of resin-extractable soil inorganic phosphate. *Rapid Communications in Mass Spectrometry*, *25*(5). https://onlinelibrary-wiley-com.uidaho.idm.oclc.org/doi/full/10.1002/rcm.4899

Williams, M. R., King, K. W., Ford, W., Buda, A. R., & Kennedy, C. D. (2016). Effect of tillage on macropore flow and phosphorus transport to tile drains. *Water Resources Research*, *52*(4). https://agupubs-onlinelibrary-wiley-com.uidaho.idm.oclc.org/doi/full/10.1002/2015WR017650

Xu, S., Gentry, L., Chen, K.-Y., & Arai, Y. (2020). Intensive agricultural management-induced subsurface accumulation of labile phosphorus in Midwestern agricultural soils dominated by tile lines. *Soil Science Society of America Journal*, *84*(4), 1094–1109. https://doi.org/10.1002/saj2.20089

Xu, Z., Huang, T., & Yin, X. (2018). Improvements in the preparation of phosphate for oxygen isotope analysis from soils and sediments. *Public Library of Science*, *13*(9). https://go-gale-com.uidaho.idm.oclc.org/ps/i.do?p=AONE&u=mosc00780&id=GALE%7CA560248536&v=2.1&it=r

Young, M. B., McLaughlin, K., Kendall, C., Stringfellow, W., Rollog, M., Elsbury, K., Donald, E., & Paytan, A. (2009). Characterizing the Oxygen Isotopic Composition of Phosphate Sources to Aquatic Ecosystems. *Environmental Science & Technology*, *43*(14), 5190–5196. https://doi.org/10.1021/es900337q

Zohar, I., Shaviv, A., Young, M., Kendall, C., Silva, S., & Paytan, A. (2010). Phosphorus dynamics in soils irrigated with reclaimed waste water or fresh water—A study using oxygen isotopic composition of phosphate. *Geoderma*, *159*(1–2), 109–121. https://doi.org/10.1016/j.geoderma.2010.07.002

Chapter 2: Phosphorus Speciation and Availability in Soils with Dairy-Derived Amendments.

2.1 ABSTRACT

Closing the circular bioeconomy of the Idaho dairy industry is necessary for managing waste streams and environmental health. Dairy manure is often applied to fields as a fertilizer, however overapplication can lead to an increase in downstream eutrophication. Recovering nutrients from fermented biosolids and lagoon manure using biochar can serve as potential P fertilizers. The objective of this research was to understand P speciation and cycling in a greenhouse study using recovered nutrients from two dairy waste streams using sequential extraction, ^{31}P-NMR, XANES, and isotopic tracing. Iron-modified biochar was used to sorb P from dairy lagoon water, suggesting that it may be used in dairy wastewater treatment. The biochar with dairy P and fermented biosolids were comprised of less than 5% water-extractable P but supplied similar amounts of plant available P as commercially available fertilizers within the rate of application. XANES analysis showed that soils consisted of mainly Ca-P (53.6% - 86.7%) and adsorbed P (0.0% - 46.4%) species. P-δ^{18}O analysis and modeling of the sequentially extracted soil pools shows that microbial cycling of P in the soils was greater in the control soils than soils with added P. The use of dairy-derived fertilizers provided similar amounts of growth as commercially available fertilizer, suggesting that lagoon water and fermented biosolids are viable options for the reuse of P from Idaho dairies. The use of multiple analytical techniques in this study provided an extensive view of P speciation and transformations in the soil.

2.2 INTRODUCTION

2.2.1 Phosphorus in Agriculture

The agriculture sector is one of the largest contributors to the Idaho economy, with a value of over $3 billion in milk yield alone generated from the Idaho dairy industry in 2021 (*USDA/NASS 2021 State Agriculture Overview for Idaho*, 2021). The dairy industry in Idaho nearly tripled from 1980 to 2012, making Idaho third in the nation for milk production (*Dairy's Economic Impact*, n.d.; Welshans, 2014). The majority of Idaho dairies are located in Southern Idaho in the Magic Valley region (Watson et al., 2014). Dairy cows produce an estimated 115 pounds of manure per day, with yearly attributions of 7 tons per cow (Fischer, 1998). This rapid expansion has serious implications for environmental and human health, as the manure waste produced can become a major source of phosphorus to nearby soils, surface water, and groundwater (Harter et al., 2002); as well as other nutrients like nitrogen and other chemicals and microbes of concern. The application of untreated dairy manure to agricultural fields has a high potential for leaching (Ghezzehei et al., 2014) and the

concentrations of nutrients from current dairies may threaten the health of waterways (Cao & Harris, 2010). However, utilization of dairy manure as a soil amendment has the potential to close the circular bioeconomy while also improving soil health (Biederman & Harpole, 2013). To realize this potential, research aimed at understanding nutrient availability and the mechanisms behind P speciation and availability in soils following amendment with dairy-derived fertilizers are needed.

Phosphorus in the soil exists in organic (P_o) and inorganic (P_i) forms. Plants take up P as phosphate ($H_2PO_4^-$, HPO_4^{2-}), which is present in low concentrations in the rhizosphere (Pierzynski et al., 2005). Primary and secondary soil minerals release P through weathering, however this process is slow and at concentrations that do not meet plant demands (Pierzynski et al., 2005). Availability of P adsorbed onto minerals is dependent on the pH of the soil and the concentration of aluminum (Al), calcium (Ca), and iron (Fe) (Hinsinger, 2001; Pierzynski et al., 2005). Low availability of P in soils often requires fertilizer inputs to sustain crop growth, which are initially plant available but can lead to build up of P stores with time (Pierzynski et al., 2005; Shen et al., 2011). P_o forms in the soil include stable inositol phosphates and phosphonates as well as more labile orthophosphate monoesters and diesters (Turner et al., 2002). Inositol phosphates tend to dominate P_o speciation in soils because they are major species of P_o input and are strongly sorbed to soil due their high charge density (Celi et al., 2000; Turner et al., 2002).

In the calcareous soils of Southern Idaho, P availability is controlled by surface adsorption and precipitation of calcium phosphate minerals, reducing leaching losses of P (Carreira et al., 2006). These reactions decrease P solubility and its availability to plants. In soils with high amounts of exchangeable cations, precipitation dominates over adsorption (Tunesi et al., 1999). In some cases, increasing the amount of fertilizer applied by 0.1 Mg ha^{-1} for every 1% free lime ($CaCO_3$) is recommended (Leytem & Mikkelsen, 2005). When fertilizer is applied to these soils, it remains soluble for a short time following application before it begins to become fixed on clay and $CaCO_3$ surfaces and precipitate to form Ca-P minerals (Leytem & Mikkelsen, 2005; Rivaie et al., 2008). Application of P sources with organic matter hinder the reaction with $CaCO_3$, making P more available (Leytem & Mikkelsen, 2005).

2.2.2 Dairy Waste Management

The reuse of waste streams as potential nutrient sources lends itself to the sustainability of the P cycle (Metson et al., 2016). Land application of manure to agricultural fields increases crop yields and can decrease the amount of synthetic fertilizer that needs to be applied. Manure storage on dairies is dependent on the solids content of the manure. Liquid manure is stored in lagoons and is characterized by low solid content allowing for land application through irrigation systems (Lorimor et al., 2004). Liquid manure is high in total P but varies in P speciation (Pagliari et al., 2013). Liquid

sources have been found to contain 10 – 70% P_o depending on the lagoon and the season (Hansen et al., 2004; Leytem & Westermann, 2005). The primary form of P in dairy lagoon water is orthophosphate (Hansen et al., 2004; Leytem & Westermann, 2005). Liquid manure applications may be more susceptible to leaching than solid manures due to application with water, which can increase movement through the soil (Hansen et al., 2004).

Anaerobic digestion (AD) systems are used on dairies to produce renewable energy from dairy wastes, reducing manure storage while leaving behind residual forms of digested products that are high in nutrients. Over 220 anaerobic digestion systems processed dairy waste in the US in 2021 (*Anaerobic Digestion on Dairy Farms | US EPA*, n.d.). Mazzini et al. (2020) found that AD solids of cattle manure contains 65% – 81% P_i depending on the AD plant (Mazzini et al., 2020). Within P_i species, anaerobic digestion waste has been found to contain stable Ca-P species than undigested manure sources, which may reduce their leaching potential (Güngör et al., 2007). Collins et al. (2020) found that anaerobically digested dairy solids provided similar amounts of P as synthetic fertilizers with no differences in crop yield. High P content in dairy AD solids may provide an alternative to synthetic P fertilizers, with a reduction in volume from traditional manure applications.

Biochar may be a sustainable and economical way to dispose of agricultural waste (Ghezzehei et al., 2014). The use of biochar for nutrient recovery from processed dairy waste, such as anaerobic digestate and manure slurries, has the potential to be used as an enriched soil amendment that is more likely to promote nutrient retention and reduce leaching losses (Ghezzehei et al., 2014; Liang et al., 2014; Sarkhot et al., 2012, 2013; Streubel et al., 2012). In alkaline soils, where biochar does not increase available P through pH increases, its ability to add P to soil is dependent on the P content of the biochar. Biochar releases P more slowly than manure sources and is less dependent on soil properties such as pH and clay content (Liang et al., 2014). Biochar has been used to remove up to 65% of P from liquid manure sources (Sarkhot et al., 2012; Streubel et al., 2012; Wang et al., 2020), which could be due to exchange with surface hydroxyl groups (Sarkhot et al., 2012). P sorbed to biochar is retained during desorption, suggesting that it could be used as a slow release fertilizer (Kizito et al., 2017; Sarkhot et al., 2012).

P recovered on biochars can be largely plant available (Streubel et al., 2012; Wang et al., 2020; Wu et al., 2020). Streubel et al. (2012) found a 30 times increase in water-extractable P from biochar with sorbed P, suggesting that recovered P biochars may increase available P in soils. Wu et al. (2020) found that, in the field, biochar increased total P compared to control soils. Although total P in soil increases with added P from dairy waste streams, low plant availability of P on biochar may reduce yield compared to synthetic fertilizers (Collins et al., 2013). Forms of Ca-P dominate P_i species in most biochars, suggesting that biochar may act as a slow release fertilizer (Robinson et al.,

2017; Rose et al., 2019; Streubel et al., 2012). P recovered from wastewaters using struvite has been used as a slow-release fertilizer with no detrimental effects on plant production compared to commercially available fertilizers (Omidire & Brye, 2022). Over multiple cropping seasons, biochars continue to release P, producing more biomass than synthetic fertilizers with one application over multiple years (Lustosa Filho et al., 2020).

2.2.3 Methods Background

To characterize P biogeochemistry requires knowledge of species of P in soils and amendments. Measuring P speciation in soils requires using multiple methods to provide a more comprehensive view of P cycling and speciation in soils. Thus, this study will use sequential extraction, solution ^{31}P-nuclear magnetic resonance spectroscopy (^{31}P-NMR), P K-edge X-ray absorption near edge structure (XANES), and P-δ^{18}O isotope tracing to characterize P in amended soils.

Characterizing P storage and mobility is dependent on properties of both the applied phosphorus and the soil. Several chemical extraction procedures are used to define phosphorus pools in soil by dissolving forms of P based on the strength of multiple reagents. One of the most common soil phosphorus extraction methods, the Hedley extraction, separates soil P_i into five operationally defined pools: resin-P, $NaHCO_3$-P, NaOH-P, HCl-P, and residual P (Hedley et al., 1982). Sequential extraction using the Hedley procedure is commonly used to operationally define soil P pools according to plant availability but does not provide information on specific P species (Hedley et al., 1982; Negassa & Leinweber, 2009). Modifications to the Hedley procedure by extracting the first pool with H_2O instead of resin are used to target P concentrations in runoff. H_2O-P, or water extractable phosphorus (WEP), was found to be a good method for determining the P available for runoff or leaching (Self-Davis et al., 2000) but is commonly the smallest P pool in the soil profile (Joshi et al., 2016). The H_2O-P and $NaHCO_3$-P are considered the most bioavailable pools and are removed first in the sequential extraction (Self-Davis et al., 2000; Tiessen et al., 1984). NaOH-P, the pool considered to be sorbed to Fe and Al minerals in soil, is moderately available in the long term relative to concentrations in other pools (Hedley et al., 1982; Joshi et al., 2016; Tamburini et al., 2012). The HCl-P pool is associated with Ca-P minerals and occluded P and is unavailable to crop plants in this form (Hedley et al., 1982; Joshi et al., 2016; Tamburini et al., 2012). There are limitations in sequential extraction methods, leading to possible differences between the true soil P pool and the extracted portion of the pool. Sample handling, time between extraction and analysis, and the presence of interfering compounds leads to bias between the measured and actual values of the extracted pools (Condron & Newman, 2011).

^{31}P-NMR is one of the most common methods for determining P_o species in soils (Abdi et al., 2014; B. Cade-Menun & Liu, 2014). ^{31}P-NMR has been utilized in past agricultural studies, however it has mainly been used in pasture systems (B. J. Cade-Menun, 2017). Because P occurs in nature as ^{31}P and not as other isotopes, the concentrations of P species can be determined (B. J. Cade-Menun, 2017). ^{31}P-NMR is capable of identifying molecular species of P in soils, especially P_o, allowing inferences to be made about concentrations in the soil and plant availability (B. J. Cade-Menun, 2017; Gatiboni et al., 2005; Turner, Manhieu, et al., 2003). ^{31}P-NMR doesn't directly observe solid phases of P_i, like orthophosphate being adsorbed onto surfaces or precipitated as Ca-P. Degradation of certain P species during extraction as well as overlapping peaks can make species identification difficult, but data processing can minimize these effects (B. Cade-Menun & Liu, 2014).

P K-edge XANES is a nondestructive molecular probe used to determine P speciation without sample alteration (Beauchemin et al., 2003; Kizewski et al., 2011; J. Liu et al., 2013). XANES is element specific and can identify between precipitated, adsorbed, and organic P species (Ajiboye et al., 2007; Beauchemin et al., 2003; Schulze & Bertsch, 1995). Linear combination fitting (LCF) is used to fit standard spectra with unique features to sample spectra to estimate the amount of each species in complex samples (Beauchemin et al., 2003; Kizewski et al., 2011). Error associated with XANES fitting can be larger than some other elements (10% - 17%) due to lack of distinct features in the spectra of many species (Ajiboye et al., 2007; Beauchemin et al., 2003). In particular, P_o species are difficult to detect with XANES analysis, requiring other techniques, such as ^{31}P-NMR to be used in combination (Prietzel et al., 2013).

Stable isotope tracing using the stable oxygen isotope of orthophosphate (P-δ^{18}O) allows for the tracing of P movements through different soil pools. P-O bonds are stable against abiotic factors and have little exchange with the oxygen in water, preserving the unique source P-δ^{18}O signature (Blake et al., 2005). Kinetic fractionation due to microbial uptake and exchange with water overwrites the original P-δ^{18}O value. The preferential uptake of lighter phosphate isotopologues by plants and microorganisms results in a ~3‰ fractionation (Blake et al., 2005). Mineralization of microbial P also has a kinetic fractionation effect, leading to isotopic values depleted in comparison to the original isotopic value (Liang & Blake, 2009). Intracellular microbial cycling of P leads to a temperature-dependent equilibrium fractionation value between the P-δ^{18}O and the ambient cellular water, which often overwrites other fractionation effects (Blake et al., 2005). As a result, the equilibrium fractionation effect is the dominant process controlling P-δ^{18}O fractionation in soils. Using both the original P-δ^{18}O signature and equilibrium fractionation effects can help to determine the amount of P cycling in soils.

Previous research has also looked at both P sorbed to biochar and anaerobic digestion solids as potential P fertilizers, with mixed results on crop yield (Bach et al., 2021; Collins et al., 2013, 2020). In alkaline soils where P is not made available through changes in pH, dairy amendments may have a different impact on P availability. Past studies have characterized P speciation in soils using sequential extraction, ^{31}P-NMR, and XANES (J. Liu et al., 2015; Weyers et al., 2016). By also determining P-δ^{18}O values in soil pools, this study will further knowledge in P cycling and leaching potential. The call for more mechanistic investigations into biochar-amended soils requires the use of multiple laboratory techniques with care taken to understand its use in specific soil types (Gelardi & Parikh, 2021).To our knowledge, no past studies have used oxygen isotope tracing on biochar amended soils. Additionally, studies on P speciation in biochar with various amendments are highly dependent on production parameters and amendment types, requiring specific studies to predict P speciation in soils. Overall, this study will provide an integrative view of P transformations in soils supplemented with various dairy-derived fertilizers.

2.2.4 Research Goals

The goal of this project is to understand the mechanisms behind P speciation, availability, and transport through calcareous soils amended with various forms of dairy-derived nutrients in a greenhouse study using multiple analytical methods, including Hedley sequential extraction, ^{31}P-NMR, P K-edge XANES, and P-δ^{18}O signatures. Our objectives were to, 1) understand P recovery from dairy waste streams and dairy amendment speciation using extractions, ^{31}P-NMR, and P K-edge XANES, 2) determine plant P availability and storage in calcareous soils using sequential extraction, and 3) quantify soil P speciation and transport following amendment application and a barley growing season using ^{31}P-NMR, P K-edge XANES, and P-δ^{18}O tracing. Information from this study will support future field-scale studies that will use biochar for P removal and integration of various dairy waste streams as alternative P fertilizers.

2.3 MATERIALS & METHODS

Barley was grown in soils collected from Parma, Idaho in a greenhouse experiment to assess P speciation and availability in three different dairy-derived P fertilizer treatments, two non-dairy biochar treatments, a commercially available P fertilizer, and an unfertilized control.

2.3.1 Dairy-Derived Amendments

Amendments were generated from two dairy waste streams at the University of Idaho dairy in Moscow, Idaho. Dairy-derived amendments included fermented dairy solids (FS), dairy lagoon P sorbed to 1% Fe-modified biochar (PBC), and fermented dairy solids mixed with unmodified biochar (FSBC). The two non-dairy biochar treatments were the unmodified biochar (UBC) and a 1% Fe-

modified biochar (1BC). A commercially available biochar (Biochar Now, Berthoud, Colorado) produced from beetle-killed and fire-damaged trees consisting of mixed conifers and sieved to 26 – 50 mesh was used for all biochar treatments. To obtain 1% Fe content, biochar was modified with $FeCl_3$ (Equation 2.2).

$$\text{Volume } FeCl_3 = \frac{m_{biochar} * \%\ \text{Fe desired}}{\%\ \text{Fe in } FeCl_3 * \text{Density } FeCl_3} \qquad \text{Equation 2.2}$$

At the University of Idaho dairy, solids and rinse water are collected in a large lagoon. A bench-scale lab test was conducted to estimate nutrient loading to Fe modified biochars at three solid:solution ratios (1:20, 1:100, and 1:400) with dairy lagoon water. Fe modified biochar was mixed with dairy lagoon water at three solid:solution ratios for two hours. The samples were centrifuged and rinsed with DI water two times before allowing the biochars to dry for three days. Biochars were digested to determine aluminum (Al), calcium (Ca), iron (Fe), potassium (K), magnesium (Mg), manganese (Mn), sodium (Na), phosphorus (P), and sulfur (S) concentrations by inductively coupled plasma optical emission spectrometry (ICP-OES) (Agilent 5110, Santa Clara, California) (Table 2.1) (Enders & Lehmann, 2012). P loading to Fe-modified biochar was greatest at a 1:400 solid:solution ratio, which had ten times more P than biochar in DI water alone. Ca, Fe, K, Mn, Na, and S also increased. Concentration of Al, Ca, Fe, K, Mg, Na, and P of the lagoon water before and after shaking with biochar were also determined by ICP-OES (Table 2.2).

Table 2.1. Al, Ca, Fe, K, Mg, Mn, Na, P, and S content in digested 0.5% Fe-modified biochars after mixing with dairy lagoon water at 1:20, 1:100, and 1:400 solid:solution ratios for two hours. 0.5% Fe-modified biochar was also mixed with DI water at 1:100 solid:solution ratio to serve as a control.

Element	BC:DI water 1:100	1:20	1:100	1:400
	mg kg^{-1}			
Al	1274.5 (279)	1110.0 (119)	1028.9 (104)	1263.1 (191)
Ca	2369.3 (54.7)	2740.3 (176)	3599.6 (70.9)	4145.9 (266)
Fe	6052.5 (248)	5771.9 (162)	7044.4 (266)	6661.7 (438)
K	866.5 (133)	1566.5 (54.4)	1446.4 (81.4)	1589.7 (172)
Mg	666.3 (63.5)	802.5 (67.4)	866.2 (33.0)	942.6 (86.1)
Na	172.9 (29.1)	649.1 (112)	576.4 (44.3)	525.8 (82.4)
P	121.3 (5.39)	324.6 (26.5)	715.2 (9.48)	1024.4 (91.3)
S	91.6 (2.83)	180.6 (17.4)	241.2 (7.65)	275.4 (25.3)

Table 2.2. Concentration of Al, Ca, Fe, K, Mg, Mn, Na, P, and S in lagoon water before and after mixing with 0.5% Fe-modified at 1:20, 1:100, and 1:400 solid:solution ratios for two hours. 0.5% Fe-modified biochar was also mixed with DI water at 1:100 solid:solution ratio to serve as a control.

	Lagoon Water	**1:100 BC:DI water**	**After 1:20**	**After 1:100**	**After 1:400**
			mg L^{-1}		
Al	0.0103 (0.002)	0.0027 (0.000)	0.0053 (0.001)	0.0047 (0.001)	0.0057 (0.001)
Ca	78.86 (0.266)	1.193 (0.114)	68.67 (0.369)	73.80 (0.139)	76.99 (0.055)
Fe	0.035 (0.003)	0.0050 (0.002)	0.0150 (0.002)	0.0113 (0.000)	0.0213 (0.001)
K	202.0 (0.646)	202.0 (0.041)	200.7 (0.331)	201.0 (0.458)	201.6 (0.186)
Mg	44.13 (0.103)	0.2297 (0.004)	41.85 (0.0933)	42.99 (0.108)	43.58 (0.072)
Na	130.9 (0.932)	0.6043 (0.045)	128.6 (0.199)	129.2 (0.654)	128.9 (0.420)
P	10.69 (0.046)	0.0027 (0.001)	5.056 (0.335)	8.558 (0.013)	10.24 (0.039)

To produce the PBC amendment used in the greenhouse, 1% Fe-modified biochar was mixed with dairy lagoon water. Fe-amended biochar was produced by mixing 1 kg of biochar in a large rotating drum with 5 gallons of deionized water. pH was adjusted to 2 to 3 with concentrated HCl and 1 M HCl. After adjusting pH, $FeCl_3$ was added to the mixture. pH was then slowly adjusted to 6 using concentrated NaOH and 1 M NaOH. Biochar was rinsed through a mesh bag filter with about 15 gallons of water until the water ran clear, then dried for one week. In total, 8 kg of 1% Fe-modified biochar was generated.

Dairy lagoon water was pumped into a 400-gallon tank. 1% Fe-modified biochar was then added to the tank at a 1:400 solid:solution ratio and mixed for two hours. After mixing, the biochar was allowed to settle for ten minutes, and then filtered through a bag filter. The recovered biochar was air-dried over three days. UBC, 1BC, and PBC were all autoclaved at 122.8 °C and 18 psi for thirty minutes before use in the greenhouse. Water samples were taken from the top foot of the tank before biochar was added and after allowing biochar to settle for ten minutes after mixing to estimate biochar effects on water quality (Table 2.3). Water samples were analyzed for pH, electrical

conductivity (EC), and turbidity in the field. The rest of the analyses were conducted by the Analytical Sciences Laboratory in Moscow, Idaho, except for total organic carbon (TOC), which was analyzed by Anatek Labs, Inc. in Moscow, Idaho. Dissolved metals were determined by ICP-MS analysis following EPA Method 200.8 (Environmental Monitoring Systems Laboratory, 1996). Alkalinity was determined by titration as per EPA Method 310.1. Nitrate (NO_3) + Nitrite (NO_2) and Ammonia were determined by EPA Method 353.2 and 350.1, respectively using flow injection analysis (FIA). To determine total P, samples were digested with persulfate. Total P and orthophosphate (OrthoP) were determined using spectrometry as per EPA Method 365.3. Total suspended solids (TSS) were determined by EPA Method 160.2. TOC was determined by SM 5310B.

Table 2.3. Summary of dairy lagoon characteristics before and after 1% Fe biochar mixing. Values are averaged from two replicate samples (±standard error).

	Units	IN	OUT
pH		8.37	8.21
EC	ppm	1410	1430
OrthoP	mg/L	4.50 (0.00)	4.3 (0.071)
Total P	mg/L	8.30 (0.495)	7.6 (0.212)
NO_3 + NO_2	mg/L	24.5 (0.354)	23.5 (0.354)
NH_4	mg/L	0.740 (0.042)	0.205 (0.060)
Turbidity	NTU	256	251
Total Suspended Solids	mg/L	225 (10.6)	225 (3.54)
Alkalinity	mg $CaCO_3$/L	665 (24.7)	690 (0.00)
Total Organic Carbon	mg/L	60.1 (0.035)	56.3 (0.00)
Ba	mg/L	0.064 (0.004)	0.066 (0.00)
Ca	mg/L	82.5 (0.354)	80 (0.707)
Cd	mg/L	<0.02	<0.02
Co	mg/L	<0.01	<0.01
Cr	mg/L	<0.05	<0.05
Cu	mg/L	<0.02	<0.02
Fe	mg/L	<0.1	<0.1
K	mg/L	365 (3.54)	360 (0.00)
Mg	mg/L	55.5 (0.354)	55 (0.00)
Mn	mg/L	0.0305 (0.004)	<0.005 (0.00)
Mo	mg/L	<0.25	<0.25
Na	mg/L	170 (0.00)	170 (0.00)
Ni	mg/L	<0.05	<0.05
V	mg/L	<0.02	<0.02
Zn	mg/L	0.098 (0.001)	0.103 (0.005)

Fermented biosolids were collected from Dr. Erik Coat's lab at the University of Idaho where fermented dairy solids are used in experiments to produce bioplastics. The fermenter is operated at a total volume of 16 L with a solids retention time (SRT) of four days. Each day, four liters of liquid is decanted from the fermenter. Coarse solids are strained out of the mixture and the remaining liquid is centrifuged at 9000 RPM for 30 minutes before being filtered to collect the fine solids. Fresh, wet manure is collected bi-weekly from the University of Idaho dairy and refrigerated until use. Manure is added to maintain 8.75 g volatile solids L^{-1} day^{-1} and mixed to 4 L with warm tap water before being added back to the fermenter. Coarse and fine fermented biosolids were collected over one week for use in this study. The solids were dried in a 50 °C oven for about 4 days until mass was stable before being combined at a 1:1 w/w ratio of fine and coarse solids (Peters, C. Personal communication, 2021).

Biochars and fermented biosolids were analyzed for chemical properties to determine their viability for use in the greenhouse (Table 2.4). Biochars (UBC, 1BC, PBC) and mixed fermented biosolids (FS) were analyzed for pH and EC at a 1:10 solid:solution ratio with 18 megaohm deionized water. H2O-P_{MR} was extracted at a 1:10 solid:solution ratio with 18 megaohm deionized water by shaking for one hour, centrifuging at 2875 x g for ten minutes, and filtering through a 0.45 μm PES filter before analyzing colorimetrically on a spectrophotometer (Genesys 10S UV-Vis, Thermo Scientific, Waltham, Massachusetts) (Self-Davis et al., 2000). Total C, N, and S were determined with a CNS analyzer (VarioMax, Elementar Analysensysteme GmbH). Biochars, coarse fermented biosolids, fine fermented biosolids, and mixed fermented biosolids were also digested using the modified dry ash method as in Enders and Lehmann (2012). Samples were placed in a muffle furnace, heated to 500 °C over a 2-h ramp-up period, held at 500 °C for 8 h, then allowed to cool to ambient temperatures. Ashed samples were extracted with 5.0 mL concentrated HNO_3 at 120 °C until dryness was reached. Then, samples were allowed to cool before 1.0 mL HNO_3 and 4.0 mL H_2O_2 were added and extracted at 120 °C until dryness was reached. 1.43 mL HNO_3 was added to the sample, vortexed, then 18.57 mL deionized water was added to achieve 5% acid concentration. Samples were filtered with 0.45 μm PES filters before analysis by ICP-OES. Biochars were analyzed for NO_3 and ammonium (NH_4) by extraction with 2 M KCl at a 1:10 solid:solution ratio (Soil Survey Staff, 2014). Samples were shaken at 200 RPM for 2 h, filtered with a Whatman 42, and analyzed with a Lachat Quikchem Flow Injection Analyzer (Hach USA, Milwaukee, Wisconsin).

Table 2.4. Summary of biochar and fermented biosolids properties. Values are averaged over replicates where applicable (± standard error).

	pH	EC	NO_3	NH_4	Total C	Total N	Total S	H_2O-P_{MR}	Al	Ca	Fe	K	Mg	Mn	Na	P	S
		µS cm^{-1}	mg kg^{-1}	mg kg^{-1}	%	%	%	mg kg^{-1}	mg kg^{-1}	mg kg^{-1}	mg kg^{-1}	mg kg^{-1}	mg kg^{-1}	mg kg^{-1}	mg kg^{-1}	mg kg^{-1}	mg kg^{-1}
UBC	9.58	528	0.295 (0.205)	6.41 (0.311)	77.7 (0.230)	0.25 (0.006)	0.08 (0.041)	3.71 (0.570)	2541	3526	4935	2789	1272	299.3	654.3	232.0	141.5
1BC	7.39	404	0.109 (0.031)	7.18 (0.445)	74.7 (0.243)	0.27 (0.014)	0.13 (0.053)	0.003 (0.00)	2104 (0.250)	2892 (0.016)	6740 (0.069)	2035 (0.105)	1022 (0.042	268.8 (0.002)	660.6 (0.001)	209.3 (0.003)	145.7 (0.008)
PBC	8.81	487	36.75 (0.500)	2.83 (0.290)	77.5 (0.291)	0.36 (0.013)	0.11 (0.013)	19.98 (0.106)	1857 (0.141)	3252 (0.074)	7621 (0.412)	2565 (0.112)	1136 (0.030)	275.5 (0.006)	852.7 (0.003)	412.1 (0.009)	303.4 (0.002)
FS	7.94	3,740	NA	NA	43.4	3.15	0.54	426.8 (19.5)	1474 (15.3)	23500 (21.9)	1770 (20.7)	10110 (10.3)	4598 (54.1)	222.0 (2.70)	3770 (56.5)	7390 (84.3)	NA

2.3.2 Greenhouse Setup

In the greenhouse the following treatments were tested: UBC, 1BC, PBC, FS, fermented biosolids plus unmodified biochar (FSBC), and a commercial fertilizer (CF). Amendments were applied at two rates with five replications to Parma agricultural soils (described in section 2.2.3). The commercial fertilizer (Expert Gardener, All-Purpose Plant Food (Gro Tec. Inc., Madison, Georgia)) had an NPK value of 12 – 5 – 7 and was chosen based on having similar N/P values as the PBC amendment. Biochars were applied at 20 Mg ha^{-1} and 100 Mg ha^{-1} based on a meta-analysis by Glaser and Lehr (2019). The authors found that biochar applications above 10 Mg ha^{-1} had a significant effect on soil P availability and that biochar applications from 20 – 40 Mg ha^{-1} had a significantly lower effect on plant availability than applications above 60 Mg ha^{-1} (Glaser & Lehr, 2019). FS and CF treatments were applied to meet equimolar total P (by HNO_3 digestion) as the PBC treatment (Table 2.4, Table 2.5). FSBC treatment was applied to meet equimolar amounts of total P as the PBC treatment, with half of the phosphorus coming from fermented biosolids and half from the unmodified biochar.

All amendments were homogenously mixed with the soil and filled into rectangular plastic pots (10 cm wide, 35 cm tall). Approximately 2.85 kg of soil were added to each pot. Biochars were added at 28.5 and 142.5 g per pot to meet low and high rates, totaling 11 and 58 mg total P per pot, respectively. FS, CF, and FSBC were applied to match total P additions in the PBC treatments (Table 2.5). Pots were watered to 25.6% soil moisture, which corresponded to 70% water holding capacity in these soils (Bach et al., 2021) using greenhouse tap water with a pH of 7.35 and electrical conductivity of 254 μS. In the greenhouse, pots were randomized in a complete block design and allowed to equilibrate after watering for two days. Two-row GemCraft barley (USDA-ARS) was initially sprouted in the lab in plastic bags. After allowing the pots to equilibrate for two days, five sprouted barley plants were planted at a depth of one inch. 11 days after planting, plants were clipped to three per pot. Moisture conditions in the pots were measured every 1 – 2 days with a soil moisture probe (HydroSense II, Campbell Scientific). Pots were watered when necessary to maintain constant moisture conditions at 70% water holding capacity. To meet N and S requirements, pots were fertilized four times with $(NH_4)_2SO_4$ and NH_4NO_3 (Thermo Scientific, Waltham, Massachusetts) at rates of 5.6 kg S ha^{-1} and 14.0 kg N ha^{-1} per application starting two weeks after planting and continuing every two weeks until the fourth application, totaling 56 kg N ha^{-1} and 22 kg S ha^{-1}. Heights and soil plant analysis development (SPAD) chlorophyll readings from barley were taken about once per week throughout the study. Heights were measured beginning four days after transplanting barley to the greenhouse. SPAD measurements were taken beginning 21 days after planting. Throughout the study, light was provided at a photoperiod of 16/8 hr day/night and

temperature varied between 16 – 27 °C. Starting at week four, blocks were rotated weekly to account for light variance.

Table 2.5. Amendment application rate and total P addition at high and low rates for each treatment.

Amendment	Rate	Application Rate	Mass Application	P Application
		Mg ha^{-1}	g	mg
Unmodified Biochar	Low	20	28.5	6.61
	High	100	142.5	33.1
1% Fe Modifed Biochar	Low	20	28.5	5.96
	High	100	142.5	29.8
1% Fe + Dairy P Modified Biochar	Low	20	28.5	11.7
	High	100	142.5	58.7
Fermented Biosolids	Low	1.12	1.59	11.7
	High	5.58	7.95	58.7
Fermented Biosolids + Unmodified Biochar	Low	18.32	25.3 g UBC + 0.8 g FS	11.7
	High	91.57	126.5 g UBC + 4.0 g FS	58.7
Commercial Fertilizer	Low	0.38	0.54	11.7
	High	1.9	2.69	58.7

2.3.3 Soil Characterization

Surface soils (0 – 30 cm) were collected for use in the greenhouse from the University of Idaho Parma Research Extension Center (43°48”03.2”N; 116°56’18.0” W). The soil is a Greenleaf-Owyhee silt loam, a fine-silty, mixed, superactive mesic Calciargid (USDA NRCS, 1999). The site receives annual rainfall of 229 mm. Mean air temperature is 10 °C. Amended and control soils were sent out for analysis (Kuo Testing Labs, Pasco, WA). All analyses at Kuo were performed according to Gavlak et al. (2005) for the Western region. Soil NO_3-N and NH_4-N was determined by method 3.10 and 3.50, respectively. Olsen P was determined using method 4.10 by ICP-OES. Ca, K, Mg, Na, and Zn were determined by method 5.10. SO_4-S, B, Mn, Cu, and Fe were determined by method 6.10.

Organic matter was determined by method 9.10. Soil pH and EC were determined at a 1:2 soil to 18-megaohm deionized water mass ratio. Total percent carbon, nitrogen, and sulfur were measured using a CNS combustion analyzer (VarioMax, Elementar Analysensysteme GmbH, Ronkonkoma, New York).

2.3.4 Barley Characterization and Harvest

After 109 days, barley was cut above the soil surface. Dry biomass was recorded after drying at 50 °C for 48 hours. Roots were picked out of the soil in the greenhouse and stored at 4 °C. Roots were washed to remove residual soil and weighed to obtain root mass. Barley yield was estimated by weighing the mass of heads. The number of heads per plant were also counted.

2.3.5 Soil Total P

Soil samples were analyzed after use in greenhouse for total P (TP) concentration by ignition with H_2SO_4 extraction (Cade-Menun & Lavkulich, 1997; Saunders & Williams, 1955). Duplicate 0.5 g subsamples of soils were oven-dried at 60 °C overnight. One 0.5 g sample was placed in a cool muffle furnace, temperature was raised to 550 °C over a 2-h heating period, maintained at 550 °C for an hour, and allowed to cool for 2 h. Both samples were extracted at a 1:60 soil to solution ratio of 0.5 M H_2SO_4, shaken for 16 h, centrifuged at 2875 x g for 15 minutes, and decanted. The unincinerated sample was analyzed colorimetrically for P (Murphy & Riley, 1962). The incinerated sample was analyzed by ICP-OES for Al, Ca, Fe, Mn, Mn, and P. The P concentration in the incinerated sample is an estimate of total P. The difference between incinerated and non-incinerated samples is considered total organic P (TP_{org}). The portion which is not TP_{org} is considered to be inorganic P The untreated soil and a Standard Reference Soil (SRM 2711 NIST) was also digested using EPA Method 3050 (aqua regia and H_2O_2 at 90 °C) and the digest analyzed for total P via ICP-OES spectrometer. P recovery of the SRM was 84% of certified value.

2.3.6 Hedley Sequential Extraction

A modified Hedley sequential extraction was used to extract P from operationally defined soil fractions (Hedley et al., 1982; Joshi et al., 2018). The Hedley sequential extraction targets P pools by increasing extractant strength each day from water-extractable P (H_2O-P) to sodium bicarbonate-extractable P ($NaHCO_3$-P), to sodium hydroxide extractable P (NaOH-P), to nitric acid extractable P (HNO_3-P). H_2O-P and $NaHCO_3$-P are considered to be plant available. The H_2O-P pool is also associated with run-off. NaOH-P is associated with Fe/Al oxides, while the HNO_3-P is associated with Ca phosphates (do Nascimento et al., 2015; Hedley et al., 1982; Joshi et al., 2018). Two samples in each experiment batch were extracted in triplicate (RSD for 26 extract triplicates ranged from 0–

11%, except for 2 replicates that had 19% and 23% RSD; Appendix Table B.1). A reference soil was extracted with each batch as a quality control assessment.

For water extraction, 0.5 g of soil were weighed into 50 mL centrifuge tubes with 30 mL of 18 megaohm deionized water and shaken for 16 h. The following day, samples were centrifuged at 2875 x g for 10 minutes, and the supernatant filtered through 0.45 μm PES membrane filter. The soils were then extracted with 0.5 M $NaHCO_3$ for 16 h at a 1:60 solid:solution ratio. The extract was centrifuged at 2875 x g, filtered with 0.45 μm PES filter. Next, soils were shaken with 0.1 M NaOH for 16 hours, centrifuged at 2875 x g and filtered with a 0.45 μm PES filter. Finally, the soils were extracted with 1 M HNO_3 at a 1:60 solid:solution ratio, shaken for 16 hours, centrifuged at 2875 x g and filtered through 0.45 μm PES filter. H_2O-P and $NaHCO_3$-P extracts were analyzed colorimetrically (Murphy & Riley, 1962). Molybdate reactive phosphorus was measured colorimetrically and is an estimate of P_i in solution (Murphy & Riley, 1962). Due to hydrolysis of organic compounds during the extraction and lack of reaction of some inorganic P compounds, we refer to this fraction as H_2O-P_{MR} and $NaHCO_3$-P_{MR} (Haygarth & Sharpley, 2000). The difference between the total H_2O-P measured by ICP and H_2O-P_{MR} is molybdate unreactive phosphorus (H_2O-P_{MU}), which primarily consists of P associated with organic, colloidal, and non-hydrolyzable forms (Haygarth & Sharpley, 2000). Aliquots from the H_2O, NaOH, and HNO_3 extractants were analyzed for multiple elements by ICP-OES. $NaHCO_3$ extracts were not analyzed on the ICP-OES due to high Na concentrations that needed dilution causing P to be below detection level (0.01 mg/L). Eight 1:10 diluted $NaHCO_3$ extract samples were selected to be analyzed by ICP-OES. For the eight samples, P concentrations determined colorimetrically were within 10% of P concentrations determined by ICP-OES (Table 2.6). Thus, we considered the colorimetric data from the $NaHCO_3$ extracts as total P in the $NaHCO_3$-P pool.

Table 2.6. Comparison of $NaHCO_3$-P_i analyzed by ICP and colorimetrically.

Sample	$NaHCO_3$-P_{MR}	$NaHCO_3$-P (ICP)	% Difference
	mg kg^{-1}		
PBCH (3)	23.3	21.6	7.4
UBCL (4)	23.3	21.6	7.4
1BCH (4)	22.2	21.6	2.9
PBCH (4)	25.1	25.2	0.26
FSH (4)	24.9	25.2	1.2
CFH (4)	24.3	25.2	3.7
PBCH (5)	24.5	22.8	7.0
CFH (5)	25.1	25.2	0.26

2.3.7 Extractable Soil P Isotopic Analysis

For isotopic analysis, soils were extracted sequentially for H_2O-P, $NaHCO_3$-P, NaOH-P, and HNO_3-P. The NaOH-P pool extractant solution was not used for isotopic analysis due to difficulties with the Ag_3PO_4 precipitation method (described below). For the total HNO_3 extraction, soils were shaken with 1 M HNO_3 at a 1:60 solid:solution ratio for 16 hours, centrifuged, and filtered through a Whatman 42 filter. Replicate treatment samples were extracted to estimate greenhouse sample variation.

For isotope analysis, a modified Nisbeth et al. (2019) protocol was used to extract silver phosphate (Ag_3PO_4) crystals from the soil samples. This method was initially developed for use in freshwater systems. Due to the nature of the soil matrix, an organic matter removal step (DAX-8) and a cation removal step were added to the protocol, as described in Tamburini et al. (2010). The complete method can be found in Appendix A. In short, magnesium-induced co-precipitation of brucite (MagIC) removes P from the sample solution, reducing sample size. Dissolved organic matter is removed using DAX-8 resin. This step was performed twice due to high OM in these samples. Cations were then removed using AG50WX8 resin, followed by removal of contaminants soluble at low pH through ammonium phospho-molybdate (APM) precipitation and removal of contaminants soluble at high pH by magnesium ammonium phosphate (MAP) precipitation. Finally, cations are removed through a cation resin wash and residual chloride ions are removed with silver nitrate ($AgNO_3$). Silver ammine solution is added to facilitate the precipitation of Ag_3PO_4. Precipitated crystals are rinsed with deionized water and dried before analyzing using a high temperature

conversion elemental analyzer coupled to a Delta V Advantage continuous flow isotope ratio monitoring mass spectrometer (TCEA-IRMS, ThermoFisher Scientific, Waltham, Massachusetts). Ag_3PO_4 and benzoic acid standards (ThermoFisher Scientific, Waltham, Massachusetts and HEKAtech GmbH, Wegberg, Germany) were used to calibrate samples. Internal standard deviation of standards was 0.4‰, thus differences of greater than 0.4‰ were not due to instrument variation. The measured P-$\delta^{18}O$ values are reported relative to Vienna Standard Mean Oceanic Water (VSMOW) in per mil (‰) notation.

2.3.8 Soil P Speciation by P-NMR Analysis

Soil samples at high amendment rates were selected for ^{31}P-NMR analysis to identify concentrations and speciation of organic P in soils. PBCH and FSBCH samples were extracted in duplicate. Amendments UBC, PBC, and FS were also extracted for NMR analysis. Standard procedures for ^{31}P-NMR analysis were used for extraction (B. J. Cade-Menun & Preston, 1996; B. Cade-Menun & Liu, 2014). 2 g dry-mass equivalent undried soil samples and biochars were suspended in 20 mL of 0.5 M NaOH and 0.1 M Na_2EDTA solution, shaken for 4 h, centrifuged at 2875 x g for 20 minutes. Fermented biosolid was extracted at a 1:20 solid:solution ratio. The extraction supernatants were decanted, with care taken to not decant any solids. If necessary, samples were filtered with a Whatman 41 to remove floating particulate matter. A 1 mL aliquot was taken from each supernatant and diluted 1:10 for analysis by ICP-OES for total P, Fe, and Mn concentrations. The rest of the sample supernatants were freeze-dried. P/(Fe+Mn) ratios in the sample were used to determine delay times for sufficient relaxation in these samples (B. Cade-Menun & Liu, 2014; R. W. McDowell et al., 2006). ^{31}P-NMR spectroscopy was conducted at the University of Idaho's Department of Chemistry. 0.25 g of freeze-dried extract powder from each sample was dissolved in 0.9 mL of NaOH-EDTA solution with added Fe and 0.1 mL D_2O. Fe was added with the NaOH-EDTA solution in order to get a 10 s relaxation time for samples (R. W. McDowell et al., 2006). The solution was vortexed, allowed to sit for 20 minutes, then centrifuged at 2875 x g for 10 minutes. 0.5 mL of sample supernatant was added to a 5 mm NMR tube. NMR spectra were obtained at 202.48 MHz on a 500 MHz Bruker Avance III spectrometer equipped with a 5 mm broadband probe. The 1D ^{31}P spectra were acquired with 45° pulses at room temperature (22°C), with proton decoupling, and a total recycle delay (pre-scan delay plus acquisition time) of 10 s for 3,000 to 8,000 scans, determined by signal-to-noise ratios. Spectra were plotted with 10 Hz line-broadening for the main spectra and 3 Hz line-broadening to assess finer details. Peak areas were computed by integration and visual inspection using SpinWorks Software (SpinWorks 4.2.11, Kirk Marat), with correction for the degradation of orthophosphate diesters (B. Cade-Menun & Liu, 2014; Schneider et

al., 2016). Peak assignments were made from the literature and confirmed using a phytate spike (B. J. Cade-Menun, 2015).

2.3.9 Phosphorus K-Edge XANES Analysis

X-ray absorption near edge structure (XANES) spectroscopy was used to determine P species present in soils. XANES spectra were collected from soils with amendments applied at a high rate. XANES spectra from biochar amendments (UBC, 1BC, PBC) were also collected. All samples were ground and sieved to less than 500 μm before mounting to sample holder with silicon (Si) free tape. P K-edge XANES spectra of biochars and standards were collected at the Soft X-ray Micro-characterization Beamline (SXRMB) at the Canadian Light Source (CLS) in Saskatoon, Canada. SXRMB uses an InSb(III) monochromator with a 300 μm x 300 μm beam size. The beamline was calibrated to 2158 eV using $ZnPO_4$ powder. Amendment spectra were collected using a Vortex detector. Spectra were collected from 2135 – 2190 eV with a step size of 1 eV on the pre edge region (2110 – 2145 eV), 0.25 eV in the near edge region (2145.25 – 2180 eV), and 0.5 eV in the post edge region (2180.5 – 2200 eV). A minimum of ten spectra were collected for each sample. Soil samples were analyzed for P K-edge XANES at Beamline 14-3a at the Stanford Synchrotron Radiation Lightsource (SSRL). Spectra were collected with a Vortex Detector. Spectra were collected from 2110 – 2290 2145.5 eV with a step size of 2.5 eV on the pre-edge region (2110 – 2145 eV), 0.1 eV in the near edge region (2145.25 – 2180 eV), and 0.25 eV in the post edge region (2180.5 – 2200 eV). Seven detectors were used (FF1-FF7), visually inspected, and averaged for each spectra. Ten spectra were collected per sample.

The collected scans were analyzed using the Athena software program (Ravel & Newville, 2005). Spectra for each sample were averaged to improve signal to noise ratio. Each spectrum was calibrated at 2151.6 eV set as the inflection point of the main edge; allowing for the main edge peak height and shape, and pre or post-edge peaks to be linearly separable elements in linear combination fitting (LCF). Background subtraction at the pre- and post-edge regions were performed on the averaged spectra. The same background subtraction parameters were used for each spectra to provide consistent background subtraction effects across the samples and standards. Supervised linear combination fitting was performed to determine speciation of each spectrum. Initially, all standards were used to fit the spectra, followed by reduction to five standards that were deemed to represent the major species possible in the sample spectra (adsorbed P, apatite, DCDP, DCDP 50:50 Ca:Mg, and phytic acid). Standards were iteratively removed if they comprised zero or less precent of the of sample fit. Previous tests of P soil XANES LCF indicated that the accuracy is approximately 5-15 percent absolute (Gustafsson et al., 2020; Ingall et al., 2011). In fitting of the spectra, it was observed that the Ca-P minerals in many cases could be substituted for each other with only a slightly

decreased fit quality, as judged by reduced chi square. Thus, the fit of these minerals is grouped for interpretation as Ca-P minerals.

2.3.10 Statistical Analysis

Data analysis was performed using R version 4.1.2 (R Studio Team, 2020). Hedley sequential extraction data, plant biomass data, and total soil P were analyzed in a generalized linear mixed model with treatment and rate of application as fixed effects and block as a random effect. Model fit was assessed by examining log-likelihoods and inspecting residual plots. Package "lme4" (Bates et al., 2015) was used for model building and ANOVA. Means comparisons were performed using R package "emmeans" (Lenth et al., 2022). Significance was determined at a $p \leq 0.05$ using a Tukey test.

Other data was tested for significance by fitting the data to the analysis of variance (ANOVA) linear models and Tukey HSD test was used for assessing for statistical differences ($P<0.05$). Pearson's correlation coefficients were used to evaluate the strength of relationships between soil properties.

2.4 RESULTS

2.4.1 Soil Characterization

Key soil properties of the amended soils were measured before use in the greenhouse (Table 2.8). Olsen P was slightly greater in the amended soils than the control soil. Percent organic matter, micronutrients (Zn, Mn, Fe), and soluble salts were higher in the amended soils than the control. Base saturation and Ca decreased slightly. pH and EC were measured for all amended soils before and after use in the greenhouse (Table 2.7). Before use in the greenhouse study, soil pH of each treatment ranged from 8.25 to 8.40. The pH of soils from after each treatment ranged from 8.33 – 8.55. After treatment and plant growth, a slight pH increase occurred in all samples, except for CF-H. EC initially increased with all amendment additions. After use in the greenhouse, EC decreased in all soils except for CF-H and the control soil.

Table 2.7. Summary of pH and EC (± standard error) of samples before and after use in the greenhouse. Time final values are averaged from five treatment replicates (n = 5).

Sample	pH (time zero)	pH (time final)	EC (µS/cm) (time zero)	EC (µS/cm) (time final)
UBCL	8.27	8.52 (0.04)	172	126 (4.50)
UBCH	8.29	8.54 (0.07)	167	128 (8.22)
1BCL	8.27	8.44 (0.06)	153	138 (8.22)
1BCH	8.31	8.45 (0.04)	169	146 (3.73)
PBCL	8.38	8.51 (0.05)	149	124 (4.02)
PBCH	8.31	8.45 (0.04)	237	157 (10.5)
FSL	8.38	8.47 (0.02)	166	131 (6.43)
FSH	8.25	8.55 (0.02)	285	131 (2.56)
FSBCL	8.40	8.54 (0.05)	151	123 (4.31)
FSBCH	8.39	8.49 (0.03)	177	136 (5.18)
CFL	8.27	8.48 (0.04)	137	127 (3.21)
CFH	8.37	8.33 (0.06)	131	184 (23.6)
Control	8.32	8.55 (0.06)	85	120 (6.06)

Table 2.8. Summary of soil characteristics of amended soil samples before use in the greenhouse. Standard errors denoted in parentheses for control (n = 3).

Sample	NO_3-N		NH_4-N		Olsen P	K	Ca	Mg	Na	SO_4-S	B	Zn	Mn	Cu	Fe	Soluble salts	OM	Total Bases	Base Saturation			
	lbs/ac	mg/kg	lbs/ac	mg/kg	mg/kg	mg/kg	meq/100g	meq/100g	meq/100g	mg/kg	mg/kg	mg/kg	mg/kg	mg/kg	mg/kg	1:01	%	meq/100g	%Ca	%Mg	%K	%Na
Control	33 (0.72)	8.3 (0.15)	15 (0.47)	3.7 (0.14)	18.7 (0.27)	355 (4.8)	17.7 (0.31)	2.8 (0.03)	0.3 (0.01)	3 (0.00)	0.57 (0.02)	2.7 (0.16)	2.9 (0.16)	1.2 (0.03)	11 (0.27)	0.25 (0.01)	1.05 (0.03)	21.8 (0.35)	81.2 (0.12)	13.1 (0.15)	4.2 (0.05)	1.4 (0.03)
UBC-L	18	9.1	5	2.3	20	363	17	2.7	0.25	5	0.58	3.2	6.5	1.4	16	0.36	1.36	20.9	81.3	13	4.3	1.2
UBC-H	17	8.7	4	2.2	20	373	16.3	2.6	0.25	5	0.55	3	8.4	1.3	14	0.38	1.46	20.2	80.7	13	5	1.2
1BC-L	15	7.3	4	1.9	19	350	16.4	2.6	0.23	4	0.53	3	4.7	1.3	14	0.28	1.4	20.2	81.4	13	4.5	1.1
1BC-H	14	6.9	4	2.2	19	334	15.6	2.5	0.24	3	0.57	3.3	7.3	1.3	14	0.48	1.48	19.2	81.5	12.8	4.7	1.2
PBC-L	18	8.9	4	2.1	22	365	16.7	2.8	0.23	4	0.53	2.9	5	1.3	12	0.32	1.31	20.6	81	13.3	4.4	1.1
PBC-H	21	10.6	5	2.3	21	357	16	2.6	0.27	8	0.56	3.2	6	1.3	13	0.48	1.4	19.7	81.2	12.9	4.6	1.4
FS-L	23	11.6	5	2.6	20	343	16.1	2.5	0.23	5	0.54	2.9	4.3	1.3	13	0.4	1.22	19.8	81.3	12.8	4.5	1.2
FS-H	17	8.4	6	2.9	20	370	16.5	2.7	0.25	5	0.52	3.2	4.6	1.3	13	0.34	1.24	20.3	81.1	13.1	4.4	1.2
FSBC-L	22	10.8	4	2	19	349	15.9	2.6	0.23	7	0.54	3.1	5	1.3	12	0.32	1.41	19.7	80.8	13.3	4.6	1.2
FSBC-H	18	9.1	4	2.2	19	381	17	2.6	0.26	5	0.55	3.1	6.5	1.4	13	0.38	1.53	20.9	81.4	126	4.8	1.2
CF-L	13	6.7	6	2.8	19	340	16.1	2.6	0.26	4	0.56	3.1	4.3	1.3	13	0.28	1.35	19.8	81.1	13.2	4.5	1.3
CF-H	14	6.8	6	3.1	19	353	16.8	2.7	0.22	4	0.54	2.9	4.1	1.3	13	0.18	1.33	20.6	81.7	13.1	4.4	1.1

2.4.2 Plant Characterization

Root mass, plant biomass, and plant yield varied across amendment type and level (Table 2.9). Differences among treatments and levels varied between root mass, biomass, yield, and number of heads. Neither treatment nor level was significant for root mass. For biomass, yield, and number of heads per plant, both treatment and level were significant. At the low level of application, plant biomass, yield, and number of heads was significantly greater than at the high level of application. Plant biomass was not significantly different for the CF, FS, and PBC treatments, however the yield of FS and PBC was significantly greater than for CF. Plant height was measured weekly for each of the treatments (Appendix Table B.2)

Pairwise comparisons of treatments within the high and low level and comparisons of each treatment at the high and low application rate are shown in Table 2.10. Plant biomass of PBC and 1BC were significantly greater at the low application rate. At the high level, 1BCH biomass was significantly less than CFH. Compared to the control, CFH, CFL, 1BCL, PBCL, FSL, and FSH were significantly greater. Yield in 1BC and CF were significantly greater at the low application rate than high application rate. In the CFH treatment the barley did not form any heads. PBCH and FSH both had significantly greater yield than CFH. Nothing had a significantly different yield from the control. $P = 0.08$ for the comparison of CFH yield to control. For the number of heads per plant, CFH was significantly less than CFL. At the high level, PBCH and FSH had greater number of heads than CFH. CFH was also the only treatment with significantly less heads than the control.

Table 2.9. Estimated marginal means for main effects of treatment and level on root mass, dried plant biomass, yield, and number of barley heads per plant. Values in parentheses are standard errors. Main effects indicated by superscript letters are statistically not different at a 95% confidence level.

	Root Mass	**Biomass**	**Yield Mass**	**# of Heads**
		g^{-1}		**$plant^{-1}$**
Main Effects				
Treatment				
UBC	3.48^{a}	10.9^{a}	2.54^{ab}	4.5^{ab}
	(0.205)	(0.488)	(0.653)	(0.992)
1BC	3.36^{a}	11.5^{a}	3.72^{ab}	6.4^{ab}
	(0.156)	(0.456)	(0.705)	(0.748)
PBC	4.21^{a}	12.2^{ab}	4.38^{b}	7.5^{b}
	(0.316)	(0.437)	(0.533)	(0.734)
FS	4.14^{a}	12.3^{ab}	4.09^{b}	6.5^{ab}
	(0.656)	(0.347)	(0.556)	(0.582)
FSBC	3.79^{a}	11.1^{a}	2.91^{ab}	5.1^{ab}
	(0.360)	(0.317)	(0.606)	(0.912)
CF	4.04^{a}	13.3^{b}	1.74^{a}	3.5^{a}
	(0.461)	(0.406)	(0.623)	(1.27)
Level				
Low	3.67^{a}	12.4^{a}	4.04^{a}	6.80^{a}
	(0.208)	(0.250)	(0.270)	(0.461)
High	4.01^{a}	11.4^{b}	2.42^{b}	4.37^{b}
	(0.243)	(0.271)	(0.419)	(0.560)

Table 2.10. Estimated marginal means for average biomass, root biomass, yield mass, and number of grain heads for GemCraft barley harvested from greenhouse pot trial. Values in parentheses are standard errors. Pairwise comparisons of treatments within each level and comparisons to control indicated by superscript letters are not statistically different at a 95% confidence level within the level of application. Significant differences at a 95% confidence level for the same treatment at high and low level of application are indicated by an asterisk.

Sample	Root Mass (g)	Biomass (g)	Yield Mass (g)	# of Heads
		g plant^{-1}		plant^{-1}
Control	4.162^{a}	10.056^{a}	3.016^{ab}	5.6^{a}
	(0.421)	(0.438)	(0.768)	(0.678)
High Level of Amendment				
UBCH	3.388^{a}	11.026^{abc}	2.300^{ab}	4.0^{ab}
	(0.346)	(0.714)	(0.969)	(1.64)
1BCH	3.184^{a}	10.378^{ab*}	2.274^{ab*}	5.0^{ab}
	(0.114)	(0.397)	(1.06)	(1.14)
PBCH	4.136^{a}	11.380^{abc*}	3.952^{b}	6.2^{ac}
	(0.357)	(0.715)	(1.04)	(1.11)
FSH	4.464^{a}	12.416^{bc}	3.716^{b}	6.2^{ac}
	(1.289)	(0.690)	(1.02)	(1.11)
FSBCH	4.652^{a*}	10.562^{abc}	2.110^{ab}	4.2^{ab}
	(0.401)	(0.495)	(1.06)	(1.28)
CFH	4.218^{a}	12.610^{c}	0.166^{a*}	0.6^{b*}
	(0.233)	(0.447)	(0.105)	(0.400)
Low Level of Amendment				
UBCL	3.566^{a}	10.766^{ab}	2.782^{a}	5.0^{a}
	(0.257)	(0.743)	(0.975)	(1.26)
1BCL	3.544^{a}	12.632^{bcd*}	5.166^{a*}	7.8^{a}
	(0.282)	(0.378)	(0.261)	(0.49)
PBCL	4.274^{a}	12.992^{cd*}	4.806^{a}	8.8^{a}
	(0.565)	(0.155)	(0.332)	(0.583)
FSL	3.824^{a}	12.202^{bcd}	4.474^{a}	6.8^{a}
	(0.473)	(0.244)	(0.525)	(0.490)
FSBCL	2.922^{a*}	11.638^{abc}	3.702^{a}	6.0^{a}
	(0.221)	(0.252)	(0.458)	(1.30)
CFL	3.862^{a}	14.034^{d}	3.312^{a*}	6.4^{a*}
	(0.941)	(0.537)	(0.706)	(1.69)

2.4.3 Soil Total P

Average TP measured by incineration and H_2SO_4 extraction ranged from 1072 mg kg^{-1} to 1142 mg kg^{-1} (Figure 2.1, Table 2.11). The untreated soil was also digested using Aqua Regia (EPA 3050) and resulted in TP concentration of 993 mg/kg vs 1102 mg/kg in the incineration H_2SO_4 digest (aqua regia digest of a certified reference material recovered 84% of the TP). Thus, TP measured by

H_2SO_4 extraction after incineration is an accurate measure of TP. TP_{org} concentrations ranged from 104 mg kg^{-1} to 170 mg kg^{-1} (10-16% of TP). There were no significant differences in TP or TP_{org} between treatments or level.

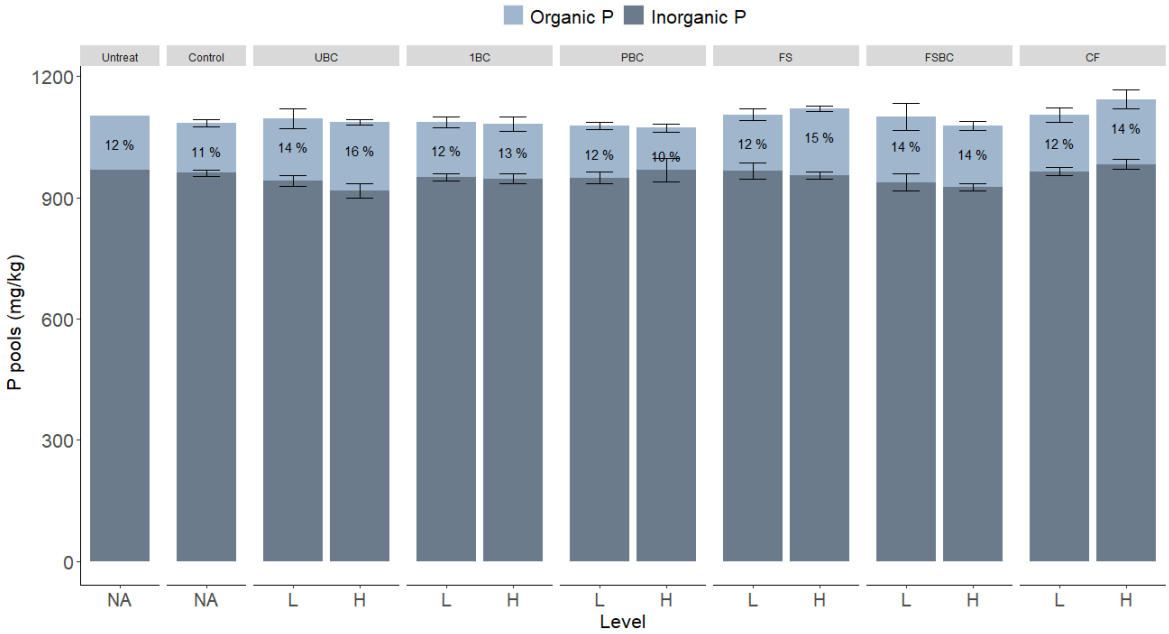

Figure 2.1. Total organic and inorganic P in soils used in greenhouse pot trials determined by difference of H_2SO_4 extraction of incinerated and non-incinerated soils. Numbers within bars are percent organic P. Error bars denote standard error (n = 5).

Table 2.11. Estimated marginal means for total P by incineration (TP), organic P (P_o), and % P_o for all treatments and levels. Values in parentheses represent standard errors.

	TP	P_o	P_o
	mg P kg^{-1}		%
Untreated Soil	1102	133.1	12.07
Control	1084	123.2	11.33
	(9.44)	(15.5)	(1.34)
High Level of Amendment			
UBC-H	1086	169.6	15.58
	(6.67)	(22.3)	(1.99)
1BC-H	1083	136.1	12.52
	(18.2)	(12.2)	(0.961)
PBC-H	1073	104.3	9.69
	(10.3)	(32.1)	(2.98)
FS-H	1121	165.5	14.77
	(7.28)	(7.47)	(0.662)
FSBC-H	1079	151.9	14.04
	(11.4)	(15.4)	(1.29)
CF-H	1143	160.3	13.92
	(23.2)	(22.9)	(1.75)
Low Level of Amendment			
UBC-L	1096	154.5	13.97
	(25.0)	(23.7)	(1.34)
1BC-L	1086	135.6	12.45
	(13.9)	(8.72)	(0.684)
PBC-L	1077	128.2	11.87
	(8.57)	(18.2)	(1.65)
FS-L	1105	138.7	12.48
	(13.7)	(26.1)	(2.26)
FSBC-L	1099	161.3	14.42
	(33.8)	(35.8)	(2.74)
CF-L	1104	139.1	12.48
	(17.3)	(25.5)	(2.09)

2.4.4 Hedley P Characterization

Concentrations in the four pools (H_2O-P, $NaHCO_3$-P, NaOH-P, and HNO_3-P) from the Hedley extraction are shown in Figure 2.2. Other elements extracted in each of the Hedley pools determined by ICP-OES are shown in Appendix Tables B.3-B.5. The total amount of P extracted was greatest in the HNO_3-P extraction and lowest in the H_2O-P extraction. H_2O-P_{MR} and H_2O-P

determined by ICP were within 3% of each other, indicating that most of the P in this pool is inorganic (Table 2.14); the $NaHCO_3$-P pool was also nearly all $NaHCO_3$-P_{MR} (Table 2.6). The $NaHCO_3$-P and NaOH-P pools extracted similar amounts of P across all treatments. The greatest amount of P in the HNO_3-P fraction indicates that this pool is the major P sink in this soil. The sum of all the sequentially extracted pools in the soils accounted for 76% – 81% of TP measured by incineration. The unextracted P (19% – 24% of remaining TP) comprises soil P that is not extractable and thus not readily available for plant uptake or leaching (Hedley et al., 1982).

Main effects of treatment and level are shown in Table 2.12. In the H_2O-P pool, treatment, level, and the interaction between treatment and level was significantly different. In the $NaHCO_3$-P pool, treatment and level were significantly different. PBC, FS, and FSBC were not significantly different from CF in the H_2O-P or $NaHCO_3$-P pools. Additionally, the no-P treatments, UBC and 1BC, had significantly less P than CF. Amendments applied at the high level supplied significantly more P than those at the low level in the H_2O-P and $NaHCO_3$-P pools. The interaction effect in the H_2O-P pool is from the increase in P at the low application of 1BCL compared to the high application. There were no significant effects in the NaOH-P pool. Treatment was significant in the HNO_3-P pool. In the HNO_3-P pool, FS and FSBC were not significantly different than CF. PBC was the only dairy-derived treatment in the HNO_3-P pool that had significantly less P than CF.

Pairwise comparisons of treatments within level as well as the comparison of treatments to each other at the high and low level provides more insight into P dynamics in these pools (Table 2.13). In the H_2O-P pool, CFH, FSBCH, PBCH, and FSH were all significantly greater than the control and 1BCH. CFH, PBCH, and FSH were also significantly greater than UBCH. Between levels, CF, FSBC, PBC, FS were all significantly greater when applied at a high rate compared to a low rate. In the $NaHCO_3$-P pool, CFH, PBCH, and FSH were significantly different than the control group. At the high level, CF was significantly greater than UBC, 1BC, and FSBC. Across levels, PBC and CF were significantly different at the high application rate than the low rate. At the high level, HNO_3-P CF was significantly greater than UBC, 1BC, and PBC. FS was also significantly greater than 1BC. At the low level, UBC and 1BC were significantly different from each other. Nothing was significantly different from the control. Overall, compared to the untreated soil, average P concentrations in the treatments decreased for H_2O-P, $NaHCO_3$-P, and HNO_3-P. Average P concentrations increased in the NaOH-P pool, but this was not significant.

Table 2.12. Estimated marginal means for main effects of treatment and level on Hedley H_2O, $NaHCO_3$, NaOH, and HNO_3 P pools. Values in parentheses are standard errors. Main effects indicated by superscript letters are statistically not different at a 95% confidence level.

	H_2O	$NaHCO_3$	NaOH	HNO_3
		mg kg^{-1}		
Main Effects				
Treatment				
UBC	8.51^{ab}	22.3^{a}	21.9^{a}	802^{ab}
	(0.243)	(0.995)	(0.501)	(10.0)
1BC	8.05^{a}	21.8^{a}	22.7^{a}	790^{a}
	(0.140)	(0.471)	(0.506)	(11.8)
PBC	9.12^{bc}	22.9^{ab}	22.5^{a}	785^{a}
	(0.283)	(0.643)	(0.399)	(9.73)
FS	9.53^{c}	24.0^{ab}	23.2^{a}	826^{b}
	(0.296)	(0.510)	(0.553)	(11.3)
FSBC	9.09^{bc}	22.9^{ab}	23.0^{a}	809^{ab}
	(0.214)	(0.538)	(0.381)	(11.0)
CF	9.38^{c}	25.1^{b}	22.5^{a}	828^{b}
	(0.299)	(0.936)	(0.485)	(8.12)
Level				
Low	8.51^{a}	22.2^{a}	22.3^{a}	813^{a}
	(0.100)	(0.271)	(0.225)	(4.90)
High	9.38^{b}	24.1^{b}	22.9^{a}	801^{a}
	(0.186)	(0.515)	(0.306)	(7.64)

Table 2.13 Estimated marginal means for Hedley H_2O, $NaHCO_3$, NaOH, and HNO_3 P pools. Values in parentheses are standard errors. Pairwise comparisons of treatments within each level and comparisons to control indicated by superscript letters are not statistically different at a 95% confidence level within the Hedley pool and level of application. Significant differences at a 95% confidence level for the same treatment at high and low level of application are indicated by an asterisk.

Treatment	H_2O-P	$NaHCO_3$-P	NaOH-P	HNO_3-P	Total P
			mg kg^{-1}		
Untreated	13.5	28.4	19.9	832	893
	(0.190)	(1.18)	(1.06)	(12.5)	(12.59)
Control	8.10^{a}	20.7^{a}	22.2^{a}	801^{ab}	852^{ab}
	(0.149)	(0.477)	(0.346)	(11.0)	(11.41)
			High Level Application		
UBC	8.75^{ab}	23.0^{ab}	22.1^{a}	784^{ab}	838^{ab}
	(0.436)	(1.98)	(0.974)	(5.15)	(6.08)
1BC	7.85^{a}	21.7^{ab}	23.2^{a}	770^{a}	823^{a*}
	(0.052)	(0.257)	(0.343)	(15.0)	(14.7)
PBC	9.88^{c*}	24.5^{bc*}	22.9^{a}	782^{ab}	839^{ab}
	(0.102)	(0.550)	(0.568)	(19.1)	(19.7)
FS	10.3^{c*}	25.0^{bc}	23.4^{a}	827^{b}	885^{b}
	(0.293)	(0.657)	(1.09)	(22.5)	(23.4)
FSBC	9.48^{bc*}	23.3^{a}	23.3^{a}	811^{ab}	868^{ab}
	(0.308)	(1.01)	(0.669)	(19.8)	(21.0)
CF	10.0^{c*}	27.2^{c*}	22.7^{a}	829^{b}	889^{b}
	(0.249)	(1.12)	(0.877)	(15.2)	(16.7)
			Low Level of Application		
UBC	8.27^{a}	21.6^{a}	21.7^{a}	820^{a}	872^{a}
	(0.218)	(0.527)	(0.406)	(15.9)	(16.25)
1BC	8.24^{a}	21.9^{a}	22.2^{a}	811^{a}	863^{a*}
	(0.257)	(0.962)	(0.957)	(13.9)	(15.3)
PBC	8.35^{a*}	21.3^{a*}	22.1^{a}	788^{a}	839^{a}
	(0.237)	(0.501)	(0.553)	(7.59)	(8.00)
FS	8.79^{a*}	23.0^{a}	23.0^{a}	825^{a}	880^{a}
	(0.196)	(0.470)	(0.420)	(8.03)	(8.52)
FSBC	8.68^{a*}	22.5^{a}	22.6^{a}	807^{a}	861^{a}
	(0.172)	(0.453)	(0.382)	(12.2)	(12.9)
CF	8.71^{a*}	23.1^{a*}	22.2^{a}	826^{a}	880^{a}
	(0.342)	(0.794)	(0.503)	(8.10)	(9.23)

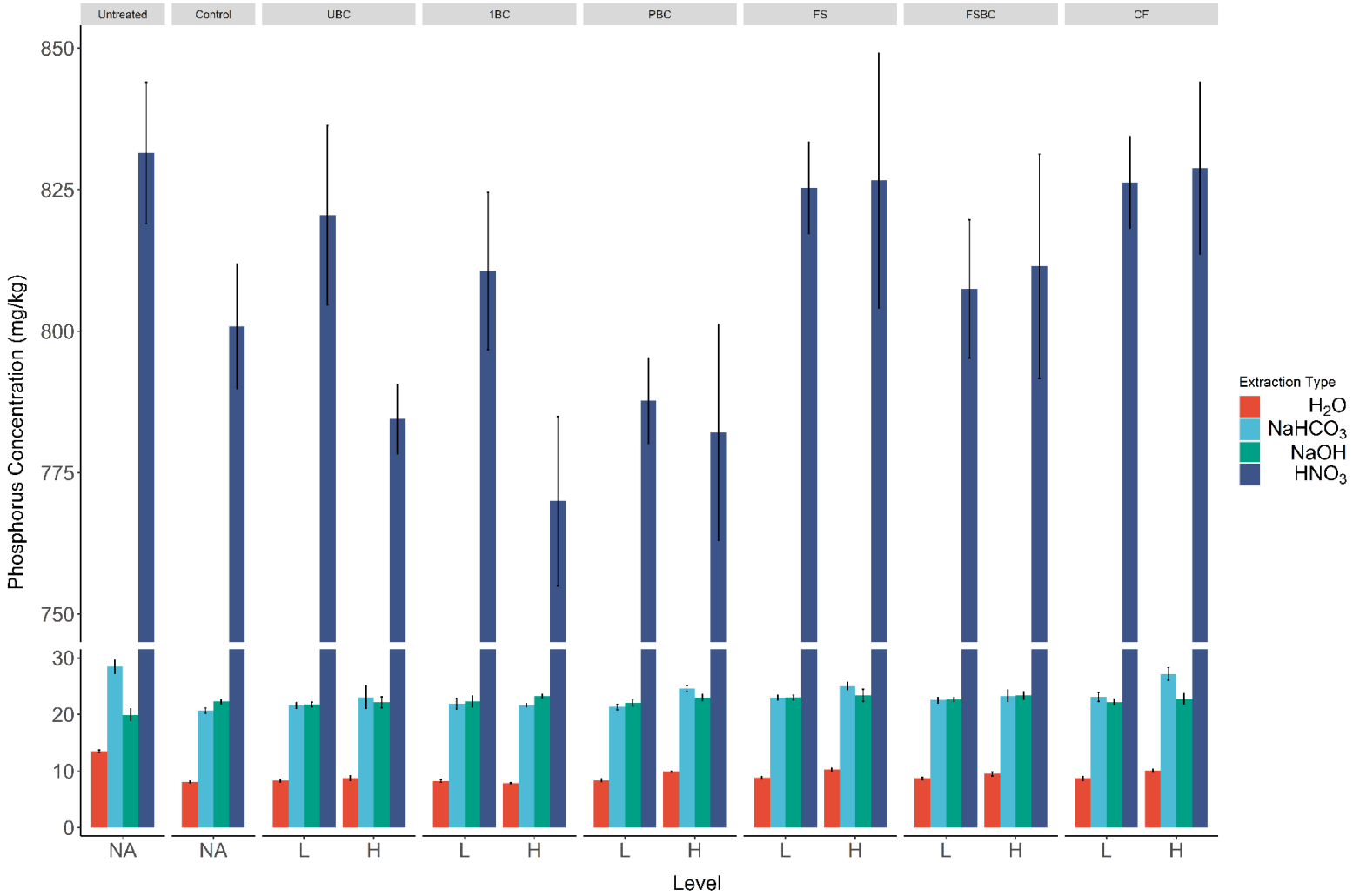

Figure 2.2. Total phosphorus extracted from soils used in greenhouse pot trial. Error bars denote standard error (n = 5).

Table 2.14. Mean H_2O-P concentrations determined by ICP and colorimetrically. Standard error in parentheses.

	H_2O-P	H_2O-P_{MR}
	mg kg^{-1}	
Control	8.07	7.89
	(0.137)	(0.302)
UBC-L	8.21	8.23
	(0.222)	(0.154)
UBC-H	8.69	8.46
	(0.412)	(0.329)
1BC-L	8.24	8.23
	(0.230)	(0.177)
1BC-H	7.85	7.79
	(0.046)	(0.081)
PBC-L	8.35	8.26
	(0.212)	(0.102)
PBC-H	9.88	9.76
	(0.091)	(0.094)
FS-L	8.80	8.71
	(0.175)	(0.263)
FS-H	10.34	10.63
	(0.217)	(0.197)
FSBC-L	8.68	8.56
	(0.154)	(0.190)
FSBC-H	9.49	9.65
	(0.275)	(0.274)
CF-L	8.71	8.57
	(0.306)	(0.144)
CF-H	10.04	10.18
	(0.222)	(0.178)

2.4.5 NMR Speciation

NaOH-EDTA extraction efficiency ranged from 18.2% – 21.2% of total P for soils (Appendix Table B.6, Table 2.11). The low extraction efficiency is similar to past studies in calcareous soils from the same region (Hansen et al., 2004; Turner, Cade-Menun, et al., 2003; Weyers et al., 2016). Phosphorus not extracted by NaOH-EDTA is considered to be mineral-bound inorganic P that is not readily available for biological cycling (B. J. Cade-Menun et al., 2015). Thus, NMR of the NaOH-EDTA extracts provides speciation information on the extractable P phases that are considered available for plant uptake and leaching.

Stacked examples of P-NMR spectra for soils are shown in Figure 2.3. Concentrations and percentage of extracted P are shown in Table 2.15. Grouping of P species into pools and compound classes are shown in Table 2.16. Chemical shifts of the identified P compounds are shown in

Appendix Table B.7. The percentage of the main P compound classes for soils and amendments are shown in Figure 2.4. Two samples were measured in replicate. Differences between P_i and P_o percentages for replicates were less than 1%.

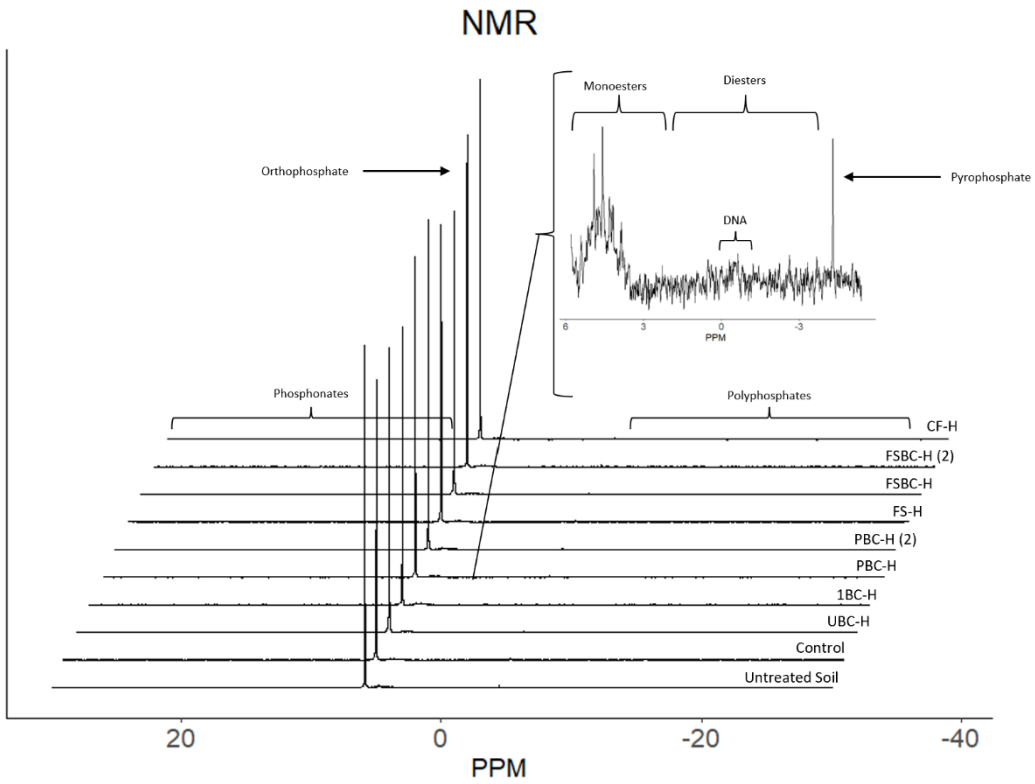

Figure 2.3. NMR spectra from NaOH-EDTA extracts of soil from all treatments at high application rate. Magnification shows monoester and diester phosphate peaks from PBC-H sample.

Inorganic P compounds identified by ^{31}P-NMR include orthophosphate, pyrophosphate, and polyphosphates. Total polyphosphates included pyrophosphate and polyphosphates. Inorganic P is the sum of orthophosphate and total polyphosphates. For the amendments, fermented biosolids had the lowest percentage of orthophosphate 70% compared to 91% in the P-biochar (PBC) (Table 2.17, Table 2.18). Pyrophosphate was present in all amendment samples from 1.5% to 3.0%. For amendments, other polyphosphates ranged from 0.1 to 3.8%, with more polyphosphates present in the biochar amendments than the fermented biosolids. Orthophosphate was the dominant inorganic P form in all soil extracts, comprising 86 – 90% of all species. Pyrophosphate was present in all soil samples and accounted for 0.3 to 0.7% of P species. Other polyphosphates accounted for 0.3 -0.5%, of soil samples with no clear trends.

Organic P compounds identified by ^{31}P-NMR include phosphonates, orthophosphate monoesters, and orthophosphate diesters. The biochar amendments were 5.2 to 5.9% organic P, while

the fermented biosolid amendment comprised of 28.4% organic P. Organic P species in the NaOH-EDTA extraction ranged from 9.9 to 14.2% in the soil samples. Phosphonate peaks were grouped together and not specifically identified. Phosphonate concentration ranged from 0.6 – 0.8% of extracted P in soil samples with no clear trends between samples.

Identified monoesters included four stereoisomers of inositol hexakisphosphate (IHP): *myo*-IHP (*m*IHP) (phytate), *scyllo*-IHP (*s*IHP), *neo*-IHP (nIHP), and D-*chiro*-IHP (*c*IHP). *myo*-IHP was the dominant form in nearly all soil samples. Other identified monoesters included glucose-6-phosphate (g6P) (0.1 – 0.3%), choline phosphate (Pchol) (0.1 – 0.4%), α-glycerophosphate (α-glc) (0.2 – 0.6%), β-glycerophosphate (β-glc) (0.5 – 0.9%), nucleotides (Nucl) (0.6 – 1.5%), and a monoester peak at 5.0 ppm (U5) which occurred in all samples (0.3 – 1.1%). α-glycerophosphate, β-glycerophosphate, and nucleotides were present in the monoester region of the spectra but originate during NaOH-EDTA extraction and ^{31}P-NMR analysis as a result of degradation of diesters in the soil samples (B. J. Cade-Menun, 2015; Schneider et al., 2016). These peak areas were subtracted from the monoester peak areas and added to the diester region.

Diester compounds were separated into DNA (0.1 - 0.5%), Diester 1 (D1) (0.2 - 1.0%), and Diester 2 (D2) (0.1 – 0.6%). Phospholipids and lipoteichoic acids are included in the Diester 1 region, while compounds in the Diester 2 region have not been specifically identified. Total diesters (cDiesters) were calculated by including the degradation compounds from the monoesters. The ratio of monoesters to diesters was greater than 1 for all soils, indicating that monoesters are the dominant form of organic P for these samples.

The control and CFH sample had slightly higher P_i than dairy and biochar amended samples, however the soil sample not used in the greenhouse trial (Untreated) had similar P_i and P_o to biochar and dairy amended soils. P_o was greatest in the samples that included unmodified biochar (UBC, FSBCH, FSBCH (2)). Total IHP values were lowest in the control and UBCH sample. When corrected, monoesters and diesters were lowest in the control and CFH samples. Total IHP comprised 30 – 54% of all monoesters, with low values in the UBCH and control samples sample.

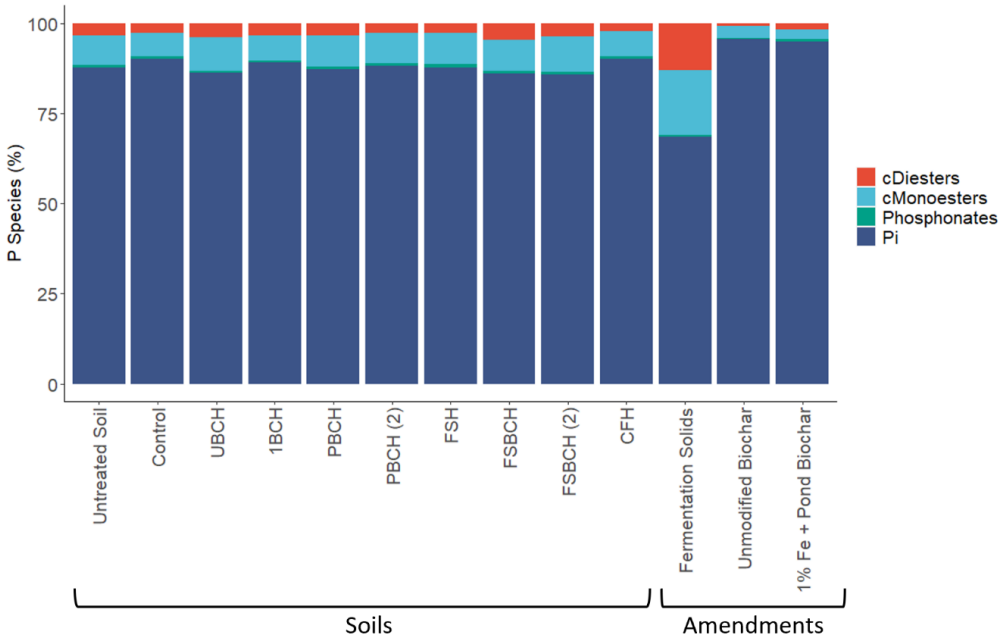

Figure 2.4. Percentage of P species in NaOH-EDTA extraction and measured using ^{31}P-NMR analysis. Monoester and diester values were corrected for degradation and denoted with "c" prefix. Inorganic P is the sum of the inorganic orthophosphate and polyphosphate compounds. Organic P is the sum of diesters, monoesters, and phosphonates.

Table 2.15. ^{31}P-NMR results from NaOH-EDTA extraction of selected soil samples.

Sample	Ortho	Pyro	Poly	Phn	*m*IHP	*s*IHP	*n*IHP	*c*IHP	α-glc	B-glc	Nucl	Pchol	g6P	U5	M1	M2	M3	DNA	Di1	Di2
									Percent Extracted P %											
Untreated	87.1	0.3	0.4	0.7	2.1	0.7	0.3	1.3	0.3	0.7	1.0	0.3	0.3	0.3	0.3	1.8	0.7	0.4	0.6	0.4
Control	89.1	0.5	0.4	0.7	1.2	0.2	0.6	0.8	0.3	0.5	1.3	0.3	0.1	0.4	0.5	2.4	0.2	0.2	0.1	0.1
UBC-H	85.5	0.4	0.4	0.6	0.9	0.3	0.2	1.3	0.6	0.7	1.2	0.4	0.2	1.1	0.7	3.4	0.6	0.4	0.8	0.3
1BC-H	88.3	0.4	0.4	0.7	1.6	0.4	0.1	1.4	0.2	0.6	1.5	0.1	0.1	0.6	0.7	1.8	0.2	0.4	0.3	0.4
PBC-H	86.3	0.6	0.3	0.6	1.0	0.3	0.4	1.7	0.3	0.9	0.6	0.2	0.1	1.0	0.3	3.1	0.6	0.3	0.8	0.6
PBC-H (2)	87.2	0.5	0.5	0.7	1.6	0.3	0.5	1.4	0.2	0.9	1.1	0.2	0.2	0.8	0.5	2.7	0.2	0.2	0.3	0.1
FS-H	86.7	0.7	0.4	0.8	2.2	0.5	0.5	1.5	0.4	0.6	1.0	0.1	0.1	0.6	0.1	2.7	0.2	0.3	0.3	0.2
FSBC-H	85.3	0.5	0.4	0.7	1.8	0.4	0.1	1.7	0.5	0.8	1.5	0.2	0.3	0.9	0.2	2.5	0.5	0.5	0.9	0.5
FSBC-H (2)	84.8	0.4	0.5	0.8	2.4	0.4	0.3	1.5	0.4	0.9	0.9	0.2	0.2	0.7	0.9	2.6	0.6	0.2	1.0	0.2
CF-H	89.1	0.6	0.4	0.7	1.9	0.3	0.4	1.0	0.3	0.5	0.9	0.1	0.2	0.4	0.7	1.9	0.2	0.1	0.2	0.2
									mg P kg^{-1} soil											
Untreated	182.0	0.6	0.8	1.5	4.4	1.5	0.6	2.7	0.6	1.5	2.1	0.6	0.6	0.6	0.6	3.8	1.5	0.8	1.3	0.8
Control	172.9	1.0	0.8	1.4	2.3	0.4	1.2	1.6	0.6	1.0	2.6	0.6	0.2	0.8	1.0	4.6	0.4	0.4	0.2	0.3
UBC-H	169.2	0.8	0.7	1.2	1.8	0.7	0.5	2.6	1.1	1.4	2.3	0.8	0.4	2.1	1.3	6.8	1.3	0.7	1.5	0.6
1BC-H	172.1	0.7	0.8	1.3	3.1	0.7	0.2	2.7	0.4	1.1	2.9	0.3	0.2	1.2	1.3	3.6	0.3	0.7	0.6	0.7
PBC-H	177.8	1.2	0.7	1.3	2.0	0.6	0.8	3.5	0.5	1.9	1.1	0.5	0.3	2.0	0.6	6.5	1.3	0.6	1.6	1.2
PBC-H (2)	171.7	1.0	0.9	1.3	3.2	0.6	0.9	2.8	0.4	1.8	2.2	0.3	0.4	1.5	1.0	5.3	0.5	0.3	0.6	0.1
FS-H	183.7	1.5	0.9	1.6	4.7	1.1	1.0	3.2	0.9	1.2	2.2	0.3	0.3	1.3	0.3	5.6	0.5	0.5	0.7	0.4
FSBC-H	173.9	1.0	0.7	1.4	3.7	0.7	0.1	3.4	0.9	1.6	3.1	0.5	0.5	1.9	0.5	5.2	1.0	0.9	1.7	1.0
FSBC-H (2)	171.3	0.9	1.1	1.6	4.9	0.7	0.6	3.0	0.9	1.7	1.9	0.4	0.4	1.4	1.7	5.3	1.3	0.5	1.9	0.5
CF-H	206.6	1.4	0.9	1.6	4.4	0.7	0.9	2.4	0.7	1.1	2.1	0.2	0.4	1.0	1.6	4.4	0.4	0.1	0.5	0.4

Table 2.16. Summed ^{31}P-NMR results from NaOH-EDTA extraction of soil samples.

	P_i	P_o	Tot Poly	Tot Phn	IHP	*myo*:other	cMonoester	cDiester	cM/D
					Percent Extracted P %				
Untreated	87.8	12.2	0.7	0.7	4.4	0.9	8.1	3.4	2.4
Control	90.0	10.0	0.9	0.7	2.8	0.8	6.7	2.6	2.5
UBC-H	86.2	13.7	0.8	0.6	2.8	0.5	9.2	3.9	2.4
1BC-H	89.0	10.9	0.8	0.7	3.5	0.9	6.9	3.3	2.1
PBC-H	87.3	12.7	0.9	0.6	3.3	0.4	8.7	3.4	2.6
PBC-H (2)	88.2	11.8	1.0	0.7	3.8	0.7	8.4	2.8	3.1
FS-H	87.8	12.2	1.1	0.8	4.7	0.9	8.6	2.8	3.1
FSBC-H	86.1	13.9	0.8	0.7	3.9	0.9	8.6	4.6	1.9
FSBC-H (2)	85.8	14.2	1.0	0.8	4.5	1.1	9.8	3.7	2.6
CF-H	90.1	9.9	1.0	0.7	3.6	1.1	7.1	2.1	3.4
					mg P kg^{-1} soil				
Untreated	183.5	25.5	1.5	1.5	9.2	0.9	16.9	7.1	2.4
Control	174.6	19.4	1.7	1.4	5.4	0.8	13.0	5.1	2.5
UBC-H	170.8	27.2	1.6	1.2	5.6	0.5	18.3	7.7	2.4
1BC-H	173.6	21.3	1.5	1.3	6.7	0.9	13.5	6.5	2.1
PBC-H	179.8	26.1	1.9	1.3	6.8	0.4	17.9	6.9	2.6
PBC-H (2)	173.7	23.3	1.9	1.3	7.5	0.7	16.5	5.4	3.1
FS-H	186.1	25.8	2.4	1.6	10.0	0.9	18.2	5.9	3.1
FSBC-H	175.7	28.3	1.7	1.4	8.0	0.9	17.6	9.3	1.9
FSBC-H (2)	173.2	28.7	2.0	1.6	9.2	1.1	19.7	7.4	2.6
CF-H	209.0	22.9	2.4	1.6	8.4	1.1	16.4	4.9	3.4

Table 2.17. ^{31}P-NMR results from NaOH-EDTA extraction of amendments.

Sample	Ortho	Pyro	Poly	Phn	*m*IHP	*s*IHP	*n*IHP	*c*IHP	α-glc	B-glc	Nucl	Pchol	g6P	U5	M1	M2	M3	DNA	Di1	Di2
									Percent Extracted P %											
Fermented Bioolids	66.3	1.9	0.2	0.7	7.8	0.0	0.0	0.6	1.9	3.9	4.5	0.6	0.6	0.0	1.3	6.4	0.6	0.7	1.9	0.1
Unmodified Biochar	92.1	3.1	0.5	0.3	0.7	0.0	0.0	0.4	0.2	0.0	0.1	0.0	0.2	0.0	1.5	0.2	0.1	0.0	0.2	0.4
1% Fe + Pond Biochar	92.6	1.7	0.6	0.7	0.8	0.0	0.0	0.5	0.2	0.6	0.6	0.1	0.0	0.0	0.7	0.6	0.0	0.1	0.2	0.1
									mg P kg^{-1} soil											
Fermented Biosolids	3886	111	11.7	41.0	457.2	0.0	0.0	35.2	111.4	228.6	263.7	35.2	35.2	0.0	76.2	375.1	35.2	41.0	111.4	5.9
Unmodified Biochar	44.5	1.5	0.2	0.2	0.3	0.0	0.0	0.2	0.1	0.0	0.1	0.0	0.1	0.0	0.7	0.1	0.1	0.0	0.1	0.2
1% Fe + P Biochar	215.9	3.9	1.5	1.6	1.8	0.0	0.0	1.1	0.4	1.3	1.3	0.1	0.1	0.0	1.7	1.4	0.1	0.2	0.5	0.2

Table 2.18. Summed ^{31}P-NMR results from NaOH-EDTA extraction of amendments.

	P_i	P_o	Tot Poly	Tot Phn	IHP	*myo*:other	cMonoester	cDiester	cM/D
					Percent Extracted P %				
Fermented Biosolids	68.4	31.6	2.1	0.7	8.4	13.0	17.9	13.0	1.4
Unmodified Biochar	95.6	4.3	3.6	0.3	1.1	1.9	3.1	0.9	3.6
1% Fe + Pond Biochar	94.9	5.1	2.3	0.7	1.2	1.7	2.7	1.7	1.6
					mg P kg^{-1} soil				
Fermented Biosolids	4009	1852	123.1	41.0	492.3	13.0	1049	761.9	1.4
Unmodified Biochar	46.2	2.1	1.7	0.2	0.5	1.9	1.5	0.4	3.6
1% Fe + Pond Biochar	221.3	11.9	5.4	1.6	2.9	1.7	6.3	4.0	1.6

2.4.7 XANES Fitting

Direct P speciation in soils can be determined by synchrotron-based X-ray absorption near-edge structure (XANES) spectroscopy (Ajiboye et al., 2007; Beauchemin et al., 2003; Prietzel et al., 2013). XANES spectrum of samples are compared with spectra of reference compounds using supervised linear combination fitting (LCF) to determine P speciation. For accurate LCF, appropriate reference compounds are necessary. The principal K-edge peak inflection for these standards was set at 2151.6 eV. This main edge peak results from the excitation of an electron from a 1*s* inner orbital due to interaction with an X-ray photon to a higher-energy orbital. The subsequent decay of high energy electrons to the unoccupied 1*s* orbitals releases photons, which are detected for XANES analysis. Pre- and post-edge features are related to the element's oxidation state, and the identity and molecular coordination of elements surrounding the central element of interest (P) (Ingall et al., 2011). Ca-P standards analyzed in this study were apatite, dicalcium phosphate dihydrate (DCDP), DCDP 50:50 Ca:Mg, monetite, and brushite (Weyers et al., 2016). Ca-P standards can be recognized by the distinct shoulder at 2155 eV and secondary peaks at 2162.5 eV and 2169 eV. Apatite has a more distinct shoulder than other Ca-P species, which may be related to the abundance of Ca in the mineral structure and decreasing number of bound H atoms (Ingall et al., 2011; Prietzel et al., 2013). The DCDP 50:50 Ca:Mg standard represents a poorly crystalline Ca-P mineral with isomorphic substitution, as evidenced by the less distinctive secondary peaks than apatite and DCDP. Other standards analyzed were Al-P, Fe-P, phytic acid, and adsorbed P (Weyers et al., 2016). Al-P minerals

are characterized by a narrow K-edge peak and lacks the shoulder present in Ca-P species (Ingall et al., 2011). Oxidized Fe-P minerals exhibit a unique pre-edge feature at 2147 eV (indicated by the arrow in Figure 2.5) in the standard used in this study, which is a useful indicator of Fe-P (Ingall et al., 2011). The adsorbed P standard is P adsorbed on goethite at pH 6.5. The adsorbed P standard has a very weak pre-edge feature compared to Fe-P, but a stronger white-line peak (Hesterberg et al., 1999). Phosphate adsorbs as an inner-sphere bidentate complex at near neutral pH (Arai et al., 2005). XANES spectra of reference P_o compounds lack recognizable pre- or post-edge features. Phytic acid, a common organic P in soil, is used as the model organic P compound. It has a prominent white-line at 2152 eV and a broad post-edge resonance (Prietzel et al., 2013). The lack distinguishable pre- or post-edge features in XANES spectra of P_o reference compounds making P_o identification difficult using P K-edge X-ray spectroscopy (Peak et al., 2002; Shober et al., 2006).

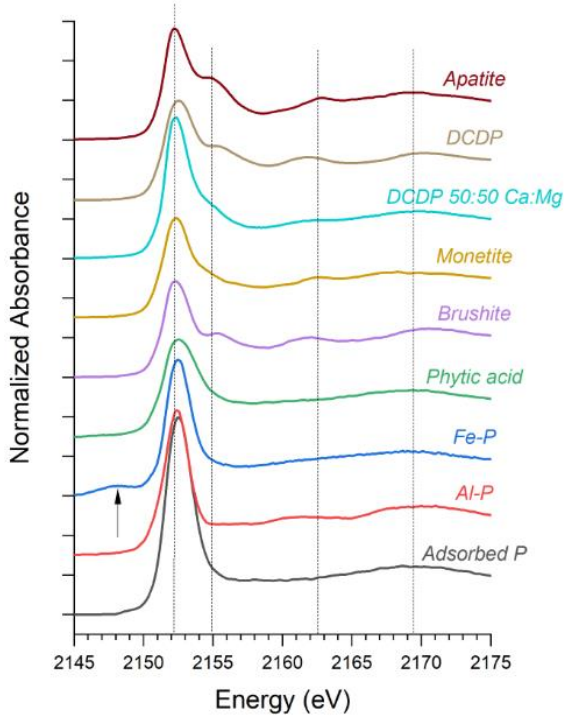

Figure 2.5. P K-edge XANES spectra for nine standards used in linear combination fitting for soil samples.

Normalized XANES spectra from the amended soils had similar features across amendment types (Figures 2.6, 2.7). In fitting the soil spectra, some standards could be replaced for each other with only small decreases in the fit quality (as judged by R-factor and reduced chi square) (Appendix Table B.8). Apatite was fit to all samples (12.9 – 74.8%) and was the predominant species in many of the samples (Table 2.19, Figure 2.8). Adsorbed P was also fit in all samples but one (13.2% – 46.4%).

The adsorbed P standard was phosphate adsorbed on goethite at pH 6.5, however spectra for phosphate adsorbed on other minerals is similar, with small variances in XANES features that are difficult to distinguish in mixed samples in soil XANES spectra (Beauchemin et al., 2003). The biochar samples, fermented biosolids, and untreated soil had a DCDP 50:50 Ca fit, with a range from 16.7% – 61.6%. To test for organic P, phytic acid was used as a standard. Phytic acid and DCDP were only fit in the CFH sample. In this sample, phytic acid was 16.3% of the fit. DCDP was only 9.0% of the fit. DCDP is a Ca-P species and, due to some difficulty separating some of the Ca-P minerals, is grouped with apatite as a Ca-P phase in the soil. Overall, Ca-P species ranged from 54% to 87% of the overall fit in the soil samples. Compared to other soil XANES spectra fits, UBCH had a poorer fit quality (R-factor = 0.0297) (Appendix Table B.8). This suggests that there may be a standard missing from our data. Based on the shoulder and lack of fit at 2155 eV, it is likely that a Ca-P species may be an important phase that is underrepresented in the LCF, but it would have to have a larger main edge peak height than the Ca-P standards to account for the higher peak height (Ca-P main edge peaks are smaller than the other standards). An amorphous Ca-P mineral may have a larger main edge peak as well as the shoulder at 2155 eV needed to fit the UBCH sample.

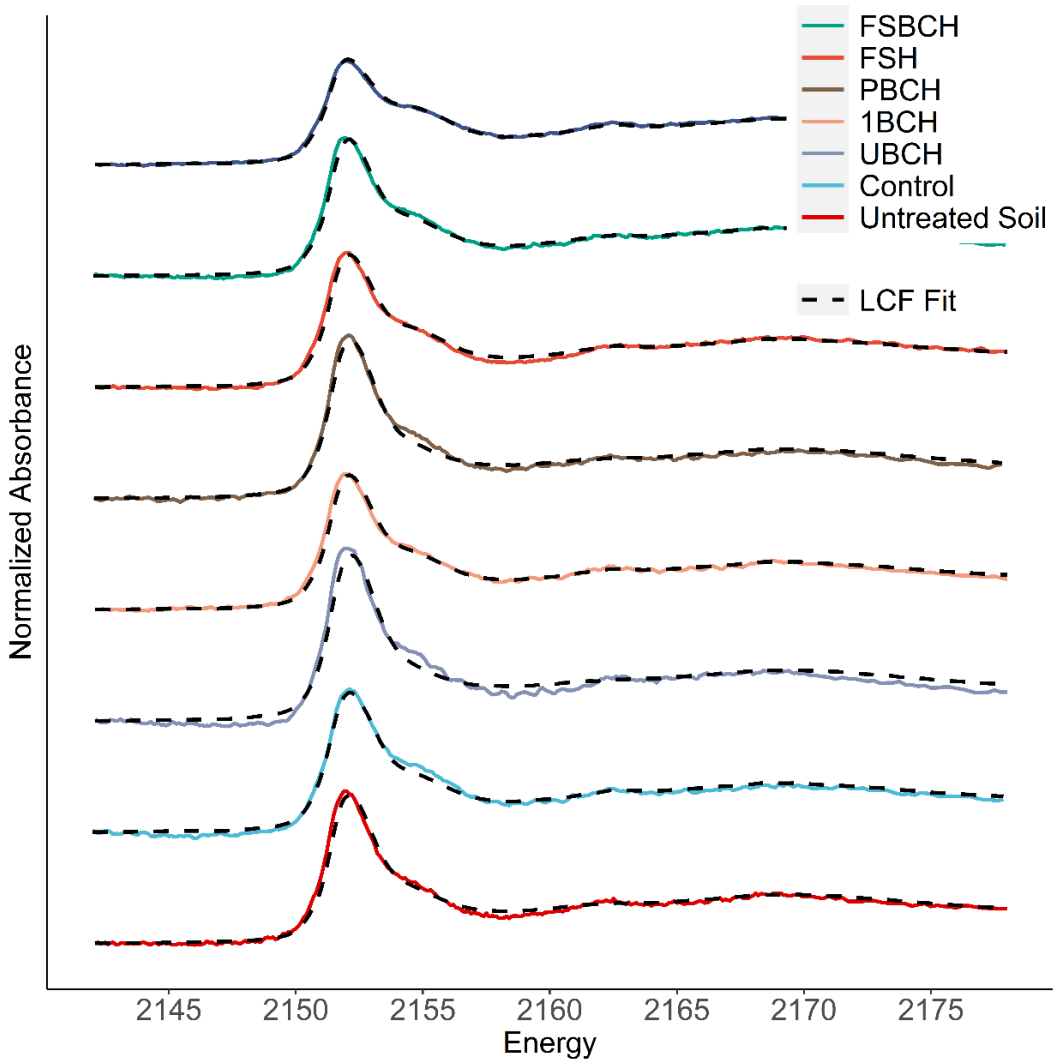

Figure 2.6. P K-edge XANES spectra for eight samples used in greenhouse pot trials.

The biochar amendment LCF suggested the presence of adsorbed P, apatite, DCDP, and phytic acid (Table 2.19, Figure 2.7, Figure 2.8). Adsorbed P accounted for the majority of the fit (43 – 65%). Ca-P species accounted for 35 - 57% of the fit.

Table 2.19. Percent composition of phosphorus species of soil samples and amendments from greenhouse pot trials determined by linear combination fitting of K-edge XANES spectra.

Sample	Adsorbed P (pH 6.5)	Apatite	DCDP	DCDP_50Ca	Phytic Acid
			%		
Untreated Soil	19.6	18.8	0.0	61.6	0.0
Control	35.4	64.6	0.0	0.0	0.0
UBCH	46.4	13.5	0.0	40.1	0.0
1BCH	17.7	51.0	0.0	31.3	0.0
PBCH	35.8	12.9	0.0	51.3	0.0
FSH	20.2	63.1	0.0	16.7	0.0
FSBCH	13.2	43.3	0.0	43.4	0.0
CFH	0.0	74.8	9.0	0.0	16.3
Unmodified BC	43.1	32.4	24.5	0.0	0.0
1% Fe Biochar	64.5	24.7	10.8	0.0	0.0
1% Fe + P Biochar	55.9	16.8	18.5	0.0	8.80

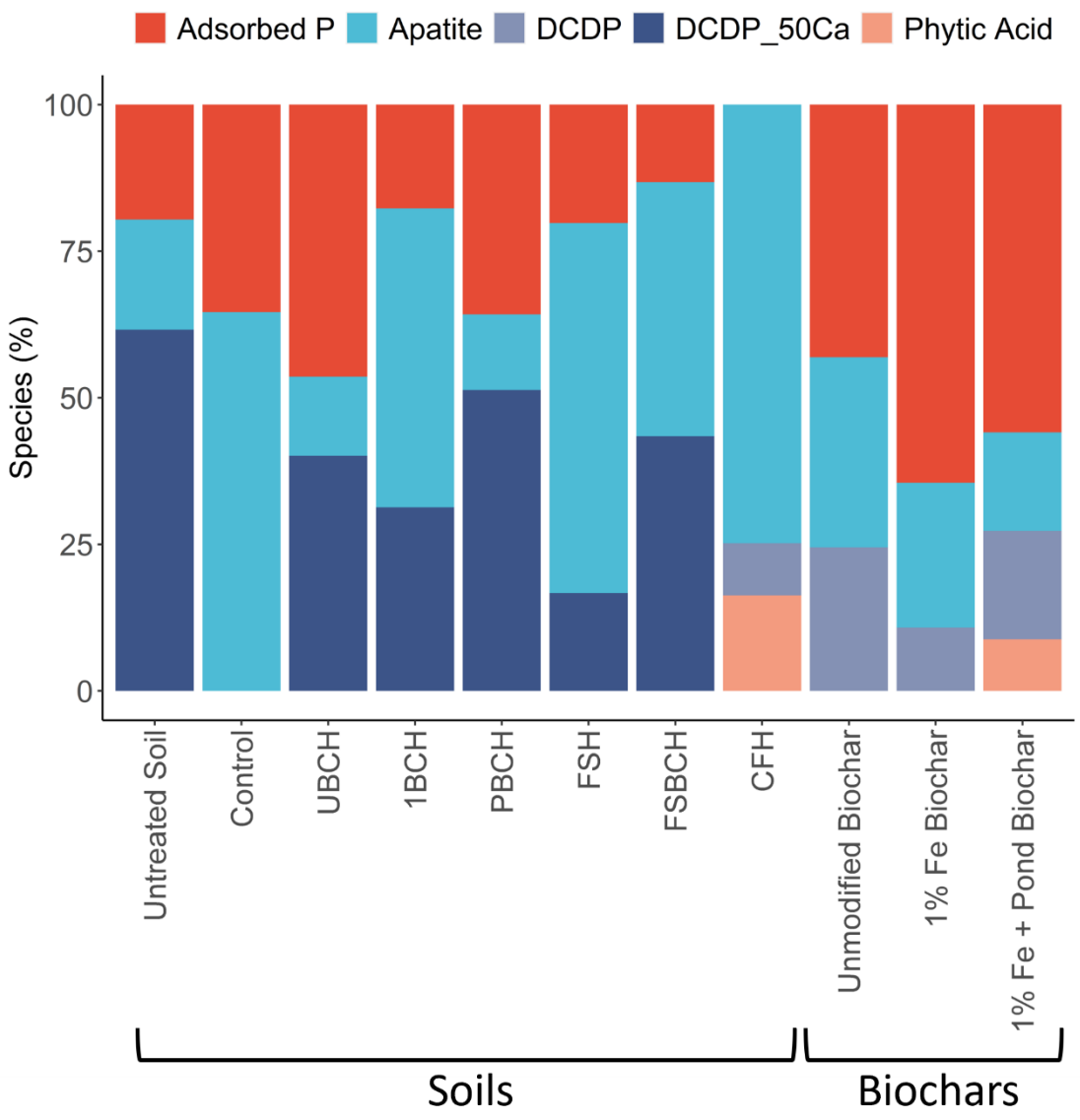

Figure 2.7. Phosphorus species composition of soil samples used in greenhouse pot trial determined by linear combination fitting of K-edge XANES spectra. Soil phosphorus was fit with phosphorus adsorbed on goethite, apatite, DCDP, DCDP 50:50 Ca:Mg, and phytic acid.

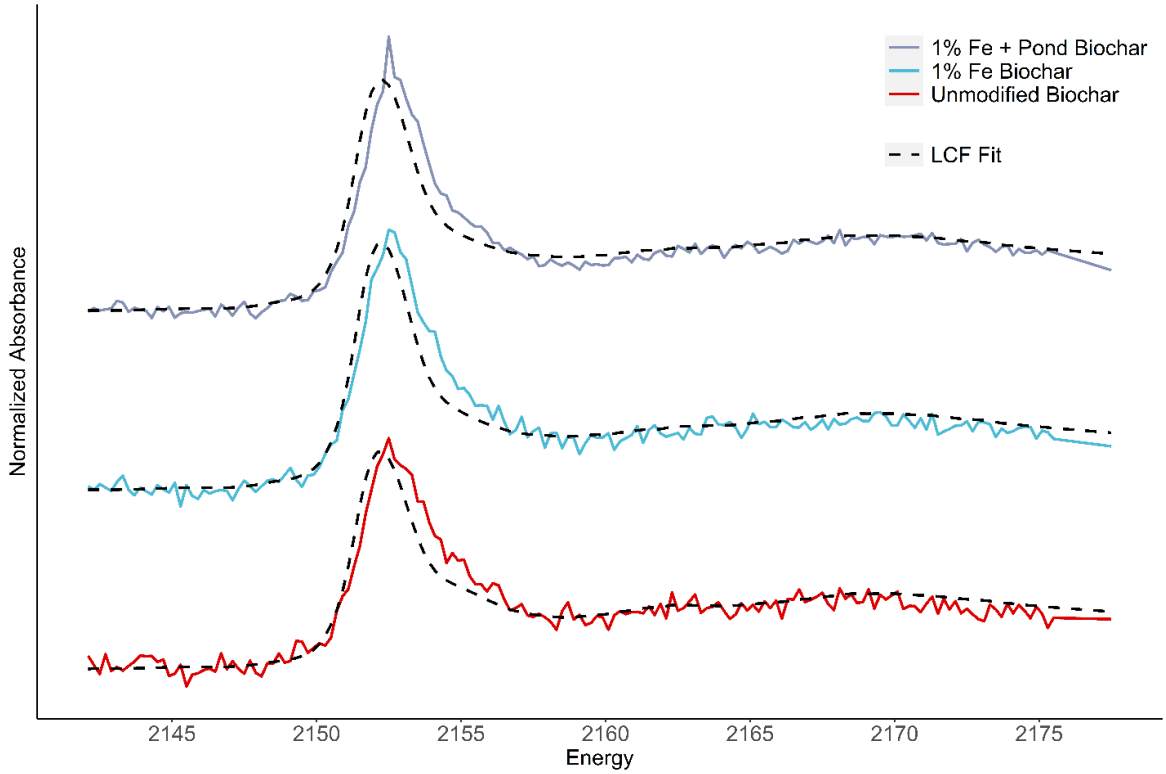

Figure 2.8. P-K edge XANES spectra for three biochar amendments used in greenhouse pot trials.

2.4.8 Hedley Isotope Extraction

Before use in the greenhouse, isotopic values of the Hedley pools were determined for the unamended soil. The isotopic composition of the untreated soil used in the greenhouse study varied slightly by pool and ranged from 9.4 – 12.8‰ (Table 2.20). The total HNO_3 isotopic value was lowest at 9.4‰ but was similar to the Hedley HNO_3 value of 10.3‰. This similarity is expected due to the majority of P in these soils is present in the HNO_3-P pool. The $NaHCO_3$-P pool was the heaviest P pool in the soil (12.8‰).

CFH and FSH samples were chosen for Hedley isotopic analysis due to differences in the water-extractable isotopic value of the amendments compared to the isotopic values of the Hedley pools in the untreated soil. The commercial fertilizer had an isotopic value of 24.2‰, which was 11.4‰ greater than the most enriched Hedley isotopic pool. The fermented biosolids had an isotopic value of 6.9‰, which was 2.5‰ lower than the most depleted Hedley isotopic pool.

The microbially-mediated equilibrium range was calculated over the last two months of the growing season using the $\delta^{18}O_w$ values from the greenhouse water and average greenhouse temperatures (Appendix Table B.9). Small variations in $\delta^{18}O_w$ and average temperatures led to an equilibrium range of 4.9 – 6.9‰. The equilibrium range upper-bound had the same P-$\delta^{18}O$ value as the fermented biosolids used in the greenhouse study.

Overall, the total isotopic extraction and $NaHCO_3$-P pools had the least amount of change in isotopic values compared to the untreated soil (Table 2.20, Figure 2.9). A slight decrease in the P-$\delta^{18}O$ values in all $NaHCO_3$-P extracts is likely due to microbially cycling in this pool, driving the value towards equilibrium. The H_2O-P and HNO_3-P pools were the most depleted compared to the untreated soil across treatments. The decrease in P-$\delta^{18}O$ of H_2O-P values towards equilibrium is also likely due to microbial cycling of this pool. The HNO_3-P pool was the most variable between replicates, with a standard deviation of 7.50 in the FSH soil. This variation could be due to the hydrolysis of P_o species that were not removed with the two resin treatments, which would lead to lighter P-$\delta^{18}O$ values (Joshi et al., 2016). The highest average H_2O-P and $NaHCO_3$-P values occurred in the CFH treated soil. The CFH and FSH treated soils followed the same pattern as the untreated soil with isotopic values from heaviest to lightest of $NaHCO_3$-P > H_2O-P > HNO_3-P.

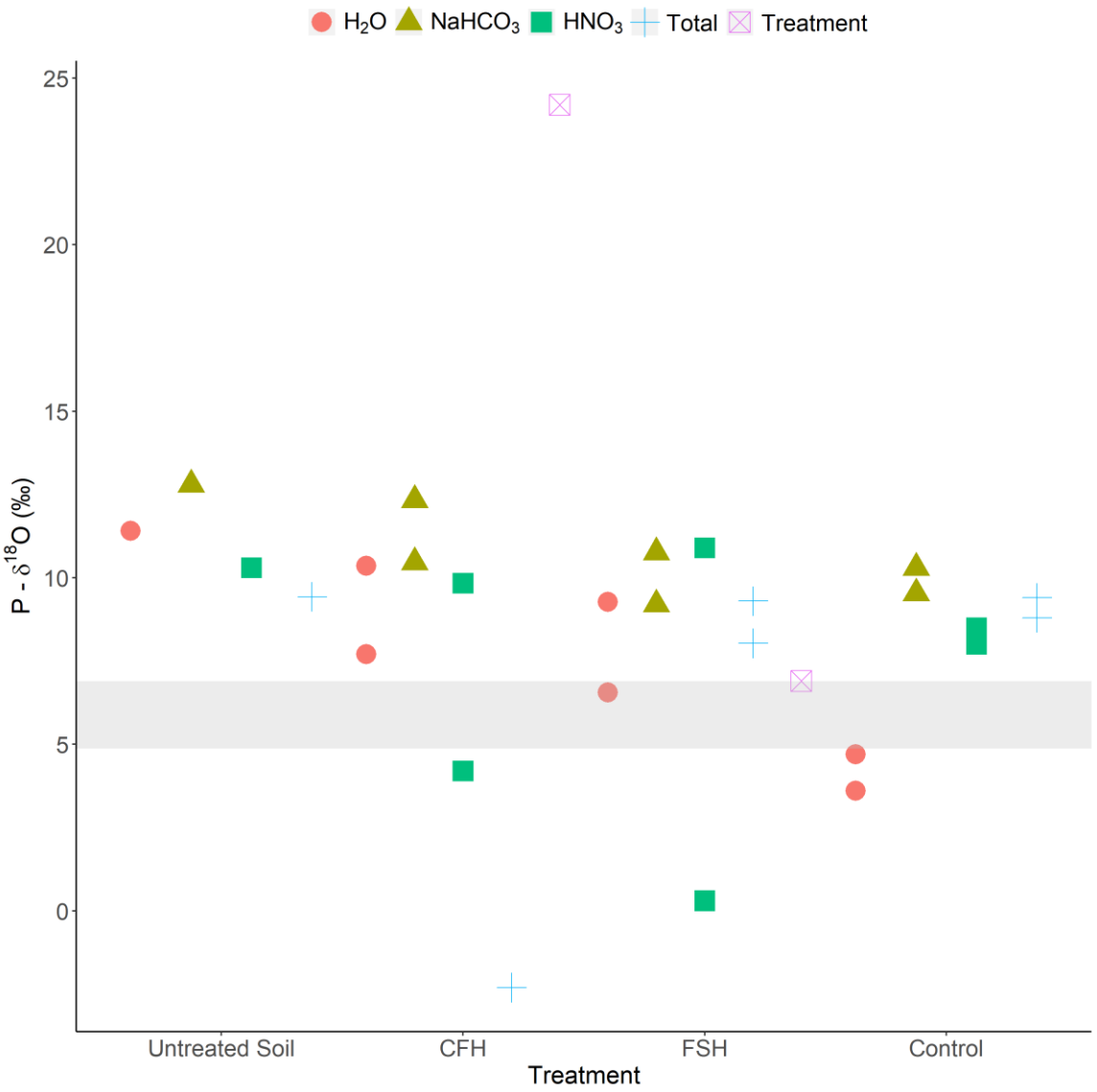

Figure 2.9. Average isotopic values (± standard deviation) for the Hedley pools for CFH, FSH, control, and untreated soils. Equilibrium range is denoted by gray bar across graph. The total isotopic value for CFH is not reported because of experimental error in extraction.

Table 2.20. Isotopic values of CF and FS amendments and Hedley pools of soils before and after use in greenhouse pot trial.

Sample	Extraction	Replicate	P-$\delta^{18}O$ Value
CFH	H_2O	1	7.7
		2	10.4
	$NaHCO_3$	1	10.5
		2	12.3
	HNO_3	1	4.2
		2	9.8
	Total	1	-2.3
		2	-
FSH	H_2O	1	6.6
		2	9.3
	$NaHCO_3$	1	9.2
		2	10.8
	HNO_3	1	10.9
		2	0.3
	Total	1	8.0
		2	9.3
Control	H_2O	1	4.7
		2	3.6
	$NaHCO_3$	1	10.3
		2	9.5
	HNO_3	1	8.0
		2	8.5
	Total	1	8.8
		2	9.4
Untreated Soil	H_2O	-	11.4
	$NaHCO_3$	-	12.8
	HNO_3	-	10.3
	Total	-	9.4
Commercial Fertilizer	H_2O	-	24.2
Fermented Biosolids	H_2O	-	6.9

2.5 DISCUSSION

2.5.1 Plant Availability of Dairy-Derived Fertilizers

P species in dairy manure may not be entirely available to crops. Nutrients in commercial fertilizers are, on the other hand, designed to be available for crop uptake upon application to the soil (Cabeza et al., 2011; Shen et al., 2011). The amendments used in this study consisted mostly of P species not extractable by water (95 – 100%). By amending with dairy lagoon water, H_2O-P in the PBC amendment had a 5.5 time increase and total P nearly doubling compared to the unmodified biochar. Streubel et al. (2012) found similar results in anaerobic digestate P recovered on biochar, with a nearly 30x and 5x increase in H_2O-P and $NaHCO_3$-P pools after AD exposure. However, in their study, over 98% of the total P was not extracted by H_2O. Compared to Streubel et al. (2012), we did not see as large of an increase in H_2O-P species. Additionally, the fermented biosolids used in this study had decreased H_2O-P compared to previous studies (Jorgensen et al., 2010). Jorgensen et al. (2010) found that H_2O-P of anaerobic digestion solids ranged from 20% - 40% of total P, depending on the technology used to treat anaerobic digestion solids. The proportion of unavailable P in the fermented biosolids may be higher in our study due to mixing of the coarse and fine solids.

Total P in the soil did not vary significantly with treatment, however based on the sequential extraction, the P species varied between the samples. When applied at a high rate, plant available P (H_2O-P and $NaHCO_3$-P) significantly increased in soils amended with most dairy-derived fertilizers compared to the control soil. The FSBCH soil was the only dairy-derived treatment with a significant increase in the H_2O-P pool and no significant increase in the $NaHCO_3$-P pool. Additionally, these treatments, except for $NaCHO_3$-P in the FSBCH treatment, supplied similar amounts of plant available P as the commercial fertilizer, even though most of the amendment P is not H_2O or $NaHCO_3$ extractable. The FSBCH treatment was applied to deliver half of P from fermented dairy solids and half of P from unmodified biochar, which likely led to its difference in $NaHCO_3$-P from CFH. Dairy-derived treatments, when applied at the high level, supply more plant available P than when applied at the low level (Table 2.13). In P-limited soils, a high rate of application of these fertilizers may be necessary to supply the required amounts of P. When soils are not P-limited, overapplication of these fertilizers may contribute to water quality issues.

2.5.2 P Speciation

Molecular speciation of the amendments used in the greenhouse was determined by ^{31}P-NMR and P K-edge XANES. Inorganic P accounted for the majority of species in each amendment. XANES LCF of the raw biochar amendments showed that they are composed of adsorbed P (49% – 74%) and Ca-P species (26% – 51%). Robinson et al. (2017) also showed that plant-based biochars are best fit with Ca-P and adsorbed P standards. The presence of Ca-P species in the XANES fit is

likely a reflection of Ca importance in plant cellular metabolism and the biogenic formation of Ca-P minerals (S. Weiner & Dove, 2003). In the PBC amendment, the 1.2% fit of phytic acid is less than the error associated with XANES LCF species determination, however ^{31}P-NMR also identified low amounts of P_o species in the PBC sample. P speciation in dairy lagoon waters varies by lagoon and season, and has been reported to range from 10% – 80% P_o (Hansen et al., 2004; Leytem & Westermann, 2005). Leytem and Westermann (2005) found that dairy lagoon water was comprised of less than 10% P_o, which is similar to the low levels of P_o in the biochar samples amended with dairy lagoon water. The fermented biosolids had the largest concentration of P_o (based on NMR) out of all amendments (Table 2.17). Similar amounts of P_o determined by ^{31}P-NMR analysis have been reported for anaerobically digested cattle waste (Mazzini et al., 2020).

Results from the chemical extraction, ^{31}P-NMR analysis, and P K-edge XANES analysis confirmed that inorganic P species made up the majority of P in soil samples. Results from ^{31}P-NMR analysis showed a majority of P in samples was orthophosphate (86.1% - 90.1%) (Table 2.15). The NaOH-EDTA extraction removes only a fraction of Total P (18% – 21%) and prevents the identification of P_i species by decoupling the cations associated with orthophosphate (J. Liu et al., 2013). So, ^{31}P-NMR results measure the speciation of P in the available soil P (extractable with NAOH- EDTA extract), while XANES analysis probes the entire sample, but has limited resolution for distinction between specific species (J. Liu et al., 2013). XANES analysis resulted in two main species present in the soils, regardless of treatment: adsorbed P (0% – 83.6%) and Ca-P (16% – 82%) (Table 2.19). Adsorbed P species are considered to have a greater potential to desorb from soil than Ca-P mineral species, which have variable solubilities, depending on the Ca-P mineral species (Hansen et al., 2004; Weyers et al., 2016). CFH treated soil was the only sample without adsorbed P fit, indicating that much of the P in this soil was quickly fixed as Ca-P, increasing unavailable P stores but potentially reducing leaching losses. This is in contrast to Kar et al. (2011), who demonstrated that application of synthetic P fertilizer resulted in both apatite and adsorbed P species in the soil. Soil P speciation by sequential extraction and XANES LCF show that the predominance of the Ca-P fit by XANES LCF agrees with the high amounts of P in the Ca-P pool determined by sequential extraction. Beauchemin et al. (2003) also found agreement between Ca-P species determined by sequential extraction and P K-edge XANES fitting in calcareous soils. In calcareous soils, P is removed from the plant available P pool through precipitation or adsorption reactions with Ca minerals, leading to large Ca-P stores in the soil (Hansen et al., 2004; Leytem & Mikkelsen, 2005; Weyers et al., 2016).

There were no distinct trends in P_o concentrations among treatments. Percent P_o determined by ignition ranged from 10 – 16%. The percent P_o distribution determined by ^{31}P-NMR ranged from

9.9 – 14.2% and was greatest in treatments that included unmodified biochar (UBCH, FSBCH), and was similar to low P_o concentrations found in soils from the same region (Hansen et al., 2004; Weyers et al., 2016). Percent P_o reported in Table 2.16 only represents a relative distribution of the P_o species in the NaOH-EDTA extraction, and not total soil P. Actual percentages of P_o determined by ^{31}P-NMR extraction when accounting for the unextracted P species is lower (Table 2.9, Appendix Table B.6). NaOH-EDTA extraction preferentially removes P_o species (B. J. Cade-Menun et al., 2015). P_o determined by ignition may be overestimated if P_i solubility increases due to ignition, or underestimated due to hydrolysis of P_o or incomplete extraction (O'Halloran & Cade-Menun, 2008). The CFH soil was the only XANES LCF combinations that included a P_o fit (Table 2.19, Table 2.21). The detection limit of P XANES is 10 – 17% of total P, so P_o may be underestimated (Ajiboye et al., 2007; Beauchemin et al., 2003). Although the fermented biosolid amendment had high P_o (Table 2.17, Table 2.20), the low amount of the amendment added did not significantly change the P_o upon amendment. Biochar amendments contributed relatively little additional P_o to the soils and P_o did not decrease in the soils through treatment and greenhouse experiments.

Table 2.21. % P_o species determined by ^{31}P-NMR, XANES LCF, and ignition.

	NaOH-EDTA	XANES LCF	Ignition
		%	
Untreated	12.2	-	12.1
Control	10.0	-	11.3
UBCH	13.7	-	15.6
1BCH	10.9	-	12.5
PBCH	12.3	-	9.7
FSH	12.2	-	14.8
FSBCH	14.0	-	14.0
CFH	9.9	17.8	13.9

Orthophosphate monoesters were the dominant form of P_o species in all the soils (Table 2.16). Included in the orthophosphate monoester group is inositol hexa*kis*phosphates (IHP). IHP forms determined by ^{31}P-NMR ranged from 2.8 – 4.7% of all soil samples and was highest in the FSH, FSBCH, and untreated samples. *myo*-IHP made up the highest proportion of P_o in most soil samples, which is consistent with other studies from cultivated fields (B. J. Cade-Menun et al., 2010). The fermented biosolids used in this study had the highest percentage of P_o (32%) out of the amendments applied, with the majority of P_o occurring as *myo*-IHP. *myo*-IHP, or phytic acid, is associated with manure and plant materials (B. J. Cade-Menun et al., 2010; Hill & Cade-Menun, 2009). An increase in *myo*-IHP values in the FS amended soils (FSH, FSBCH) compared to all other samples is likely due to high *myo*-IHP concentrations in the fermented biosolid amendment. Even though phytic acid was used as a standard in XANES LCF analysis, low concentration of IHP forms in these soil samples were not identified by LCF, and it is unlikely that other P_o forms would be identified (Prietzel et al., 2013). Immobilized P_o species, like phytic acid can be strongly adsorbed in calcareous soils, reducing its availability (Celi et al., 2000). Even with greater phytic acid concentrations, plant availability in fermented biosolid-amended soils was not lower than other treatments in this study, indicating that other P species were contributing to plant availability.

2.5.3 Dairy-derived fertilizer impacts on plant biomass

Treatment and level of fertilizer application impacted plant biomass production. In general, dried plant biomass from soils treated with dairy-derived fertilizers did not differ from the commercial fertilizer. FSBCL was the only dairy-derived P treatment with significantly less biomass than the corresponding CFL soil. The reason for this is unclear, as FSBCL supplied similar amounts of plant available P as CFL and other treatments, as judged by the H_2O-P and $NaHCO_3$-P fractions in

the sequential extraction (Table 2.13). At the high treatment rate, FSH and CFH had significantly greater biomass than the control soil, as well as significantly more plant available P than the control soil. Biochar with no added P treatments at the high rate did not have significantly different biomass than the control, indicating that biochar alone did not improve plant growth. At the low application rate, 1BCL, PBCL, FSL, and CFL had significantly greater biomass than the control, but no differences in plant available P. These amendments may be supplying other nutrients that were not measured in this study that is causing the difference in biomass. Other studies have found correlations with plant biomass and P availability in agricultural soils for both recycled P treatments and conventional fertilizer (Bach et al., 2021).

Most dairy-derived fertilizers had greater yield at high rate than the commercial fertilizer. The FSBCH soil was the only dairy-derived treatment that did not have a significantly different yield than the commercial fertilizer. FSBCH also had significantly lower $NaHCO_3$-P than the other treatments, which could account for decrease in plant yield. P availability was not, however, correlated with plant biomass or yield (Appendix Figure B.1). Additionally, CFH plants did not head – which is why the yield is significantly higher for all dairy-derived treatments. The reason for the failed yield in the CFH crop is unclear but could be due to overapplication of nutrients that stimulated continued plant growth with little energy being directed toward reproduction. At both the high and low application rate, there were no significant differences in yield between dairy-derived treatments and the control. The lack of differences from the control soil shows that dairy-derived P fertilizer can be an effective fertilizer alternative to commercially available P fertilizers.

Single doses of dairy-derived P fertilizers applied at an equimolar amount resulted in an equivalent amount of available P, plant biomass, and plant yield as a commercial fertilizer when applied at both a high and low rate. Across all treatments, the low rate of P application did not significantly reduce plant biomass or yield, but in all P-added treatments labile P was significantly reduced in either the H_2O- or $NaHCO_3$-P pools when applied at a low rate. The lack of an effect on biomass suggests that these soils were not P-limited, and as such, lower rates of fertilizer application could reduce losses due to leaching. Often in calcareous soils, overapplication of P is used to overcome P fixation in the soil (Farrell et al., 2014; Leytem & Mikkelsen, 2005). Yield or biomass were both significantly decreased when applied at a high rate for PBC and 1BC. Other studies have also reported decreased plant production at high biochar application rates (>60 Mg ha^{-1}) (Aller et al., 2018; Mia et al., 2014; Rondon et al., 2007). Decreased yield with biochar application may be due to high C:N ratios of biochar stimulating microbial N immobilization and removing N from the plant available pool (Aller et al., 2018; Deenik et al., 2010; Rondon et al., 2007).

2.5.4 P Cycling as Determined by P-$\delta^{18}O$ Signatures

P-$\delta^{18}O$ values from Hedley extraction of the treated soils provide insight into transformations between extracted P pools in the soil. Recent work by Joshi et al. (2016) suggests a step-wise transformation of P from plant available pools to acid-extractable pools, which can be explained through isotopic signatures. Some preservation of the isotopic source signature from these pools is preserved through the transformation between pools and provides insight into the potential sources and the fate of P. The close proximity of isotopic values of the pools (Table 2.20) indicates that the soils have a long-term history of fertilization that is more dominant than geological influences (Joshi et al., 2016). Isotopically, all P-$\delta^{18}O$ values decreased from the untreated soil after use in the greenhouse towards the microbially-driven equilibrium range. The control soil had the greatest difference from the equilibrium P-$\delta^{18}O$, likely due to P limitations in the system

Coefficients of variation were used to qualitatively understand the spread of data across pools (Table 2.22). P-$\delta^{18}O$ values in the H_2O-P pool showed the largest variation in values across treatments (Figure 2.9). Other studies also show large variation in H_2O-P of soil (Angert et al., 2011, 2012). The variation likely stems from microbial turnover, as all microbes catalyze H_2O-P oxygen isotope exchange, cycling H_2O-P to equilibrium at different rates (Blake et al., 2005; Joshi et al., 2016; Liang & Blake, 2009). The H_2O-P pool was also the closest, on average, to equilibrium values. Labile P pools are driven to equilibrium over short time frames by microbial cycling (Angert et al., 2011, 2012; Gross et al., 2015; Gross & Angert, 2015; Joshi et al., 2016; Zohar et al., 2010). In our study, the CFH H_2O-P samples were the farthest from equilibrium. The P-$\delta^{18}O$ values in the CFH soil are caused by the heavier P-$\delta^{18}O$ value of the treatment (24.2‰). The FSH treatment was heavier than equilibrium by 1.2‰, while the control sample was at a value lower than equilibrium (Figure 2.9). Angert et al. (2012) proposed that P-$\delta^{18}O$ values below equilibrium, such as those in the control soil, may retain low isotopic values from the hydrolysis of P_o, which are cycled to equilibrium, partially erasing the large fractionation effect of hydrolysis. The amended soils (CFH, FSH) used in this study had higher average isotopic values than the control soil in the H_2O-P pool, by 4.9‰ and 3.8‰, respectively. Gross et al. (2015) also found a larger deviation from equilibrium in labile P soil pools with P additions than in control soils, indicating that the rate of microbial P turnover is faster when biomass is P-limited. Other studies, however, have found that five months after fertilizer application, the H_2O-P pool was at equilibrium (Joshi et al., 2016). P concentrations in the CFH and FSH samples were significantly greater than the control soil, suggesting that microbial communities in CFH and FSH were not P-limited, slowing microbial cycling.

Across treatments, P-$\delta^{18}O$ values remained heavier than equilibrium in the $NaHCO_3$-P pool. Average $NaHCO_3$-P values remained heaviest in the CFH treatment (11.4‰) compared to FSH

(10‰) and control soils (9.9‰) (Table 2.20). Similar to heavier P-$\delta^{18}O$ values in the CFH H_2O-P pool, this is indicative of the enriched source value from the commercial fertilizer. The variation in $NaHCO_3$-P is much lower than in the H_2O-P pool. Zohar et al. (2010) also found low variation in the $NaHCO_3$-P pool across treatments with different P-$\delta^{18}O$ values. Joshi et al. (2016) found that the $NaHCO_3$ pool remained heavier than equilibrium five months after fertilizer application. The rate of microbial cycling is slower in the $NaHCO_3$-P pool than in the H_2O-P pool, and is only consumed by microorganisms after H_2O-P (Joshi et al., 2016). On average, the $NaHCO_3$ P-$\delta^{18}O$ values across treatments were enriched by 3.5‰ from the top of the equilibrium range. Gross et al. (2015) found ~3.5‰ enrichment in resin P-$\delta^{18}O$ values for both P- and No-P added treatments compared to equilibrium, suggesting a steady-state had been reached between the uptake of lighter isotopologues by plants and microorganisms and equilibrium values, leaving the remaining soil pool soil pool enriched (Gross et al., 2015). In laboratory studies, a 3‰ fractionation was reported by Blake et al. (2005) due to the uptake of light isotopologues by *Escherichia coli*. In the plant available $NaHCO_3$-P pool, the preferential uptake of lighter isotopologues by plants and microorganisms in this study may be reaching an enriched steady state with equilibrium, regardless of the treatment.

The HNO_3-P pool values had relatively little variation between samples compared to the more labile pools. Stepwise transformations from the H_2O and $NaHCO_3$-P pools into the HNO_3-P pool drive isotopic values in this pool, not biological cycling (Joshi et al., 2016). These transformations, in the absence of fractionation effects, record signatures of more labile P pools (Angert et al., 2011). The coefficient of variation for the HNO_3 pool was 0.308 (Table 2.22), which is similar to variation in the H_2O pool. However, when the low CFH P-$\delta^{18}O$ value is removed from this calculation, the coefficient of variation drops to 0.141, suggesting that the rest of the values are similar in magnitude. The low CFH P-$\delta^{18}O$ value could be due to P_o hydrolysis during sample preparation, or may reflect low values from the labile pool species precipitating as HNO_3 (Jaisi & Blake, 2010; Joshi et al., 2016). The discussion for this pool will disregard this outlier to better understand trends in the system. The amended soils had heavier P-$\delta^{18}O$ values in the HNO_3-P pool than the control soil. Low P-$\delta^{18}O$ values in the control HNO_3 pool reflect the lower H_2O P-$\delta^{18}O$ values of the control group, which are the likely source of the newly formed HNO_3-P pools. Similarly, P-$\delta^{18}O$ values in the CFH and FSH HNO_3 pools are the result of P transformations from the enriched H_2O-P pool in these treatments. Even though concentrations of P did not significantly differ across the three treatments in the HNO_3 pool, isotopic values show that various degrees of P transformations between the pools occurred.

Average total P values decreased slightly towards equilibrium after the greenhouse study and across all treatments, suggesting that overall isotopic compositions are slow to reflect changes in the

soil (Joshi et al., 2018). Decreases in the total P pool are likely from step wise transformations of microbially cycled pools becoming lighter, and precipitating into the HNO_3 pool, which makes up the majority of P in the soil. Isotopic values of the bulk soil represent multiple generations of various P_i pools existing at the same time (Jaisi & Blake, 2010; Joshi et al., 2016), making the interpretation of the mechanisms behind changes in isotopic signatures difficult. Cycling between all P pools in soils is dynamic, which may not be shown using chemical extraction techniques alone.

To determine the relative turnover time of the soil pools, a model was developed based on the difference between initial P-$\delta^{18}O$ values in each of the pools before amendments, equilibrium values predicted based on equation 2.1, and measured isotopic values in each of the pools ~150 days after amending the soils, assuming that cycling to equilibrium follows an exponential decay function:

$$P\text{-}\delta^{18}O_1 = (P\text{-}\delta^{18}O_i - P\text{-}\delta^{18}O_e)*e^{\frac{-t}{\tau}} + P\text{-}\delta^{18}O_e \qquad \text{Equation 2.3}$$

where τ is the effective time constant of the system in days and t is the sampling time in days from the beginning of the greenhouse study. Subscripts i, 1, and e represent initial, sampling at day 150, and equilibrium P-$\delta^{18}O$ values. Values of τ were optimized for each soil individually based on the three observed P-$\delta^{18}O$ values. Averages for each treatment replicate and for each pool were also calculated (Figure 2.9, Table 2.22). The derivation of Equation 2.3 is based on the Olson (1963) model for the net rate of change in material in ecological systems, where τ represents the approximate time it takes for decomposition to 37% of the initial level (Olson, 1963).

Individual values of τ reflect the large amount of variation in the system. The parameterized model of P-$\delta^{18}O$ equilibrium cycling as a function of time fit the measured data well. In all pools, the replicate average τ values reflect faster microbial cycling of control soils than the in the amended soils. Total averaged τ for all treatments within each pool show that the H_2O-P pool is microbially-cycled faster than $NaHCO_3$ and HNO_3 pools. The average τ of the total P pool for all treatments confirms slow isotopic turnover in the soil. Variation in τ calculated in the CFH treatment across all pools reflects the difficulty into fitting a model to natural systems. The CFH soil was the only soil with evidence that the amendment P-$\delta^{18}O$ signature was influencing soil pool isotopic values, resulting in enriched soil P-$\delta^{18}O$ values. The interaction between microbial cycling and the application of an enriched amendment relative to equilibrium values may be causing this variation.

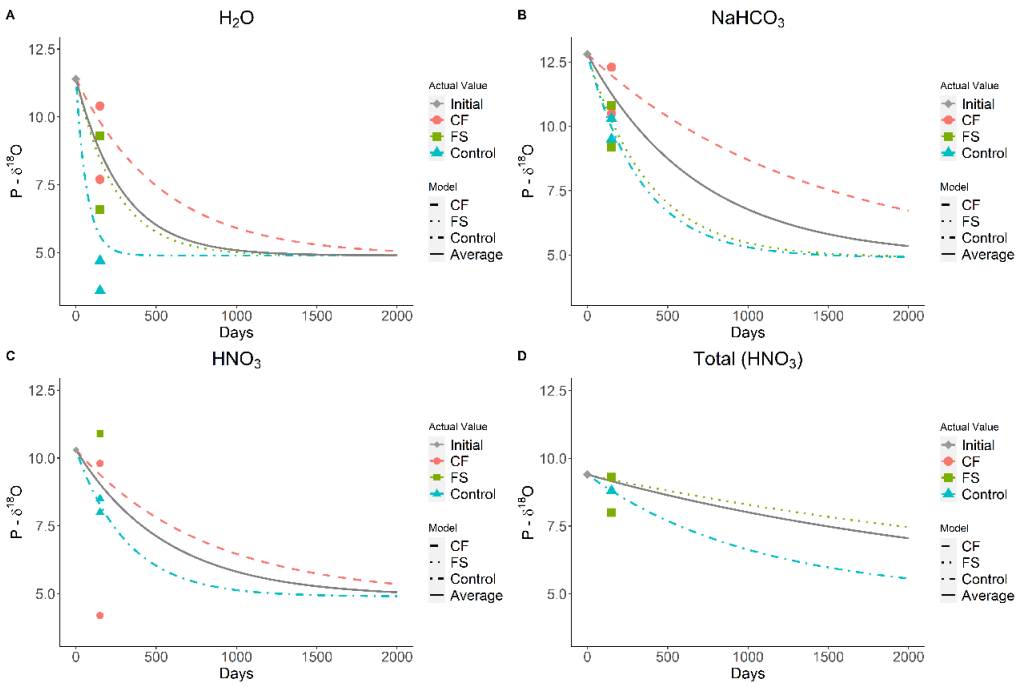

Figure 2.10. Modelled turnover times of P-$\delta^{18}O$ signatures present in the a) H_2O, b) $NaHCO_3$, c) HNO_3, and d) Total extractable soil pools. Points are measured values of P-$\delta^{18}O$ signatures and lines are predictions from the numerical model with average τ calculated for each amendment and for the entire average soil pool.

Table 2.22. Optimized τ values for individual samples, averaged within treatment for each extractable soil pool and treatment, and total average for the extractable soil pool. Coefficients of variation were calculated to determine the spread of values in each pool.

Treatment	P-$\delta^{18}O$ (‰)	Coefficient of Variation	τ	Average τ - Amendment	Average τ - Pool
			H_2O		
CF-H (1)	7.7	0.371	178	538	285
CF-H (2)	10.4		898		
FS-H (1)	6.6		112	248	
FS-H (2)	9.3		384		
Control (1)	4.7		43.1	68	
Control (2)	3.6		93.2		
			$NaHCO_3$		
CF-H (1)	10.5	0.105	436	1365	694
CF-H (2)	12.3		2294		
FS-H (1)	9.2		247	380	
FS-H (2)	10.8		514		
Control (1)	10.3		394	336	
Control (2)	9.5		277		
			HNO_3		
CF-H (1)	4.2	0.308	73.4	807	564
CF-H (2)	9.8		1544		
FS-H (1)	10.9		N/A	N/A	
FS-H (2)	N/A		N/A		
Control (1)	8.0		270	320	
Control (2)	8.5		370		
			Total (HNO_3)		
CF-H (1)	N/A	0.075	N/A	N/A	2708
CF-H (2)	N/A		N/A		
FS-H (1)	8.0		402.5	3539	
FS-H (2)	9.3		6675		
Control (1)	8.8		1048	1048	
Control (2)	9.4		N/A		

2.6 CONCLUSION

Applying unprocessed manure to soil has implications for environmental health, and transport costs limit the movement of this waste to locations far from origin. Alternative dairy-derived fertilizers utilizing P from liquid and solid waste streams are a potential value-added product for the Idaho dairy industry. Biochar removed P from dairy lagoon water, suggesting that biochar can be

used in dairy wastewater treatment to remove excess nutrients. The fermented biosolids, used as a proxy for anaerobic digestion solids, also concentrated nutrients into a smaller weight than typical manure applications. At large scale operations in dairies, further techniques used for solids separation and dewatering could reduce the AD biosolids weight even further, making transportation and utilization more likely. The dairy wastes used in this study, lagoon water and fermented dairy solids, consisted of mainly inorganic P species. The unamended biochars and dairy-derived fertilizers used in this study were comprised of less than 5% water-extractable P, compared to synthetic fertilizers which are designed to be immediately accessible for crop uptake, potentially reducing losses from the soil by acting as a slow-release fertilizer, thus preserving waterway health.

The calcareous soils of Southern Idaho pose a unique challenge to managing P storage and availability. Fixation of P into adsorbed and Ca-P species reduces plant availability, and requires overapplication of P to overcome this limitation in some areas (Leytem & Mikkelsen, 2005). Dairy-derived amendments provided similar amounts of plant available P as the applied commercial fertilizer, resulting in similar amounts of barley biomass production across treatments and level of application. Applications of fertilizers at a low rate did not significantly reduce plant biomass, but in some, cases, did reduce labile P. Similarities in the amount of plant available P being supplied by dairy-derived amendments supports the benefits of recovering nutrients from dairy waste streams. The production of similar amounts of biomass in soils with dairy-derived amendments and commercially available fertilizer further supports the idea that these fertilizers can sustain crop production.

Using these products as a soil amendment requires specific studies into the mechanisms behind P speciation and availability in soils following dairy-derived fertilizer application. Mechanistic studies using multiple analytical methods show the benefits of using a variety of techniques to accurately quantify and categorize soil P (Ajiboye et al., 2007; Gelardi & Parikh, 2021; Peak et al., 2012). Speciation results suggest that the majority of P in all the soils used in the greenhouse experiment was Ca-P species, such as hydroxyapatite, and adsorbed P. Fixation of P into Ca-P species reduces plant availability and likelihood of P losses from the soil. NMR speciation showed no major trends in P_o speciation with dairy-derived amendment application. Within the sequentially extracted pools, isotopic cycling determined that P from available pools is microbially cycled before precipitating into more unavailable P pools. Modelling of isotopic values suggests that movement of P to more unavailable pools is slow and is dependent on the isotopic value of the amendment applied. Minimal changes in soil P speciation with dairy-derived amendment application compared to commercial fertilizer application is likely due to the short-time frame of the study and small amounts of P being added via amendments compared to P in the unamended soils.

Results from this study provide an important mechanistic and agronomic overview of the use of P recovered from various dairy waste streams. Understanding the mechanisms of P transformation and transport in the soil is important for further improving these potential fertilizers. P fertilizers generated from dairy waste streams can help to close the gap in the circular bioeconomy of the dairy industry by reducing potential P losses and maintaining crop yields.

2.7 REFERENCES

Abdi, D., Cade-Menun, B. J., Ziadi, N., & Parent, L.-Étienne. (2014). Long-Term Impact of Tillage Practices and Phosphorus Fertilization on Soil Phosphorus Forms as Determined by 31P Nuclear Magnetic Resonance Spectroscopy. *Journal of Environmental Quality*, *43*(4), 1431–1441.

Ajiboye, B., Akinremi, O. O., & Jürgensen, A. (2007). Experimental Validation of Quantitative XANES Analysis for Phosphorus Speciation. *Soil Science Society of America Journal*, *71*(4), 1288–1291.

Aller, D. M., Archontoulis, S. V., Zhang, W., Sawadgo, W., Laird, D. A., & Moore, K. (2018). Long term biochar effects on corn yield, soil quality and profitability in the US Midwest. *Field Crops Research*, *227*, 30–40. https://doi.org/10.1016/j.fcr.2018.07.012

Anaerobic Digestion on Dairy Farms | US EPA. (n.d.). Retrieved May 25, 2022, from https://www.epa.gov/agstar/anaerobic-digestion-dairy-farms#fn1

Angert, A., Weiner, T., Mazeh, S., & Sternberg, M. (2012). Soil Phosphate Stable Oxygen Isotopes across Rainfall and Bedrock Gradients. *Environmental Science & Technology*, *46*(4), 2156–2162.

Angert, A., Weiner, T., Mazeh, S., Tamburini, F., Frossard, E., Bernasconi, S. M., & Sternberg, M. (2011). Seasonal variability of soil phosphate stable oxygen isotopes in rainfall manipulation experiments. *Geochimica et Cosmochimica Acta*, *75*(15), 4216–4227. https://doi.org/10.1016/j.gca.2011.05.002

Arai, Y., Sparks, D. L., & Davis, J. A. (2005). Arsenate Adsorption Mechanisms at the Allophane−Water Interface. *Environmental Science & Technology*, *39*(8), 2537–2544. https://doi.org/10.1021/es0486770

Bach, I.-M., Essich, L., & Müller, T. (2021). Efficiency of Recycled Biogas Digestates as Phosphorus Fertilizers for Maize. *Agriculture*, *11*(6), 553. https://doi.org/10.3390/agriculture11060553

Bates, D., Machler, M., Bolker, B., & Walker. (2015). Fitting Linear Mixed-Effects Models Using lme4. *Journal of Statistical Software*, *67*(1), 1–48. https://doi.org/10.18637/jss.v067.i01

Beauchemin, S., Hesterberg, D., Chou, J., Beauchemin, M., & al, et. (2003). Speciation of phosphorus in phosphorus-enriched agricultural soils using x-ray absorption near-edge structure spectroscopy and chemical fractionation. *Journal of Environmental Quality*, *32*(5), 1809–1819.

Biederman, L. A., & Harpole, W. S. (2013). Biochar and its effects on plant productivity and nutrient cycling: A meta-analysis. *Global Change Biology. Bioenergy; Oxford*, *5*(2), 202–214. http://dx.doi.org.uidaho.idm.oclc.org/10.1111/gcbb.12037

Blake, R. E., O'Neil, J. R., & Surkov, A. V. (2005). Biogeochemical cycling of phosphorus: Insights from oxygen isotope effects of phosphoenzymes. *American Journal of Science*, *305*(6–8), 596–620. https://doi.org/10.2475/ajs.305.6-8.596

Cabeza, R., Steingrobe, B., Römer, W., & Claassen, N. (2011). Effectiveness of recycled P products as P fertilizers, as evaluated in pot experiments. *Nutrient Cycling in Agroecosystems*, *91*(2), 173–184. https://doi.org/10.1007/s10705-011-9454-0

Cade-Menun, B. J. (2015). Improved peak identification in 31P-NMR spectra of environmental samples with a standardized method and peak library. *Geoderma*, *257–258*, 102–114. https://doi.org/10.1016/j.geoderma.2014.12.016

Cade-Menun, B. J. (2017). Characterizing phosphorus forms in cropland soils with solution 31P-NMR: Past studies and future research needs. *Chemical and Biological Technologies in Agriculture*, *4*(1), 19. https://doi.org/10.1186/s40538-017-0098-4

Cade-Menun, B. J., He, Z., Zhang, H., Endale, D. M., Schomberg, H. H., & Liu, C. W. (2015). Stratification of Phosphorus Forms from Long-Term Conservation Tillage and Poultry Litter Application. *Soil Science Society of America Journal*, *79*(2), 504–516. https://doi.org/10.2136/sssaj2014.08.0310

Cade-Menun, B. J., & Lavkulich, L. M. (1997). A comparison of methods to determine total, organic, and available phosphorus in forest soils. *Communications in Soil Science and Plant Analysis*, *28*(9–10), 651–663. https://doi.org/10.1080/00103629709369818

Cade-Menun, B. J., & Preston, C. M. (1996). A comparison of soil extraction procedures for 31P NMR Spectroscopy. *Soil Science*, *161*(11), 770–785.

Cade-Menun, B., & Liu, C. W. (2014). Solution Phosphorus-31 Nuclear Magnetic Resonance Spectroscopy of Soils from 2005 to 2013: A Review of Sample Preparation and Experimental Parameters. *Soil Science Society of America Journal*, *78*(1), 19–37.

Cao, X., & Harris, W. (2010). Properties of dairy-manure-derived biochar pertinent to its potential use in remediation. *Bioresource Technology*, *101*(14), 5222–5228. https://doi.org/10.1016/j.biortech.2010.02.052

Carreira, J. A., Viñegla, B., & Lajtha, K. (2006). Secondary CaCO3 and precipitation of P–Ca compounds control the retention of soil P in arid ecosystems. *Journal of Arid Environments*, *64*(3), 460–473. https://doi.org/10.1016/j.jaridenv.2005.06.003

Celi, L., Lamacchia, S., & Barberis, E. (2000). Interaction of inositol phosphate with calcite. *Nutrient Cycling in Agroecosystems*, *57*(3), 271–277. https://doi.org/10.1023/A:1009805501082

Collins, H. P., Kimura, E., & Smith, D. R. (2020). Sweet Corn Phosphorus Uptake from Sandy Soil Amended with Anaerobically-digested Manure. *Communications in Soil Science and Plant Analysis*, *51*(18), 2398–2413. https://doi.org/10.1080/00103624.2020.1836208

Collins, H. P., Streubel, J., Alva, A., Porter, L., & Chaves, B. (2013). Phosphorus Uptake by Potato from Biochar Amended with Anaerobic Digested Dairy Manure Effluent. *Agronomy Journal*, *105*(4), 989–998.

Condron, L. M., & Newman, S. (2011). Revisiting the fundamentals of phosphorus fractionation of sediments and soils. *Journal of Soils and Sediments*, *11*(5), 830–840. http://dx.doi.org.uidaho.idm.oclc.org/10.1007/s11368-011-0363-2

Dairy's Economic Impact. (n.d.). Idaho Dairymen's Association. Retrieved November 21, 2020, from https://www.idahodairymens.org/economic-impact

Deenik, J. L., McClellan, T., Uehara, G., Antal, M. J., & Campbell, S. (2010). Charcoal Volatile Matter Content Influences Plant Growth and Soil Nitrogen Transformations. *Soil Science Society of America Journal*, *74*(4), 1259–1270.

do Nascimento, C. A. C., Pagliari, P. H., Schmitt, D., He, Z., & Waldrip, H. (2015). Phosphorus Concentrations in Sequentially Fractionated Soil Samples as Affected by Digestion Methods. *Scientific Reports*, *5*(1), 17967. https://doi.org/10.1038/srep17967

Enders, A., & Lehmann, J. (2012). Comparison of Wet-Digestion and Dry-Ashing Methods for Total Elemental Analysis of Biochar. *Communications in Soil Science and Plant Analysis*, *43*(7), 1042–1052. https://doi.org/10.1080/00103624.2012.656167

Environmental Monitoring Systems Laboratory. (1996). DETERMINATION OF TRACE ELEMENTS IN WATERS AND WASTES BY INDUCTIVELY COUPLED PLASMA - MASS SPECTROMETRY. In *Methods for the Determination of Metals in Environmental Samples* (pp. 88–145). Elsevier. https://doi.org/10.1016/B978-0-8155-1398-8.50011-2

Farrell, M., Macdonald, L. M., Butler, G., Chirino-valle, I., & Condron, L. M. (2014). Biochar and fertiliser applications influence phosphorus fractionation and wheat yield. *Biology and Fertility of Soils*, *50*(1), 169–178. https://doi-org.uidaho.idm.oclc.org/10.1007/s00374-013-0845-z

Fischer, D. B. (1998, August 6). *Energy Aspects of Manure Management*. Dairy Cattle: Illinois Livestock Trail. http://livestocktrail.illinois.edu/dairynet/paperDisplay.cfm?ContentID=274

Gatiboni, L. C., Rheinheimer, D. dos S., Flores, A. F. C., Anghinoni, I., Kaminski, J., & Lima, M. A. S. de. (2005). Phosphorus Forms and Availability Assessed by 31P-NMR in Successively Cropped Soil. *Communications in Soil Science and Plant Analysis*, *36*(19–20), 2625–2640. https://doi.org/10.1080/00103620500301917

Gavlak, R., Horneck, D., & Miller, R. O. (2005). *Soil, Plant and Water Reference Methods for the Western Region* (3rd ed.).

Gelardi, D. L., & Parikh, S. J. (2021). Soils and Beyond: Optimizing Sustainability Opportunities for Biochar. *Sustainability*, *13*(18), 10079. https://doi.org/10.3390/su131810079

Ghezzehei, T. A., Sarkhot, D. V., & Berhe, A. A. (2014). Biochar can be used to capture essential nutrients from dairy wastewater and improve soil physico-chemical properties. *Solid Earth*, *5*, 953–962.

Glaser, B., & Lehr, V.-I. (2019). Biochar effects on phosphorus availability in agricultural soils: A meta-analysis. *Scientific Reports*, *9*(1), 9338. https://doi.org/10.1038/s41598-019-45693-z

Gross, A., & Angert, A. (2015). What processes control the oxygen isotopes of soil bio-available phosphate? *Geochimica et Cosmochimica Acta*, *159*, 100–111. https://doi.org/10.1016/j.gca.2015.03.023

Gross, A., Turner, B. L., Wright, S. J., Tanner, E. V. J., Reichstein, M., Weiner, T., & Angert, A. (2015). Oxygen isotope ratios of plant available phosphate in lowland tropical forest soils. *Soil Biology and Biochemistry*, *88*, 354–361. https://doi.org/10.1016/j.soilbio.2015.06.015

Güngör, K., Jürgensen, A., & Karthikeyan, K. G. (2007). Determination of Phosphorus Speciation in Dairy Manure using XRD and XANES Spectroscopy. *Journal of Environmental Quality*, *36*(6), 1856–1863.

Gustafsson, J. P., Braun, S., Tuyishime, J. R. M., Adediran, G. A., Warrinnier, R., & Hesterberg, D. (2020). A Probabilistic Approach to Phosphorus Speciation of Soils Using P K-edge XANES Spectroscopy with Linear Combination Fitting. *Soil Systems*, *4*(2). https://www.mdpi.com/2571-8789/4/2/26/htm

Hansen, J. C., Cade-Menun, B. J., & Strawn, D. G. (2004). Phosphorus Speciation in Manure-Amended Alkaline Soils. *Journal of Environmental Quality*, *33*(4), 1521–1527. https://doi.org/10.2134/jeq2004.1521

Harter, T., Davis, H., Mathews, M. C., & Meyer, R. D. (2002). Shallow groundwater quality on dairy farms with irrigated forage crops. *Journal of Contaminant Hydrology*, *55*(3), 287–315. https://doi.org/10.1016/S0169-7722(01)00189-9

Haygarth, P. M., & Sharpley, A. N. (2000). Terminology for phosphorus transfer. *Journal of Environmental Quality*, *29*(1), 10.

Hedley, M. J., Stewart, J. W. B., & Chauhan, B. S. (1982). Changes in Inorganic and Organic Soil Phosphorus Fractions Induced by Cultivation Practices and by Laboratory Incubations. *Soil Science Society of America Journal*, *46*(5), 970–976.

Hesterberg, D., Zhou, W., Hutchison, K. J., Beauchemin, S., & Sayers, D. E. (1999). XAFS study of adsorbed and mineral forms of phosphate. *Journal of Synchrotron Radiation*, *6*(3), 636–638. https://doi.org/10.1107/S0909049599000370

Hinsinger, P. (2001). Bioavailability of soil inorganic P in the rhizosphere as affected by root-induced chemical changes: A review. *Plant and Soil*, *237*(2), 173–195.

Ingall, E. D., Brandes, J. A., Diaz, J. M., de Jonge, M. D., Paterson, D., McNulty, I., Elliott, W. C., & Northrup, P. (2011). Phosphorus K-edge XANES spectroscopy of mineral standards. *Journal of Synchrotron Radiation*, *18*(Pt 2), 189–197. https://doi.org/10.1107/S0909049510045322

Jaisi, D. P., & Blake, R. E. (2010). Tracing sources and cycling of phosphorus in Peru Margin sediments using oxygen isotopes in authigenic and detrital phosphates. *Geochimica et Cosmochimica Acta*, *74*(11), 3199–3212. https://doi.org/10.1016/j.gca.2010.02.030

Jorgensen, K., Magid, J., Luxhoi, J., & Jensen, L. S. (2010). Phosphorus Distribution in Untreated and Composted Solid Fractions from Slurry Separation. *Journal of Environmental Quality*, *39*(1), 393–401. https://doi.org/10.2134/jeq2009.0168

Joshi, S. R., Li, W., Bowden, M., & Jaisi, D. P. (2018). Sources and Pathways of Formation of Recalcitrant and Residual Phosphorus in an Agricultural Soil. *Soil Systems*, *2*(3), 45. https://doi.org/10.3390/soilsystems2030045

Joshi, S. R., Li, X., & Jaisi, D. P. (2016). Transformation of Phosphorus Pools in an Agricultural Soil: An Application of Oxygen-18 Labeling in Phosphate. *Soil Science Society of America Journal*, *80*(1), 69–78. https://doi.org/10.2136/sssaj2015.06.0219

Kar, G., Hundal, L. S., Schoenau, J. J., & Peak, D. (2011). Direct Chemical Speciation of P in Sequential Chemical Extraction Residues Using P K-Edge X-Ray Absorption Near-Edge Structure Spectroscopy. *Soil Science*, *176*(11), 589–595. https://doi.org/10.1097/SS.0b013e31823939a3

Kizewski, F., Liu, Y.-T., Morris, A., & Hesterberg, D. (2011). Spectroscopic Approaches for Phosphorus Speciation in Soils and Other Environmental Systems. *Journal of Environmental Quality*, *40*(3), 751–766.

Kizito, S., Luo, H., Wu, S., Ajmal, Z., Lv, T., & Dong, R. (2017). Phosphate recovery from liquid fraction of anaerobic digestate using four slow pyrolyzed biochars: Dynamics of adsorption, desorption and regeneration. *Journal of Environmental Management*, *201*, 260–267. https://doi.org/10.1016/j.jenvman.2017.06.057

Lenth, R. V., Buerkner, P., Herve, M., Love, J., Miguez, F., Riebl, H., & Singmann, H. (2022). *emmeans: Estimated Marginal Means, aka Least-Squares Means* (1.7.3) [Computer software]. https://CRAN.R-project.org/package=emmeans

Leytem, A. B., & Mikkelsen, R. L. (2005). *The Nature of Phosphorus in Calcareous Soils*. *89*(2), 3.

Leytem, A. B., & Westermann, D. T. (2005). Phosphorus Availability to Barley from Manures and Fertilizers on a Calcareous Soil. *Soil Science*, *170*(6), 401–412. https://doi.org/10.1097/01.ss.0000169914.17732.69

Liang, Y., & Blake, R. E. (2009). Compound- and enzyme-specific phosphodiester hydrolysis mechanisms revealed by δ18O of dissolved inorganic phosphate: Implications for marine P cycling. *Geochimica et Cosmochimica Acta*, *73*(13), 3782–3794. https://doi.org/10.1016/j.gca.2009.01.038

Liang, Y., Cao, X., Zhao, L., Xu, X., & Harris, W. (2014). Phosphorus Release from Dairy Manure, the Manure-Derived Biochar, and Their Amended Soil: Effects of Phosphorus Nature and Soil Property. *Journal of Environmental Quality*, *43*(4), 1504–1509.

Liu, J., Hu, Y., Yang, J., Abdi, D., & Cade-Menun, B. J. (2015). Investigation of Soil Legacy Phosphorus Transformation in Long-Term Agricultural Fields Using Sequential Fractionation, P K-edge XANES and Solution P NMR Spectroscopy. *Environmental Science & Technology*, *49*(1), 168–176. https://doi.org/10.1021/es504420n

Liu, J., Yang, J., Cade-Menun, B. J., Liang, X., Hu, Y., Liu, C. W., Zhao, Y., Li, L., & Shi, J. (2013). Complementary Phosphorus Speciation in Agricultural Soils by Sequential Fractionation, Solution 31P Nuclear Magnetic Resonance, and Phosphorus K-edge X-ray Absorption Near-Edge Structure Spectroscopy. *Landscape and Watershed Process*, *42*(6), 1763–1770.

Lorimor, J., Powers, W., & Sutton, A. (2004). *Manure Characteristics: Manure Management System Series*. Iowa State University MidWest Plan Service.

Lustosa Filho, J. F., Carneiro, J. S. da S., Barbosa, C. F., de Lima, K. P., Leite, A. do A., & Melo, L. C. A. (2020). Aging of biochar-based fertilizers in soil: Effects on phosphorus pools and availability to Urochloa brizantha grass. *Science of The Total Environment*, *709*, 136028. https://doi.org/10.1016/j.scitotenv.2019.136028

Mazzini, S., Borgonovo, G., Scaglioni, L., Bedussi, F., D'Imporzano, G., Tambone, F., & Adani, F. (2020). Phosphorus speciation during anaerobic digestion and subsequent solid/liquid separation. *Science of the Total Environment*, *734*.

McDowell, R. W., Stewart, I., & Cade-Menun, B. J. (2006). An Examination of Spin-Lattice Relaxation Times for Analysis of Soil and Manure Extracts by Liquid State Phosphorus-31 Nuclear Magnetic Resonance Spectroscopy. *Journal of Environmental Quality*, *35*(1), 293–302.

Metson, G. S., MacDonald, G. K., Haberman, D., Nesme, T., & Bennett, E. M. (2016). Feeding the Corn Belt: Opportunities for phosphorus recycling in U.S. agriculture. *Science of The Total Environment*, *542*, 1117–1126. https://doi.org/10.1016/j.scitotenv.2015.08.047

Mia, S., van Groenigen, J. W., van de Voorde, T. F. J., Oram, N. J., Bezemer, T. M., Mommer, L., & Jeffery, S. (2014). Biochar application rate affects biological nitrogen fixation in red clover conditional on potassium availability. *Agriculture, Ecosystems & Environment*, *191*, 83–91. https://doi.org/10.1016/j.agee.2014.03.011

Murphy, J., & Riley, J. P. (1962). A modified single solution method for the determination of phosphate in natural waters. *Analytica Chimica Acta*, *27*, 31–36.

Negassa, W., & Leinweber, P. (2009). How does the Hedley sequential phosphorus fractionation reflect impacts of land use and management on soil phosphorus: A review. *Journal of Plant Nutrition and Soil Science*, *172*(3), 305–325. https://doi.org/10.1002/jpln.200800223

Nisbeth, C. S., Tamburini, F., Kidmose, J., Jessen, S., & O'Connell, D. W. (2019). Analysis of oxygen isotopes of inorganic phosphate ($\delta^{18}O_p$) in freshwater: A detailed method description. *Hydrology and Earth System Sciences Discussions*, 1–18. https://doi.org/10.5194/hess-2019-469

O'Halloran, I. P., & Cade-Menun, B. J. (2008). Total and Organic Phosphorus. In M. R. Carter & E. G. Gregorich (Eds.), *Soil Sampling and Methods of Analysis* (2nd ed., pp. 265–291). CRC Press.

Olson, J. S. (1963). Energy Storage and the Balance of Producers and Decomposers in Ecological Systems. *Ecology*, *44*(2), 322–331. https://doi.org/10.2307/1932179

Omidire, N. S., & Brye, K. R. (2022). Wastewater-recycled struvite as a phosphorus source in a wheat–soybean double-crop production system in eastern Arkansas. *Agrosystems, Geosciences & Environment*, *5*(2), e20271. https://doi.org/10.1002/agg2.20271

Pagliari, P. H., Laboski, C. A., & M. (2013). Dairy manure treatment effects on manure phosphorus fractionation and changes in soil test phosphorus. *Biology and Fertility of Soils*, *49*(8), 987–999. http://dx.doi.org.uidaho.idm.oclc.org/10.1007/s00374-013-0798-2

Peak, D., Kar, G., Hundal, L., & Schoenau, J. (2012). Kinetics and Mechanisms of Phosphorus Release in a Soil Amended With Biosolids or Inorganic Fertilizer. *Soil Science*, *177*(3), 183–187. https://doi.org/10.1097/SS.0b013e31823fd478

Peak, D., Sims, J. T., & Sparks, D. L. (2002). Solid-State Speciation of Natural and Alum-Amended Poultry Litter Using XANES Spectroscopy. *Environmental Science & Technology*, *36*(20), 4253–4261. https://doi.org/10.1021/es025660d

Pierzynski, G. M., McDowell, R., & Sims, J. T. (2005). Chemistry, Cycling, and Potential Movement of Inorganic Phosphorus in Soils. In *Phosphorus: Agriculture and the Environment*. https://doi.org/10.2134/agronmonogr46.c3

Prietzel, J., Dümig, A., Wu, Y., Zhou, J., & Klysubun, W. (2013). Synchrotron-based P K-edge XANES spectroscopy reveals rapid changes of phosphorus speciation in the topsoil of two glacier foreland chronosequences. *Geochimica et Cosmochimica Acta*, *108*, 154–171. https://doi.org/10.1016/j.gca.2013.01.029

R Studio Team. (2020). *RStudio: Inegrated Development for R* [RStudio]. PBC. http://www.rstudio.com/

Ravel, B., & Newville, M. (2005). ATHENA, ARTEMIS, HEPHAESTUS: Data analysis for X-ray absorption spectroscopy using IFEFFIT. *Journal of Synchrotron Radiation*, *12*(4), 537–541. https://doi.org/10.1107/S0909049505012719

Rivaie, A. A., Loganathan, P., Graham, J. D., Tillman, R. W., & Payn, T. W. (2008). Effect of phosphate rock and triple superphosphate on soil phosphorus fractions and their plant-availability and downward movement in two volcanic ash soils under Pinus radiata plantations in New Zealand. *Nutrient Cycling in Agroecosystems*, *82*(1), 75–88. http://dx.doi.org/10.1007/s10705-008-9170-6

Robinson, J. S., Baumann, K., Hu, Y., Hagemann, P., Kebelmann, L., & Leinweber, P. (2017). Phosphorus transformations in plant-based and bio-waste materials induced by pyrolysis. *Ambio*, *47*(1), S73–S82.

Rondon, M. A., Lehmann, J., Ramírez, J., & Hurtado, M. (2007). Biological nitrogen fixation by common beans (Phaseolus vulgaris L.) increases with bio-char additions. *Biology and Fertility of Soils*, *43*(6), 699–708. https://doi.org/10.1007/s00374-006-0152-z

Rose, T. J., Schefe, C., Weng, Z. (Han), Rose, M. T., Zwieten, L. van, Liu, L., & Rose, A. L. (2019). Phosphorus speciation and bioavailability in diverse biochars. *Plant and Soil*, *443*(1–2), 233–245. https://doi.org/10.1007/s11104-019-04219-2

Sarkhot, D. V., Berhe, A. A., & Ghezzehei, T. A. (2012). Impact of Biochar Enriched with Dairy Manure Effluent on Carbon and Nitrogen Dynamics. *Journal of Environmental Quality*, *41*(4), 1107–1114.

Sarkhot, D. V., Ghezzehei, T. A., & Berhe, A. A. (2013). Effectiveness of Biochar for Sorption of Ammonium and Phosphate from Dairy Effluent. *Journal of Environmental Quality*, *42*(5), 1545–1554.

Saunders, W. M. H., & Williams, E. G. (1955). Observations on the Determination of Total Organic Phosphorus in Soils. *Journal of Soil Science*, *6*(2), 254–267. https://doi.org/10.1111/j.1365-2389.1955.tb00849.x

Schneider, K. D., Cade-Menun, B. J., Lynch, D. H., & Voroney, R. P. (2016). Soil Phosphorus Forms from Organic and Conventional Forage Fields. *Soil Science Society of America Journal*, *80*(2), 328–340. https://doi.org/10.2136/sssaj2015.09.0340

Schulze, D. G., & Bertsch, P. M. (1995). *Synchrotron X-Ray Techniques in Soil, Plant, and Environmental Research* (D. L. Sparks, Ed.; Vol. 55, pp. 1–66). Academic Press. https://doi.org/10.1016/S0065-2113(08)60537-4

Self-Davis, M. L., Moore, P. A., & Joern, B. C. (2000). Determination of Water- and/or Dilute Salt-Extractable Phosphorus. In J. L. Kovar & G. M. Pierzynski (Eds.), *Methods of Phosphorus Analysis for Soils, Sediments, Residuals, and Waters* (pp. 24–26). Southern Extension/Research Activity-Information Exchange Group 17-A USDA-CSREES Regional Commiittee. http://www.sera17.ext.vt.edu/Documents/P_Methods2ndEdition2009.pdf

Shen, J., Yuan, L., Zhang, J., Li, H., Bai, Z., Chen, X., Zhang, W., & Zhang, F. (2011). Phosphorus Dynamics: From Soil to Plant. *Plant Physiology*, *156*(3), 997–1005. https://doi.org/10.1104/pp.111.175232

Shober, A. L., Hesterberg, D. L., Sims, J. T., & Gardner, S. (2006). Characterization of Phosphorus Species in Biosolids and Manures Using XANES Spectroscopy. *Journal of Environmental Quality*, *35*(6), 1983–1993.

Soil Survey Staff. (2014). *Kellogg Soil Survey Methods Manual* (Burt and Soil Survey Staff, Ed.; Version 5). US Department of Agriculture, Natural Resources Conservation Service.

Streubel, J. D., Collins, H. P., Tarara, J. M., & Cochran, R. L. (2012). Biochar Produced from Anaerobically Digested Fiber Reduces Phosphorus in Dairy Lagoons. *Journal of Environmental Quality*, *41*(4), 1166–1174.

Tamburini, F., Bernasconi, S. M., Angert, A., Weiner, T., & Frossard, E. (2010). A method for the analysis of the δ18O of inorganic phosphate extracted from soils with HCl. *European Journal of Soil Science*, *61*(6), 1025–1032. https://doi.org/10.1111/j.1365-2389.2010.01290.x

Tamburini, F., Pfahler, V., Bünemann, E. K., Guelland, K., Bernasconi, S. M., & Frossard, E. (2012). Oxygen Isotopes Unravel the Role of Microorganisms in Phosphate Cycling in Soils. *Environmental Science & Technology*, *46*(11), 5956–5962. https://doi.org/10.1021/es300311h

Tiessen, H., Stewart, J. W. B., & Cole, C. V. (1984). Pathways of Phosphorus Transformations in Soils of Differing Pedogenesis. *Soil Science Society of America Journal*, *48*(4), 853–858.

Tunesi, S., Poggi, V., & Gessa, C. (1999). Phosphate adsorption and precipitation in calcareous soils: The role of calcium ions in solution and carbonate minerals. *Nutrient Cycling in Agroecosystems*, *53*(3), 219–227. http://dx.doi.org/10.1023/A:1009709005147

Turner, B. L., Cade-Menun, B. J., & Westermann, D. T. (2003). Organic phosphorus composition and potential bioavailability in semi-arid arable soils of the Western United States. *Soil Science Society of America Journal*, *67*(4), 1168.

Turner, B. L., Manhieu, N., & Condron, L. M. (2003). Phosphorus-31 nuclear magnetic resonance spectral assignments of phosphorus compounds in soil NaOH-EDTA extracts. *Soil Science Society of America Journal*, *67*(2), 497–510.

Turner, B. L., Papházy, M. J., Haygarth, P. M., & McKelvie, I. D. (2002). Inositol Phosphates in the Environment. *Philosophical Transactions: Biological Sciences*, *357*(1420), 449–469.

USDA NRCS. (1999). *Official Series Description—GREENLEAF Series*. https://soilseries.sc.egov.usda.gov/OSD_Docs/G/GREENLEAF.html

USDA/NASS 2021 State Agriculture Overview for Idaho. (2021). https://www.nass.usda.gov/Quick_Stats/Ag_Overview/stateOverview.php?state=IDAHO

Wang, H., Xiao, K., Yang, J., Yu, Z., Yu, W., Xu, Q., Wu, Q., Liang, S., Hu, J., Hou, H., & Liu, B. (2020). Phosphorus recovery from the liquid phase of anaerobic digestate using biochar derived from iron−rich sludge: A potential phosphorus fertilizer. *Water Research*, *174*, 115629. https://doi.org/10.1016/j.watres.2020.115629

Watson, P., Brown, A., Lewin, P., & Taylor, G. (2014). *The Contribution of the Dairy Industry to the Idaho Economy: 2011 and 2012*. 30.

Weiner, S., & Dove, P. M. (2003). An Overview of Biomineralization Processes and the Problem of the Vital Effect. *Reviews in Mineralogy & Geochemistry*, *54*(1), 1–29.

Welshans, K. (2014, November 8). *Analysis: Idaho dairy industry flourishing*. Feedstuffs. http://www.feedstuffs.com/story-analysis-idaho-dairy-industry-flourishing-61-119976

Weyers, E., Strawn, D. G., Peak, D., Moore, A. D., Baker, L. L., & Cade-Menun, B. (2016). Phosphorus Speciation in Calcareous Soils Following Annual Dairy Manure Amendments. *Soil Science Society of America Journal*, *80*(6), 1531–1542. https://doi.org/10.2136/sssaj2016.09.0280

Wu, L., Zhang, S., Wang, J., & Ding, X. (2020). Phosphorus retention using iron (II/III) modified biochar in saline-alkaline soils: Adsorption, column and field tests. *Environmental Pollution*, *261*, 114223. https://doi.org/10.1016/j.envpol.2020.114223

Zohar, I., Shaviv, A., Young, M., Kendall, C., Silva, S., & Paytan, A. (2010). Phosphorus dynamics in soils irrigated with reclaimed waste water or fresh water—A study using oxygen isotopic composition of phosphate. *Geoderma*, *159*(1–2), 109–121. https://doi.org/10.1016/j.geoderma.2010.07.002

Appendix A. Supplemental Tables and Figures for Chapter 1.

Appendix A.1. P-$\delta^{18}O$ Extraction Protocol.

Step 1. H_2O-P_i Extraction.

MRP concentrations in samples determined the amount of soil used per sample for isotopic analysis, which requires a minimum of 20 μmol of PO_4^{3-} for sufficient Ag_3PO_4 precipitation (Nisbeth et al., 2019). The necessary amount of soil to obtain 20 μmol PO_4^{3-} was then extracted with DI water at a 1:10 solid:solution ratio for one hour at 100 rotations per minute (RPM) using the Self-Davis method (Self-Davis et al., 2000). Soil samples were centrifuged at 4000 RPM for 20 minutes then filtered under vacuum through Whatman 42 (pore size 2.5 μm) filter paper followed by 0.45 μm polycarbonate filters.

Step 2. Brucite Precipitation.

3 M magnesium chloride brine (Mg-brine) was added at a ratio of 1:50 Mg-brine:sample volume and shaken vigorously. 1 M sodium hydroxide (NaOH) was then added at a volume to 0.5% of the sample and shaken. At this stage, pH should be between 9 to 10. Continue to add 1 M NaOH until this pH range is reached. Following the addition of 1 M NaOH, brucite ($Mg(OH)_2$) flocs began to precipitate, adsorbing PO_4^{3-}. Flocs were allowed to settle, then supernatant was siphoned. Flocs were centrifuged at 3500 RPM for 10 minutes in acid-washed 1 L centrifuge bottles. There is possibility for storage at this point.

Solutions used:

3 M magnesium brine (Mg-brine)

Dissolve 610 g $MgCl_2 \cdot 6H_2O$ in DDI-water to 1 L volume. Filter through Whatman GF/F filter.

1 M NaOH

Dissolve 40 g NaOH in DDI-water to 1 L volume.

Step 3. DOM Removal.

High levels of dissolved organic matter found in water and soil samples interfere with Ag_3PO_4 formation. The Nisbeth et al (2019) method suggests dissolving and precipitating flocs in 1 M HNO_3 and 1 M NaOH, respectively, to remove DOM. We found our samples to have to high of a DOM concentration for sufficient removal in this manner. So, a DOM removal step from Tamburini et al (2012) was included. 100 mL of DAX-8 resin was conditioned by shaking in HPLC-grade methanol (MeOH) for 15 minutes followed by a 15 minute rinse with DDI-water. Flocs were then dissolved in 1 M HNO_3 (pH ~ 1) and conditioned resin slurry was added. The mixture was shaken for

three hours and then filtered through 0.2 μm polycarbonate filters and the resin was rinsed with 10 mL DDI water. The resin was reconditioned using acetonitrile and MeOH before being used again. Following the removal of resin, the Nisbeth (2019) protocol was continued by adding 1 M NaOH to pH 10. Flocs are then centrifuged at 3500 RPM for 10 minutes and supernatant is discarded. If DOM removal was successful, flocs should be white. Chance of storage in fridge at this point.

Solutions Used:

1 M HNO_3

Add 66 mL concentrated HNO_3 to 934 mL DDI-water

Step 4. APM Precipitation.

If sample was stored in fridge, allow to come to room temperature. Dissolve flocs in 1 M HNO_3 (pH <1) and filter using a 0.7 μm GF/F filter. Transfer solution to a 250 mL Erlenmeyer flask and place in a 50°C water bath. Add 25 mL 35% ammonium nitrate (NH_4NO_3) to the dissolved mixture, followed by a slow addition of 40 mL 10% ammonium molybdate. The solution should turn bright yellow and milky yellow crystals should begin to form. Color of the solution may be green if the soils were calcareous or if a H_2O extraction was used. Adjust pH to ~1 with 1 M sulfuric acid (H_2SO_4) if necessary. Ammonium phospho-molybdate (APM) crystals should begin to form. If no APM crystals precipitate after 15 minutes, check pH and adjust if needed. If no crystals precipitate and pH is <1, add 35% NH_4NO_3 and 10% ammonium molybdate at a 2.5:4 mL ratio with pH adjustments if necessary, until precipitation occurs. Shake solution in 50°C water bath at 30 RPM overnight. The next day, filter APM crystals using a 0.2 μm cellulose acetate filter and wash with 250 mL 5% NH_4NO_3. Place the filter with the APM in a 125 mL Erlenmeyer flask. Add ammonium citrate solution (15 – 50 mL) while stirring to dissolve APM crystals. This step could take ~15 minutes until all the crystals are dissolved. The solution should turn clear. If the solution is not clear but yellow color is gone, remove filter and filter with 0.2 μm cellulose nitrate filter. The solution may turn different colors depending on the extracted matrix or formation of silicate molybdate complexes (Nisbeth et al., 2019).

Solutions Used:

35% ammonium nitrate

Dissolved 538.5 g ammonium nitrate in 1000 mL DDI-water.

10% ammonium molybdate

This solution must be made fresh. Dissolve 5.56 g ammonium molybdate (tetrahydrate) in 50 mL DDI-water. This is enough for one sample.

5% ammonium nitrate

Dissolve 105.5 g ammonium nitrate in 2 L DI water.

Ammonium citrate

Working under fume hood, add 300 mL DDI-water and 140 mL concentrated NH_4OH to 10 g of citric acid.

Step 5. MAP Precipitation.

Slowly add 25 mL magnesium reagent (Mg-reagent) to solution while stirring. Then, slowly add 7 mL 1:1 ammonia. Magnesium ammonium phosphate (MAP) crystals should begin to precipitate immediately. Check to see if pH is between 8-9. More 1:1 ammonia solution may be necessary to achieve the correct pH. Leave the solution to stir overnight. The next day, filter crystals using a 0.2 μm cellulose nitrate filter and wash with 250 mL 1:20 ammonia. This step removes excess chloride (Cl^-) ions which can interfere with Ag_3PO_4 precipitation.

Step 6. Cation Removal.

Condition AG50WX8 resin in 7 M HNO_3 by shaking overnight with 1.5 times the volume of resin. The next day, rinse resin with >1 L DDI water to bring it to neutrality, then filter using a 0.45 μm polycarbonate filter. Add 6 mL of the resin slurry to the sample and shake overnight. Filter solution using a 0.2 μm polycarbonate filter and rinse with 2 mL DDI water. Collect resin and recondition using 1 M HNO_3.

Step 7. Chloride Removal.

Add a few $AgNO_3$ crystals to the remaining solution to remove residual Cl^- ions. If Cl^- ions are present, AgCl will precipitate and the solution will turn a milky white color. Let sit ~5 minutes. Filter solution using the same 0.2 μm filter as in the previous step. Continue to add $AgNO_3$ and filter until no AgCl precipitates. Filter before preceding to next step.

Step 8. Ag_3PO_4 Precipitation

At this step, the solution has been reduced to ~10 mL. Add ~5 mL Ag-ammine to the solution. The solution will turn briefly white or yellow at pH 7, then transparent at pH > 7. The sample is then placed in the oven at 50°C for two days. Yellow Ag_3PO_4 crystals should begin to form. If no crystals begin to form after 1-2 days, adjust pH (~7) using ammonium hydroxide (NH_4OH) or HNO_3. After crystals form, vacuum-filter using a 0.2 μm polycarbonate filter and rinse with >250 mL DDI water to remove oxygen bearing compounds. Place the filter with washed sample in a petri dish

and dry in an oven at 50°C overnight. The next day, remove samples from filters and transfer to small glass vials. Samples may need to be scratched off filters. Store in a desiccator until analysis.

Solutions Used:

Ag-ammine

Dissolve 10.2 g $AgNO_3$ and 9.6 g NH_4NO_3 in 81.5 mL DDI-water. Add 18.5 mL concentrated NH_4OH. Store in an amber bottle in the dark.

Step 9. TCEA-IRMS analysis

Weigh Ag_3PO_4 crystals into silver capsules (~300 ug) with a small amount of nickelized carbon to aid in pyrolysis. Ag_3PO_4 crystals are analyzed using a high temperature elemental analyzer coupled with an isotope ratio mass spectrometer (TCEA-IRMS). Internal phosphate standards of Ag_3PO_4 and benzoic acid were used for calibration (Nisbeth et al., 2019). To ensure quality control, industrial APM was used to precipitate Ag_3PO_4 crystals in conjunction with each sample to confirm variation between samples is related to precision of the TCEA-IRMS and not the protocol.

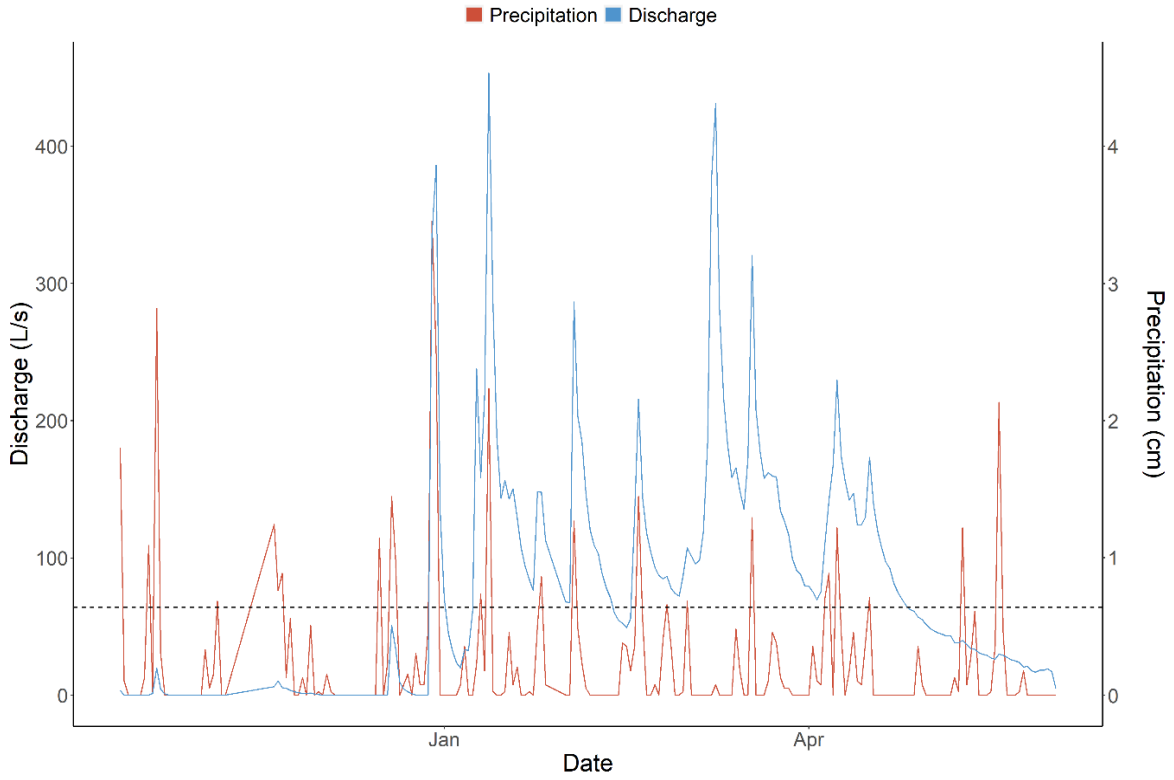

Figure A.1. Precipitation and no till tile drain discharge from the 2018 water year. Dashed line at 0.64 cm is the threshold determined for when to sample storms.

Table A.23. Estimated marginal means for main effects of catchment and month for soil $H_2O\text{-}P_{TF}$, $H_2O\text{-}P_{MR}$, and $P\text{-}\delta^{18}O$ values. Values in parentheses are standard errors.

	$H_2O\text{-}P_{TF}$	$H_2O\text{-}P_{MR}$	$P\text{-}\delta^{18}O$
	mg kg^{-1}		‰
Main Effects			
Month			
November/ December	7.79 (1.22)	5.20 (1.09)	16.1 (0.677)
February	7.70 (1.12)	4.30 (0.682)	16.9 (0.522)
May	4.79 (0.674)	4.31 (0.488)	16.2 (2.69)
Catchment			
CT	5.09 (0.724)	3.44 (0.423)	15.7 (0.423)
NT	8.42 (0.768)	5.77 (0.562)	17.1 (0.561)

Table A.24. Estimated marginal means and p-values for differences in H_2O-P_{TF} by catchment for each month.

Month	Catchment	Mean	P-value
November/December	CT	5.62	0.0432
	NT	9.95	
February	CT	5.88	0.0697
	NT	9.52	
May	CT	3.79	0.2459
	NT	5.80	

Table A.25. Estimated marginal means and p-values for differences in $H_2O\text{-}P_{MR}$ by catchment for each month.

Month	Catchment	Mean	P-value
November/December	CT	3.30	0.0375
	NT	7.09	
February	CT	3.40	0.2171
	NT	5.21	
May	CT	3.63	0.3300
	NT	5.00	

Table A.26. Estimated marginal means and p-values for differences in P-$\delta^{18}O$ values by catchment for each month.

Month	Catchment	Mean	P-value
November/December	CT	16.2	0.9277
	NT	16.1	
February	CT	16.5	0.4498
	NT	17.3	
May	CT	14.4	0.0254
	NT	18.0	

Appendix B. Supplemental Introduction, Discussion, Tables and Figures for Chapter 2.

Appendix B.1. Supplementary Material for Chapter 2 Introduction

The total maximum daily load (TMDL) for the Snake River Watershed, where the majority of Idaho dairies are located, is 0.075 mg L^{-1} of total P (Buhidar, 2005; Watson et al., 2014). Nutrient management plans are required for all dairies to control for potential losses associated with manure application (Hines et al., 2012). The application of P fertilizers or manures to fields is restricted to what is removed by the crop in this area if Olsen P is greater than 40 mg kg^{-1} in the top foot of the soil (Carey et al., 2011; Hines et al., 2012). Expensive transportation costs inhibits the amount of manure that can be transported off-site, and thus excessive local application can lead to an accumulation of nutrients in the soil (Sheffield et al., 2008). Limits on manure application in this area requires careful consideration of how to best manage dairy waste streams.

Currently, P loading from agriculture to freshwater systems is a leading cause or eutrophication in many areas of the world (Holly et al., 2018; Jarvie, Sharpley, Withers, et al., 2013; Sharpley et al., 2003). In the decade between 1994 and 2004, the USGS determined that animal manure was responsible for 40% of P inputs to agricultural water basins (Dubrovsky et al., 2010). Dairy manures, in particular, have high N and P concentrations (Pagliari et al., 2020). The high nutrient concentrations of dairy wastewaters make it a beneficial amendment to soils to meet plant nutrient requirements, however continuous manure and fertilizer application has led to a buildup of legacy P in soils (R. W. McDowell & Sharpley, 2001). In Idaho, over 40% of P purchased for dairy feed and fertilizer ends up in manure (Holly et al., 2018). Overapplication of manure to fields in regards to P requirements is common in spite of the fact that manure application can increase P losses to downstream waterways (Carey et al., 2011; Carpenter et al., 1998; R. W. McDowell & Sharpley, 2001; Palmer-Felgate et al., 2009). Manures are typically applied to soils at rates needed to meet plant nitrogen (N) requirements, thus exceeding P requirements by up to 6 times (Carey et al., 2011). Manure application increases TP found in soil (R. W. McDowell & Sharpley, 2001; Ojekanmi et al., 2011), but the speciation of P in the soil profile can vary based on manure type and processing (Hansen et al., 2004; Turner & Leytem, 2004). McDowell et al. (2001) found a significant correlation between water extractable P from soils with long term manure amendments and P from leaching studies, suggesting that increasing manure application may increase P loss to waterways. As a result, concern regarding leaching from fields treated with manure into aquatic systems has emerged (Ghezzehei et al., 2014). An increase in high-risk agricultural practices, such as dairy production, has been linked to an increase in P found in sediments in surrounding streams (Palmer-Felgate et al.,

2009) and a correlation between the rates of manure application and TP loading to surrounding aquatic systems has also been suggested (Carpenter et al., 1998). Seemingly inconsequential P losses can have huge impacts of freshwater systems, highlighting the importance of the balance between agricultural P inputs and exports (Holly et al., 2018). Closing the bioeconomy of Idaho dairies through the recycling of these nutrients is an important step in increasing efficiency and preserving environmental health.

The risk of eutrophication from runoff related to dairy manure has led to a push for better solutions for waste management. Interest in biochar, a promising soil amendment produced from biomass pyrolysis, has increased over the past decade due to its benefits in sequestering carbon, reducing nutrient losses, and improving soil water holding capacity. Biochar production and its subsequent application to soils has been proposed to reduce atmospheric CO_2 concentrations. While growing, plants store carbon in their biomass (Lackner, 2003). When added back to the soil, this biomass is decomposed, releasing carbon dioxide (Lehmann, 2007a). Pyrolyzing organic material, however, stabilizes carbon in aromatic structures that prevent microbial mineralization, storing carbon in soils for longer amounts of time than non-biochar organic materials(Lehmann et al., 2006; Woolf et al., 2010). The addition of biochar to soils may also increase soil physical and chemical properties, thus enhancing soil quality and health (Biederman & Harpole, 2013; Woolf et al., 2010).

Research suggests that, in regards to phosphorus, biochar enhances crop P nutrition (Slavich et al., 2013; Van Zwieten et al., 2015), mobilizes Fe and Al bound hydroxides in acidic soils by increasing pH (Van Zwieten et al., 2015), and reduces nutrient leaching losses, resulting in decreased fertilizer application (Laird et al., 2010). Physical properties of biochar, which are primarily dependent on pyrolysis temperature and the feedstock used, includes high porosity, surface area, and sorption capacity for both cations and anions (Ghezzehei et al., 2014; Lehmann, 2007b). In acidic soils, biochars have been shown to increase pH, thus increasing P availability to plants, but in alkaline soils, biochars are not useful for pH adjustment (Biederman & Harpole, 2013). Additionally, nutrient availability in biochars varies greatly depending on feedstock and pyrolysis conditions (Biederman & Harpole, 2013). While a meta-analysis by Bierderman and Harpole (2013) found that on average, biochar additions improved soil conditions, the authors found major variability in system responses to various types biochar that added uncertainty to the positive effects.

In cultivated fields, ^{31}P-NMR mostly identifies orthophosphate due to high fertilizer inputs, with phytic acid as the dominant P_o species (B. J. Cade-Menun, 2017). In arid soils, ^{31}P-NMR has characterized lower amounts of P_o than in similarly cultivated fields in other areas, likely due to differences in climate which effect microbial activity (Hansen et al., 2004; Turner, Cade-Menun, et al., 2003; Weyers et al., 2016). P_o species in arid soils consist mostly of orthophosphate monoesters,

which are preserved in soils due to high charge density, while orthophosphate diesters are preferentially degraded (Turner, Cade-Menun, et al., 2003). In manure-amended soils, ^{31}P-NMR was used to determine that liquid manure may be more mobile in soils than solid manures, resulting in more P in subsurface soils (Hansen et al., 2004).

P K-edge XANES has been used in a variety of soil matrices. Beauchemin et al. (2003) used P K-edge XANES together with sequential extraction to identify specific P species within soil pools. In calcareous soils, Ca-P has been found to be the dominant P species, with adsorbed P species also occurring (Beauchemin et al., 2003). Robinson et al. (2017) determined that Ca-P species are the dominant form of P in biochars produced from plant materials, providing important insight into P availability from these sources. In soils amended with biosolids, Kar et al. (2011) found that P applied as biosolids contributed more to Ca-P stores than synthetic fertilizers, which added more adsorbed P. Understanding P speciation at this scale is helpful for understanding P transformations in soils with respect to soil additions.

Oxygen isotope tracing has been used to trace sources of P_i in agricultural systems amended with conventional fertilizers and manure applications (Tonderski et al., 2017). Sequential extraction using the Hedley procedure has been used to characterize P-δ^{18}O values in the four operationally-defined pools, providing information on P cycling between soil pools and potential for P leaching (Joshi et al., 2016; Tamburini et al., 2014; Zohar et al., 2010). Using P-δ^{18}O values, Joshi et al. (2016) found that stepwise transformations occurred from more labile P pools to unavailable pools in the soil, which could not be determined from changes in Hedley pool concentrations alone. P-δ^{18}O signatures can also be used to provide insight into biological cycling. In soils treated with wastewaters, biological cycling effects may be more pronounced than in soils with synthetic fertilizers (Zohar et al., 2010). Zohar et al. (2014) used P-δ^{18}O signatures in conjunction with ^{31}P-NMR to determine that once in soil, wastewater P speciation is controlled by biological and geochemical cycling. Isotopic signatures are a powerful tool for understanding P cycling in agricultural soils.

Appendix B.2. Supplementary Material for Chapter 2 Discussion.

Many other studies have found an increase in available P compared to control soils with biochar application (Chathurika et al., 2016; Collins et al., 2013; Nelson et al., 2011). Biochars often improve P availability in acidic soils through an increase in pH which reduces P sorption to Fe and Al oxides (Chan et al., 2007; Doydora et al., 2011; Glaser & Lehr, 2019; Lehmann et al., 2003). In alkaline soils, such as these (Table 2.7), there was minimal pH increase, and thus increases in plant available P are due to P in the dairy-derived inputs. Comparing available P in biochar-amended soils to soils amended with synthetic fertilizers has yielded mixed results by other researchers (Chathurika et al., 2016; Collins et al., 2013; Nelson et al., 2011). Chathurika et al. (2016) found that biochar applied with synthetic fertilizer significantly increased plant available P compared to synthetic fertilizer alone. Collins et al. (2013) found decreased P availability from dairy-amended biochars compared to commercial fertilizers due to low P availability of the amendments. Nelson et al. (2011) found that, when applied with added P, biochar increased plant available P in soils, which may be due to biochar inhibiting P adsorption or precipitation reactions. The non-dairy reacted biochar treatments (UBC and 1BC) were not significantly different from the control soils in supplying plant available P. In a meta-analysis by Glaser and Lehr (2019), the authors found that across 108 studies, biochar application significantly increased plant available P. For wood derived biochars alone, however, the authors found no effect on P availability. Anaerobic digestion solids have also been shown to increase plant available P and have similar yields to mineral fertilizers (Bachmann et al., 2011; Hupfauf et al., 2016; Insam et al., 2015), which could be extrapolated to the fermented biosolids used in this study that also showed increased P availability (Tables 2.12, 2.13).

Past studies on biochar in soil have typically shown an increase in Ca-P species following incubation (Morshedizad et al., 2018; Peng et al., 2021; Siebers et al., 2013). The untreated soil, UBCH, and PBCH were the only samples where apatite was not the major P species fit by XANES LCF (Table 2.19). In the sequential extraction, the UBCH and PBCH treatments had less HNO_3 extractable P (Ca-P) than all other treatments, though the difference was not significant. 1BCH also had lower amounts of Ca-P determined by sequential extraction, but this is not reflected in the XANES fit. Biochar amended soils and the untreated soil included a DCDP 50:50 Ca:Mg fit, which is a more soluble form of Ca-P than apatite. DCDP transforms into apatite in the absence of organic matter at supersaturated conditions (Borkiewicz et al., 2010; Grossl & Inskeep, 1991, 1992). When organic matter is present, DCDP that is associated with OM may form preferentially over the more stable apatite due to the coating of Ca-P particles, inhibiting growth (Grossl & Inskeep, 1991, 1992). Peak et al (2002) found that in poultry litter, large amounts of organic matter favor the formation of DCDP over apatite. Delgado et al (2002) found that in calcareous soils amended with humic and

fulvic acids, DCDP formation was favored over more stable Ca-P forms. %OM was greater in the biochar amended soil samples by 0.25%. Kar et al (2011) found that in soils amended with biosolids, poorly crystalline DCDP was fit to the P XANES spectra, while soils amended with mineral fertilizers were fit with apatite. In the CFH soil, apatite was responsible for over 80% of the XANES LCF fit (Table 2.19). In calcareous soils, synthetic fertilizers are quickly precipitated into unavailable Ca-P species, reducing plant availability (Delgado et al., 2002; Leytem & Westermann, 2005). If P application with biochar produces soluble Ca-P species but remains plant available, it may be a more effective form of slow-release fertilizer.

Past studies have attempted to trace P-$\delta^{18}O$ signatures of various fertilizer sources through extractable soil pools with varying success (Gross et al., 2015; Joshi et al., 2016; Zohar et al., 2010). Joshi et al. (2016) used labelled synthetic fertilizer that was ~16‰ heavier than the most enriched soil pool. Gross et al. (2015) used fertilizers with P-$\delta^{18}O$ signatures that varied above and below the values of soil pools. Zohar et al. (2010) used 14.3‰ wastewater compared to 28‰ freshwater for irrigation. We attempted to trace natural abundance P-$\delta^{18}O$ values in the fertilizers through the different soil pools as assessed in sequential extraction. Similar to Granger et al. (2017), only the water-extractable values for the amendments was determined in this study, and thus some important signals from the more unavailable P pools in the amendments cannot be evaluated. However, the water-extractable P-$\delta^{18}O$ signature likely reflects the P that was most available to transform in the short timescale of this greenhouse study. The commercial fertilizer was 11.4‰ heavier than the heaviest soil pool ($NaHCO_3$) (Table 2.20). The fermented biosolids were 2.5‰ lighter than the lightest soil pool (Total P).

Table B.27. %RSD values for analytical replicates in each run.

			H_2O		$NaHCO_3$		NaOH		HNO_3	
Run	**Treatment**	**Rep**	**mg P kg^{-1}**	**%RSD**	**mg P kg^{-1}**	**%RSD**	**mg P kg^{-1}**	**%RSD**	**mg P kg^{-1}**	**%RSD**
1	Control (2)	A	9.0	3.29	19.7	6.64	25.2	11.2	701	10.5
	Control (2)	B	8.4		21.0		21.6		839	
	Control (2)	C	8.4		22.5		20.4		852	
	CF-L (2)	A	9.0	3.01	22.5	3.30	22.8	0.00	849	2.40
	CF-L(2)	B	9.6		23.9		22.8		848	
	CF-L(2)	C	9.6		22.7		22.8		814	
2	FSBC-H(2)	A	10.5	2.22	38.6	22.51	23.0	18.8	848	1.96
	FSBC-H (2)	B	10.02		27.6		22.7		882	
	FSBC-H(2)	C	10.02		25.9		31.2		863	
	PBC-H(2)	A	9.72	0.78	26.7	1.64	24.12	1.69	845	1.88
	PBC-H(2)	B	9.54		25.9		24.84		814	
	PBC-H(2)	C	9.66		26.4		24.84		829	
3	FS-H(4)	A	10.56	2.73	23.9	9.79	23.3	2.06	770	0.82
	FS-H(4)	B	11.04		23.1		22.8		782	
	FS-H(4)	C	11.28		27.7		23.8		773	
	FSBC-L(4)	A	8.76	2.01	21.1	0.80	21.36	0.65	758	0.32
	FSBC-L(4)	B	8.58		21.4		21.12		763	
	FSBC-L(4)	C	8.34		21.2		21.12		761	
4	FS-H(5)	A	9.78	1.00	23.3	2.63	22.8	1.06	876	6.19
	FS-H(5)	B	9.90		22.1		22.6		787	
	FS-H(5)	C	9.66		22.8		22.3		790	

Table B.28. Plant height measurements (cm) taken weekly and averaged across treatment (± standard error).

	10/13/21	10/18/21	10/25/21	11/1/21	11/12/21	11/17/21	11/22/21	11/29/21	12/7/21	12/13/21	12/29/21	1/4/22	1/17/22
Control	10.2	24.0	36.8	40.2	53.2	56.6	59.0	58.2	61.8	62.8	69.8	70.4	70.8
	(0.374)	(0.632)	(1.02)	(1.20)	(1.43)	(0.510)	(1.82)	(1.46)	(1.32)	(1.85)	(2.33)	(3.66)	(1.36)
UBC-L	10.8	24.8	36.6	37.8	53	57.2	56.8	59.2	59.0	61.4	67.2	71.4	69.6
	(0.735)	(1.32)	(1.08)	(2.46)	(1.30)	(0.860)	(2.08)	(0.860)	(1.92)	(1.50)	(1.32)	(0.678)	(1.57)
UBC-H	10.2	23.2	34.8	38.0	51.6	55.0	55.6	56.6	58.2	59.8	68.4	72.2	73.6
	(0.374)	(0.583)	(0.583)	(1.67)	(2.49)	(1.64)	(1.81)	(1.72)	(2.69)	(2.99)	(2.91)	(2.62)	(0.927)
1BC-L	10.8	26.0	38.0	42.2	55.0	60.2	57.4	59.8	61.0	64.4	70.2	71.4	70.6
	(0.374)	(1.14)	(1.95)	(1.11)	(2.42)	(2.15)	(0.927)	(0.583)	(1.48)	(1.54)	(1.85)	(2.20)	(2.14)
1BC-H	10.6	23.2	35.0	38.0	52.4	57.2	56.2	57.8	58.6	61.8	67.2	70.6	70.2
	(0.510)	(1.07)	(2.02)	(1.70)	(2.11)	(1.59)	(0.800)	(1.39)	(1.75)	(1.85)	(1.39)	(1.91)	(2.24)
PBC-L	11.2	25.2	37.4	38.2	53.2	58.6	58.4	60.6	62.2	64.8	67.4	71.2	71.2
	(0.860)	(0.917)	(1.86)	(2.13)	(1.80)	(1.89)	(1.33)	(0.980)	(0.200)	(0.583)	(0.812)	(0.583)	(0.583)
PBC-H	11.2	25.6	38.8	38.4	51.8	54.0	54.6	60.2	60.4	63.0	67.4	72.2	69.8
	(0.490)	(0.400)	(0.583)	(1.44)	(2.73)	(2.26)	(3.17)	(1.16)	(2.46)	(2.88)	(1.25)	(1.46)	(1.85)
FS-L	10.6	25.4	36.6	38.2	52.8	58.0	56.0	58.2	59.8	62.8	69.0	72.4	70.0
	(0.510)	(0.600)	(0.678)	(1.36)	(1.43)	(0.837)	(1.18)	(0.800)	(0.800)	(0.970)	(1.00)	(1.63)	(0.894)
FS-H	10.4	25.0	36.6	40.8	54.4	56.8	57.6	59.4	62.0	64.0	69.4	69.4	67.8
	(0.510)	(1.14)	(1.03)	(0.970)	(1.28)	(1.83)	(1.96)	(3.20)	(1.70)	(1.92)	(2.16)	(1.36)	(1.62)
FSBC-L	11.0	24.4	39.8	39.4	54.8	57.2	55.2	58.4	62.0	63.8	71.2	72.8	69.2
	(0.548)	(1.03)	(0.583)	(2.11)	(1.04)	(2.13)	(1.32)	(1.29)	(1.90)	(2.31)	(1.46)	(1.74)	(1.85)
FSBC-H	10.4	24.4	37.2	40.0	53.0	56.4	56.4	57.8	59.4	60.0	68.8	70.6	69.8
	(0.245)	(0.678)	(0.490)	(1.38)	(1.17)	(1.75)	(0.871)	(1.24)	(1.69)	(2.43)	(2.31)	(1.75)	(1.59)
CF-L	12.0	25.6	38.0	42.0	52.4	57.8	56.4	58.2	60.4	61.2	64.4	68.2	65.2
	(0.447)	(0.600)	(1.14)	(1.92)	(1.40)	(1.85)	(1.96)	(1.43)	(1.44)	(1.02)	(1.91)	(0.735)	(2.08)
CF-H	11.8	26.2	39.6	41.2	54.0	60.6	58.2	60.0	60.0	60.8	64.4	65.4	63.0
	(0.490)	(1.16)	(0.510)	(2.35)	(1.23)	(0.678)	(1.50)	(1.00)	(2.10)	(2.13)	(0.678)	(1.50)	(0.316)

Table B.29. Average concentrations for Al, Ca, Fe, Mg, Mn (± standard error) for the H_2O-P Hedley extraction.

	Al	**Ca**	**Fe**	**Mg**	**Mn**
			mg kg^{-1}		
Control	28.61	354.5	26.30	45.44	0.236
	(5.68)	(4.87)	(5.70)	(1.03)	(0.066)
UBCL	23.77	352.2	21.12	44.04	0.240
	(6.53)	(4.77)	(6.20)	(1.52)	(0.099)
UBCH	33.65	348.8	30.89	46.10	0.384
	(10.3)	(2.55)	(9.84)	(1.75)	(0.088)
1BCL	18.14	356.6	15.43	43.84	0.312
	(2.73)	(5.08)	(2.60)	(1.13)	(0.079)
1BCH	16.60	353.5	14.34	42.88	0.204
	(1.75)	(2.41)	(1.82)	(0.410)	(0.052)
PBCL	23.60	352.2	20.74	44.11	0.312
	(8.16)	(2.16)	(7.96)	(1.48)	(0.074)
PBCH	23.58	350.4	21.39	44.36	0.340
	(5.10)	(1.23)	(5.05)	(0.945)	(0.066)
FSL	21.54	357.7	19.21	44.60	0.324
	(6.21)	(4.14)	(6.30)	(1.28)	(0.075)
FSH	15.49	356.5	13.09	44.20	0.184
	(1.28)	(4.18)	(1.17)	(0.476)	(0.053)
FSBCL	22.33	352.4	19.91	43.98	0.304
	(11.8)	(1.74)	(5.30)	(0.865)	(0.075)
FSBCH	18.94	350.6	16.88	44.12	0.188
	(3.51)	(1.44)	(3.52)	(0.675)	(0.050)
CFL	35.04	367.3	32.30	48.06	0.396
	(12.63)	(2.77)	(12.32)	(2.45)	(0.084)
CFH	23.50	391.1	22.55	48.89	0.300
	(6.98)	(3.57)	(6.16)	(1.19)	(0.076)

Table B.30. Average concentrations for Al and Ca (± standard error) for the NaOH-P Hedley extraction.

	Al	Ca
	mg kg^{-1}	
Control	553.6 (10.6)	49.83 (15.2)
UBCL	564.6 (2.55)	49.51 (15.9)
UBCH	547.3 (8.77)	49.18 (15.5)
1BCL	563.3 (6.38)	50.45 (14.3)
1BCH	547.5 (5.71)	63.48 (15.1)
PBCL	561.3 (6.39)	62.54 (15.6)
PBCH	550.5 (4.48)	64.45 (15.7)
FSL	564.2 (5.63)	64.20 (15.7)
FSH	558.3 (2.95)	51.10 (15.5)
FSBCL	558.7 (3.51)	50.77 (15.3)
FSBCH	553.1 (7.08)	51.67 (15.4)
CFL	568.7 (4.44)	50.90 (15.4)
CFH	571.9 (1.56)	51.5 (15.4)

Table B.31. Average concentrations for Al, Ca, Fe, Mg, and Mn (± standard error) for the HNO_3-P Hedley extraction.

	Al	Ca	Fe	Mg	Mn
			mg kg^{-1}		
Control	2603 (68.5)	17113 (204)	6333 (158)	4817 (92.8)	343.4 (5.39)
UBCL	2655 (36.8)	17525 (279)	6439 (91.6)	4890 (59.6)	350.6 (4.67)
UBCH	2585 (47.2)	17088 (122)	6274 (115)	4755 (64.7)	344.4 (3.61)
1BCL	2672 (35.8)	17449 (651)	6582 (95.3)	4976 (113)	342.9 (6.88)
1BCH	2564 (35.2)	16280 (414)	6265 (105)	4599 (95.5)	338.8 (9.54)
PBCL	2628 (34.8)	16548 (232)	6413 (78.4)	4766 (54.2)	344.3 (2.56)
PBCH	2582 (33.5)	16674 (441)	6336 (76.0)	4721 (87.3)	339.7 (8.71)
FSL	2722 (35.3)	17528 (350)	6619 (79.1)	4962 (62.9)	354.8 (10.1)
FSH	2666 (48.6)	17175 (378)	6496 (109)	4901 (88.3)	345.6 (4.97)
FSBCL	2657 (41.3)	16986 (303)	6428 (108)	4843 (86.9)	348.4 (7.90)
FSBCH	2637 (53.3)	17206 (494)	6359 (129)	4822 (118)	344.7 (8.28)
CFL	2687 (35.8)	17259 (157)	6506 (153)	4895 (82.5)	382.6 (30.3)
CFH	2695 (36.1)	17634 (267)	6527 (95.8)	4952 (72.6)	348.2 (3.45)

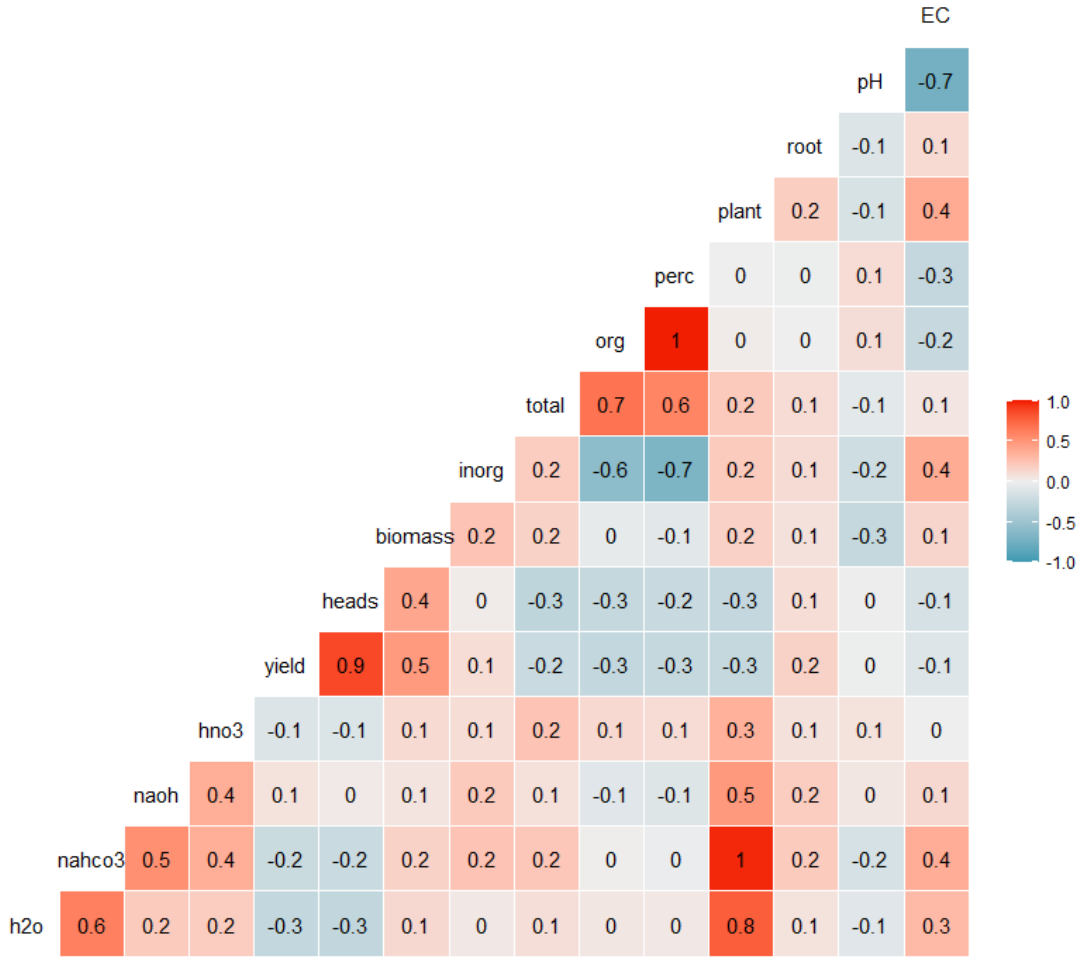

Figure B.1. Pearson correlation coefficients for soil properties, plant characteristics, Hedley pool concentrations, total P, and total organic P.

Table B.32. Elemental concentrations in freeze-dried NMR extracts.

	Dried Sample Wt	Al	Ca	Fe	Mg	Mn	P
	g			mg kg^{-1}			
Soils							
Untreated Soil		203	16290	1	269	5	209
Control	0.5196	189	15236	1	288	4	194
UBC-H (1)	0.4654	192	15362	2	300	6	198
1BC-H (1)	0.485	195	15138	2	297	6	195
PBC-H (1)	0.4656	187	15742	2	268	5	206
PBC-H (2)	0.5103	192	14740	3	291	6	197
FS-H (1)	0.5141	189	16054	1	262	4	212
FSBC-H (1)	0.5124	192	15552	2	285	6	204
FSBC-H (2)	0.4856	191	14878	2	286	6	202
CF-H (1)	0.5167	192	15692	1	274	4	232
Amendment							
UBC	`0.2355	64	987	32.8	119	28.7	48.3
1BC	0.2455	92.2	753	113.7	83.0	16.1	46.3
PBC	0.2323	54.3	1223	59.8	215	18.3	233
FS	0.3594	26.6	16866	58.0	2269	114	5860

Table B.33. Chemical shifts of peaks detected in ^{31}P-NMR spectra.

Category	P Form or Compound Class	Chemical Shift (ppm)
Inorganic P		
	OrthoP	6
	Pyrophosphate	-4.317
	Polyphosphates	-4.006 to -25
Organic P		
	Phosphonates	29.2 to 8.6
Orthophosphate Monoesters		
	myo-IHP	5.64, 4.70. 4.32, 4.23
	scyllo-IHP	3.842
	neo-IHP	6.540, 4.526
	D-*chiro*-IHP 4e/2a	6.756, 5.422, 4.131
	D-*chiro*-IHP 4a/2e	6.239, 4.868, 4.493
	Glucose-6-phosphate	5.442
	α-glycerophosphate	5.038
	B-glycerophosphate	4.620
	Mononucleotides	4.586, 4.554, 4.407, 4.363
	Choline phosphate	3.995
	Unknown	4.939
	Monoester 1	7.064, 6.351, 6.172
	Monoester 2	5.798, 5.242,5.215, 5.167, 5.126, 4.997, 4.903, 4.802, 3.973, 3.898
	Monoester 3	3.607, 3.443, 3.350, 2.939, 2.620
Orthophosphate Diesters		
	Other Diester 1	2.135, 2.056, 1.739, 0.920, 0.502, 0.194, 0.063
	DNA	-0.463, -0.549
	Other Diester 2	-0.849, -1.29, -1.69, -2.09

Table B.34. R-Factors for LCF processing of XANES soil samples.

Sample	R-Factor
Soils	
Untreated Soil	0.0151
Control	0.0128
UBC-H	0.0297
1BC-H	0.0105
PBC-H	0.0122
FS-H	0.0117
FSBC-H	0.0111
CF-H	0.0038
Amendments	
UBC	0.0520
1BC	0.0696
PBC	0.0620

Table B.35. Average $\delta^{18}O_w$ values from collected greenhouse water (± standard error) and average high and low equilibrium values calculated using high and low average greenhouse temperatures.

Date	$\delta^{18}O_W$ (‰)	Equilibrium (Low Temp)	Equilibrium (High Temp)
11/24/2022	-28.319 (0.193)	5.97	5.14
11/30/2022	-28.105 (0.322)	6.25	5.42
12/16/2022	-28.043 (0.258)	6.40	5.58
12/29/2022	-27.623 (0.229)	6.89	6.06
1/04/2022	-27.813 (0.263)	6.63	5.80
1/11/2022	-28.534 (0.23)	5.70	4.87